MASTER THESIS

MESOZOIC AND CENOZOIC FAULT SYSTEMS IN THE MOLASSE BASIN:

THE EXAMPLE OF THE TRATTNACH AREA (UPPER AUSTRIA)

LEOBEN, 2010

Author:

Stefan Sageder, BSc.

Advisor of the Chair of Petroleum Geology:

Univ.-Prof. Mag. rer. nat. Dr. mont. Reinhard F. Sachsenhofer

I declare in lieu of oath, that I wrote this thesis and performed the associated research myself, using only literature cited in this volume.

Leoben, October 2010

ACKNOWLEDGEMENTS

At first I thank my supervisor Professor Sachsenhofer for the support and expert guidance throughout the thesis.

My gratitude goes to RAG for readily providing the data and to Schlumberger making Petrel available to the University of Leoben. Especially I would like to thank Mr. Linzer and Reingruber for the inspiring discussions.

Special thanks to the Chair of Petroleum Geology team for all the lively discussions, brilliant remarks and great laughs we had.

In addition I would like to thank my family, friends and especially Vilja for all the truly outstanding support.

TABLE OF CONTENTS

ABSTRACT

The Mesozoic and Cenozoic fault inventory of the Molasse Basin and its Mesozoic basement was studied using the example of the Trattnach area (~40 km WSW Linz).

To achieve these objectives, 3D seismic data, acquired in 2007 and kindly provided by Rohöl-Aufsuchungs AG to the University of Leoben within the frame of the "Trattnach project", was interpreted.

As a first step a number of key horizons were mapped in the Mesozoic and Cenozoic succession. Thereafter, stratigraphic intervals ranging from the Jurassic to the Upper Puchkirchen Formation were identified and their seismic facies was described.

The interpreted faults and horizons were used to analyze the Mesozoic and Cenozoic tectonic evolution recorded in the area of interest. Attributes were derived from migrated data and from semblance cubes. Especially semblance data was important for this study because maps created from it helped in identifying discontinuities and structural features.

The area of investigation is part of the Alpine Foreland Basin. The most obvious deformation patterns are those related to Cenozoic normal faulting. Normal faulting in the Molasse Basin is the response of the European foreland to the advancing Alpine nappe system. In addition there is a deformation record older than that dating back to Mesozoic times. To some extent these older fault systems predefined the orientation of Cenozoic normal faulting.

Within the study area three deformational events can be distinguished:
(1) During a Late Cretaceous deformation phase horizontal stresses were approximately E-W directed. In response a N-S trending bulge formed during the Turonian to Coniacian. This structural element is about 3 km long and 500 m wide and its steeper western flank it is bordered by a reverse fault. Along with this bulge NNW-SSE trending reverse faults were formed. These deformational structures have not yet been described for the area of investigation. The deformation is caused by E-W directed horizontal stresses originating from sea floor spreading in the N-Atlantic realm. Besides that it is suggested that

contemporaneous NE-SW directed horizontal stresses were induced on the European foreland by the convergence of Africa towards Iberia-Europe.

(2) During the Paleocene, triggered by the collision of the Austro-Alpine unit with the European foreland, a pulse of NE-SW directed intraplate compression affected Europe. In the area of investigation the Paleocene stress pattern caused the formation of the NNW-SSE trending Trattnach reverse fault which borders a broad anticline on the W-side. As the structurally highest points of this anticline the Trattnach Anticline and the Altenhof Anticline were formed. The Trattnach Anticline hosts an oil deposit ("Trattnach Oil Field") which has been produced since the 1970's.

(3) The Cenozoic fault pattern in the Upper Austrian Molasse Basin originates from flexural down-bending of the foreland crust due to the load exerted by the advancing Alpine nappe system. Down-bending was accommodated by E-W trending, N- and S-dipping normal faults. Faulting commenced during latest Eocene and Early Oligocene times. The S-dipping normal faults remained active until the end of the Egerian. This is indicated by the increasing throw from top to bottom.
During the deposition of the Lower Puchkirchen Formation (Egerian) a local block-rotation took place. This block-rotation is documented by an angular unconformity within the deposits of the Lower Puchkirchen Formation.

KURZFASSUNG

Das mesozoische und känozoische Störungsinventar des Molassebeckens und ihres mesozoischen Untergrundes wurden am Beispiel des Trattnach Gebietes untersucht. Dieses Gebiet befindet sich etwa 40 km WSW von Linz.

Um diese Untersuchungen durchzuführen wurden 3D Seismikdaten verwendet, die der Montanuniversität Leoben von der Rohöl-Aufsuchungs AG zur Verfügung gestellt wurden. Diese Daten wurden 2007 gemessen.

Als erster Schritt wurden einige Schlüsselhorizonte des Mesozoikums und Känozoikums kartiert. Danach sind stratigraphische Intervalle, die sich vom Jura bis zur Oberen Puchkirchen-Formation erstrecken, identifiziert und deren seismische Fazies beschrieben worden.

Die kartierten Horizonte und Störungen wurden verwendet um die tektonische Entwicklung im Untersuchungsgebiet während des Mesozoikum und Känozoikum zu analysieren. Um dies zu erreichen war es notwendig verschiedene seismische Attribute aus den vorhanden Daten zu gewinnen. Dabei haben sich die "Semblance" Daten als sehr hilfreich erwiesen, da mit Hilfe dieser das Erkennen von Diskontinuitäten und strukturellen Eigenschaften vereinfacht wurde. Die Interpretationsarbeit erfolgte vorwiegend mit einem "Pre-Stack Time Migrated" (PrSTM) Datensatz.

Das untersuchte Gebiet ist ein Teil des Alpenvorlandes. Die augenscheinlichsten Störungsmuster sind känozoische Abschiebungen. Gebildet wurden diese Abschiebungen als Reaktion des europäischen Vorlandes auf das herannahenden alpine Deckensystem. Darüber hinaus gibt es wesentlich ältere, mesozoische, Deformationsstrukturen im Untergrund des Molassebeckens. Diese Störungssysteme haben, bis zu einem gewissen Grad, die Orientierung känozoischer Abschiebungen beeinflusst.

Im Gebiet konnten drei Deformationsereignisse unterschieden werden:

(1) Während einer Deformationsphase in der späten Kreide kam es zu E-W gerichteten Einengung. Als Folge daraus bildet sich während des Turoniums und

Coniaciums ein N-S streichender Rücken aus. Dieses Strukturelement ist in etwa 3 km lang und 500 m breit und wird an seiner steileren westlichen Flanke von einer Aufschiebung begrenzt. Gemeinsam mit diesem Rücken kam es zur Ausbildung von weiteren Aufschiebungen. Diese Deformationsstrukturen wurden für das untersuchte Gebiet bisher noch nicht beschrieben. Ausschlaggebend für eine E-W gerichtete Einengung am europäischen Vorland war "Sea-Floor Spreading" im Bereich des Nordatlantiks. Zeitgleich kam es zu NE-SW gerichteten Spannungen, hervorgerufen durch die Konvergenz der afrikanischen Platte mit Iberia-Europa.

(2) Im Paleozän wird Europa von NE-SW gerichteter Kompression erfasst, was durch die Kollision der Ostalpen mit dem europäischen Vorland hervorgerufen wurde. Im Gebiet des Trattnach Ölfeldes kam es deswegen zur Ausbildung einer NNW-SSE verlaufenden Aufschiebung. Diese begrenzt eine weitgespannte, gleich alte Antiklinale im Westen. Als strukturell höchste Punkte dieser Antiklinale wurden die Trattnach- und Altenhofen Antiklinale gebildet. In der ersteren befindet sich das Trattnach Ölfeld, das seit Mitte der 1970er Jahre produziert wird.

(3) Das känozoische Störungsmuster in der oberösterreichischen Molassezone wurde durch die Flexur des Vorlandes, bedingt durch die Auflast der alpinen Deckenstapel, angelegt. Die durch das Verbiegen der Kruste hervorgerufenen Dehnungsspannungen wurden von E-W gerichteten Abschiebungen aufgenommen. Diese Brüche tauchen entweder nach Norden oder Süden ab und wurden ab dem spätesten Eozän und jüngstem Oligozän angelegt. Die nach S einfallenden Brüche waren bis zum Ende des Egeriums aktiv, was durch den von oben nach unten zunehmenden Versatz angezeigt wird.
Während der Ablagerung der Unteren Puchkirchen-Formation (Egerium) kam es zu einer lokalen Blockrotation. Dabei kippte der Block nach Norden und wurde im Süden erodiert. Dies ist durch eine Winkeldiskordanz dokumentiert.

INTRODUCTION

The Molasse Basin including its Mesozoic basement is characterized by a multi-stage evolution characterized by diverse tectonic events. The main aim of the present thesis is to study the tectonic evolution of the Molasse Basin using the example of the Trattnach area, which is located in the Upper Austrian Molasse Basin about 40 km WSW of the city of Linz. The study is based mainly on a high quality 3D seismic data (acquired in 2007) covering an area of 65 km². The seismic data were generously provided by Rohöl-Aufsuchungs AG (RAG) together with data from wells and drill core samples within the framework of the "Trattnach project". The Trattnach project is a corporation between RAG and the University of Leoben. Besides that RAG also provided support on technical questions.

Understanding the Mesozoic and Cenozoic tectonic evolution of the area today occupied by the Upper Austrian Molasse Basin is a crucial part in unraveling the regional geological history of the Molasse Basin.

Moreover, the majority of oil and gas reservoirs in Upper Austria is linked to faults, which provide trapping structures and act either as migration pathways or as sealing elements. Hence an understanding of the processes forming these faults is desirable.

Existing literature dealing with faulting in the Molasse Basin and the underlying Mesozoic is somehow inconclusive. Nachtmann & Wagner (1987) suggested a dextral transpressional deformation event at the transition from the Cretaceous to the Tertiary. Bachmann (1987) described Cretaceous reverse faults in the German Molasse Basin, whereas Nachtmann (1995) postulated that pre-Cenozoic and Cenozoic faults were created mainly by extension and were modified by N-S compression during the Early Miocene. At that time seismic data was limited in number and moreover in quality and resolution. Hence faults were frequently indentified as normal faults, which is not in accordance with today's findings.
Recent unpublished investigations suggest the existence of NNW-SSE trending reverse faults and younger E-W striking normal faults.

Considering the previous work, a detailed interpretation of deformational structures and fault systems based on 3D seismic data should help in clarifying the tectonic evolution and related paleostress regimes. The 3D seismic data used was kindly provided by RAG who acquired the data in 2007. Integrating regional geology, seismic interpretation along with seismic attributes helps to explain the evolution of Mesozoic and Cenozoic fault patterns in the Upper Austrian Molasse and its underlying Mesozoic succession.
Accordingly, the important Mesozoic and Cenozoic horizons were mapped in order to describe the stratigraphic record. Subsequently a large number of individual faults was mapped, analyzed and dated. Every fault was interpreted in terms of dip, dip direction, age and sense of displacement (e.g. reverse or normal fault)

Combining all the information gathered from seismic interpretation, regional geology and literature makes it possible to explain deformation structures and associated deformation phases.

GEOLOGICAL SETTING

The Molasse Basin is a part of the North Alpine Foreland Basin (Fig. 1). The basin extends from France, through Switzerland across Southern Germany (Bavaria) and Austria to the Czech Republic (Nachtmann and Wagner 1987). In the eastern part, the northern margin of the Cenozoic Molasse Basin is delineated by the outcropping Bohemian Massif, whereas its southern margin corresponds to the Alpine thrust front (Wagner 1996). It attains a maximum width of 150 km in Bavaria and narrows to some 20 km near its

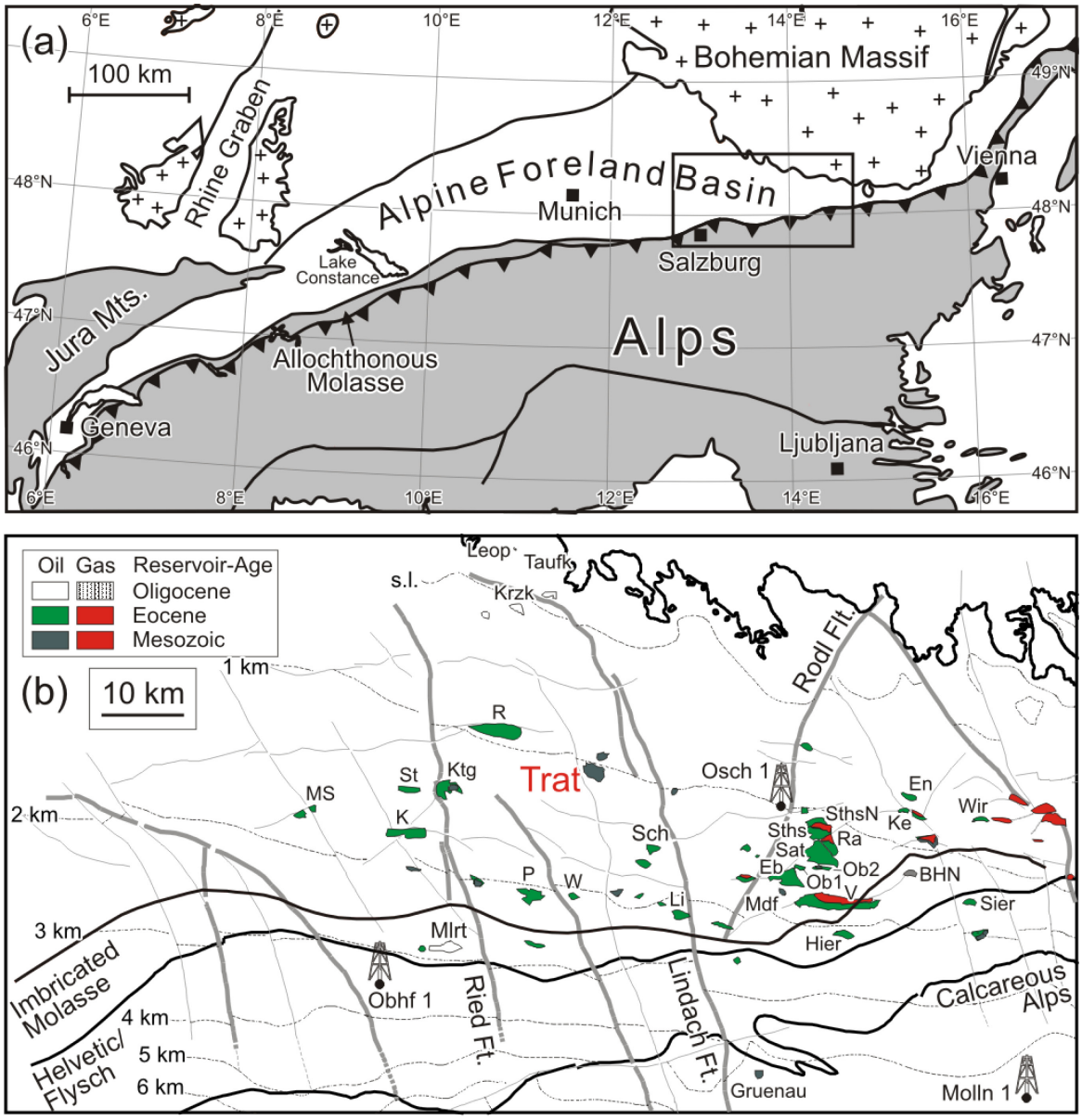

Fig. 1. **a) Overview of the North Alpine Foreland Basin.**
b) Map showing the depth of the pre-Cenozoic basement and the distribution of oil and thermal gas deposits in the Austrian part of the Alpine Foreland Basin (after Sachsenhofer et al. (2010)).

eastern and western ends. The fill of the asymmetrically shaped basin predominantly consists of Oligocene and Miocene syn-orogenic shallow- to deep-marine and continental clastics. The Cenozoic Molasse sediments are generally underlain by Mesozoic rocks which have been profoundly truncated. The Mesozoic deposits locally cover Paleozoic rocks preserved in graben structures or crystalline basement rocks (Sissingh 1997). The crystalline basement, in Upper Austria represented by the Bohemian Massif, is composed of Precambrian to Paleozoic metamorphic rocks and Variscian granitic plutonites (Kollmann 1977).

A system of NW-SE and NE-SW trending faults is dissecting the Bohemian Massif (Wagner 1998). These faults were predominantly formed during Permo-Carboniferous times and however reactivated in the Early Jurassic, Early Cretaceous and Early Cenozoic.

OUTLINE OF THE TECTONIC EVOLUTION

The area of the present-day Upper Austrian Molasse Basin started to subside during Middle Jurassic time, when clastic sediments overlain by a vast Middle to Upper Jurassic carbonate platform were laid down.

During Middle Jurassic time rift and wrench tectonics culminated in the Central and Western Tethys. By the Late Jurassic, sea-floor spreading in the central Atlantic became dominant and induced sinistral translation between Africa and Europe followed by the transtensional opening of the Alboran-Ligurian-Penninic Ocean. At that time the central Tethys sea-floor spreading axis became overpowered and a subduction system developed along the NE-margin of the Hellenic-Dinaric ocean (Ziegler 1987). The Early Cretaceous was dominated by apparently transpressional wrench deformation and differential uplift of individual fault blocks followed by erosion and karstification of Jurassic carbonates. Early Cretaceous deformations were polyphase with a first tectonic event during Berriasian to Hauterivian followed by a second pulse during the Aptian. These deformation events coincide with rift and wrench tectonics in NW-Europe, related to crustal extension in the N-Atlantic and Norwegian-Greenland Sea areas (Nachtmann and Wagner 1987). Sinistral translation between Africa and Europe continued during the Early Cretaceous. Thereafter, in response to the gradual opening to the Atlantic-Indian Ocean, Africa drifted northwards causing progressive subduction of the South Penninic-Piedmont

Ocean (Ziegler 1987). During the Albian to Turonian the closure of the Penninic Ocean was followed by the collision of the Alpine subduction zone with the passive margin of the European craton.

The Late Cretaceous evolution of the Molasse Basin is characterized by the deposition of shallow-marine sands and shales. During the Cenomanian marine transgression advanced from the S and W towards N and E and initiated the development of the Upper Austrian Cretaceous Basin.

In the Late Turonian to Early Senonian the orogenic front reached the passive margin of the Helvetic Shelf of the Eastern Alps and the Carpathians. This was accompanied by the reactivation of intra-plate discontinuities in the Alpine Foreland together with the reactivation of Permo-Carboniferous fracture zones, which transected the Bohemian Massif, and the uplift of major basement blocks along wrench and steep reverse faults. Late Cretaceous and Paleocene tectonic deformations resulted in an uplift of the Central-Swell-Zone (Fig. 2), erosion and the formation of NW-SE trending faults.

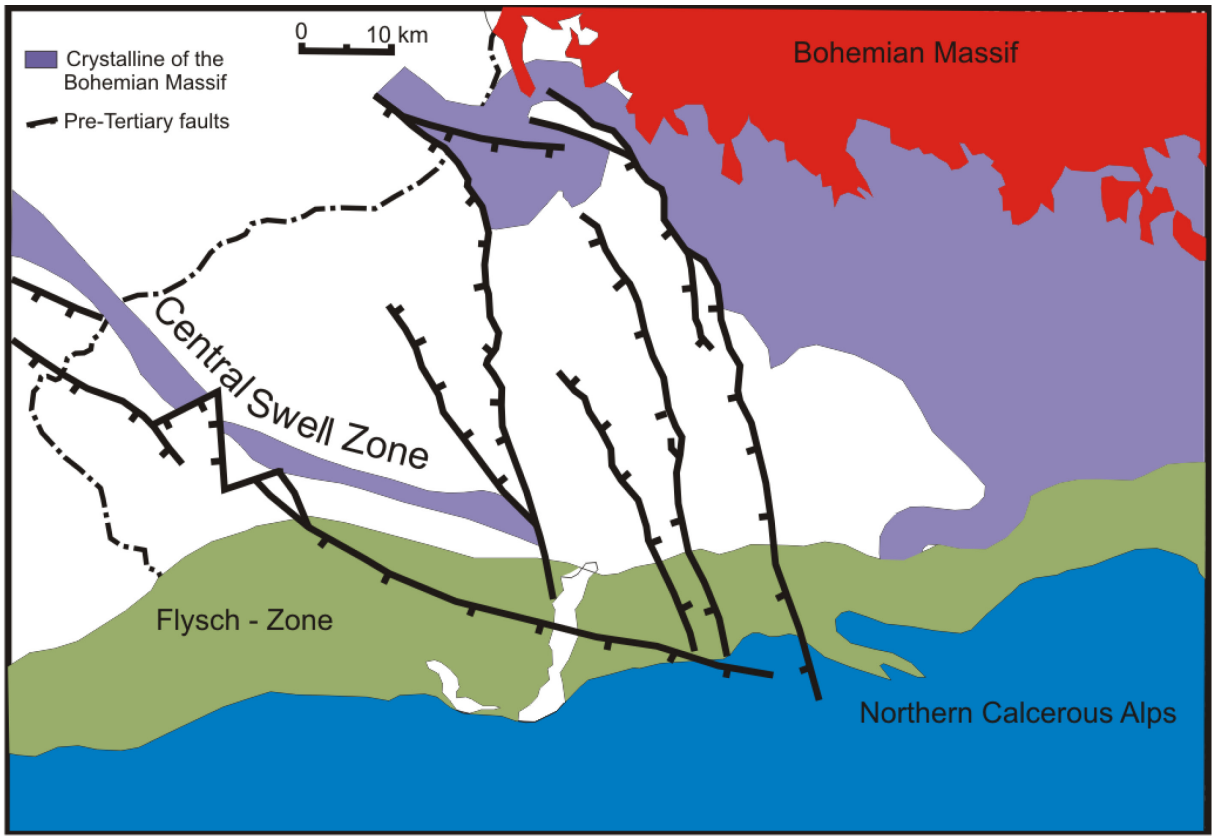

Fig. 2. Map of the Austrian Molasse Basin displaying pre-Tertiary faults and the Central Swell Zone (Nachtmann and Wagner 1987).

Whereas Late Cretaceous and Early Paleocene processes are traditionally interpreted to be triggered by the collision of the Alpine-Carpathian orogen with Europe's southern margin (Ziegler, Cloething and van Wees 1995), recent investigations (Kley and Voigt 2008) propose that Late Cretaceous compressional deformation in Europe reflects the onset of Africa-Iberia-Europe convergence and is unrelated to the early orogeny of the Alps. Furthermore efficient mechanical coupling of the Alps and Europe was only achieved during the Cenozoic Alpine orogeny. A summary of the Mesozoic tectonic evolution of different European domains according to Kley and Voigt (2008) is provided by Fig. 3.

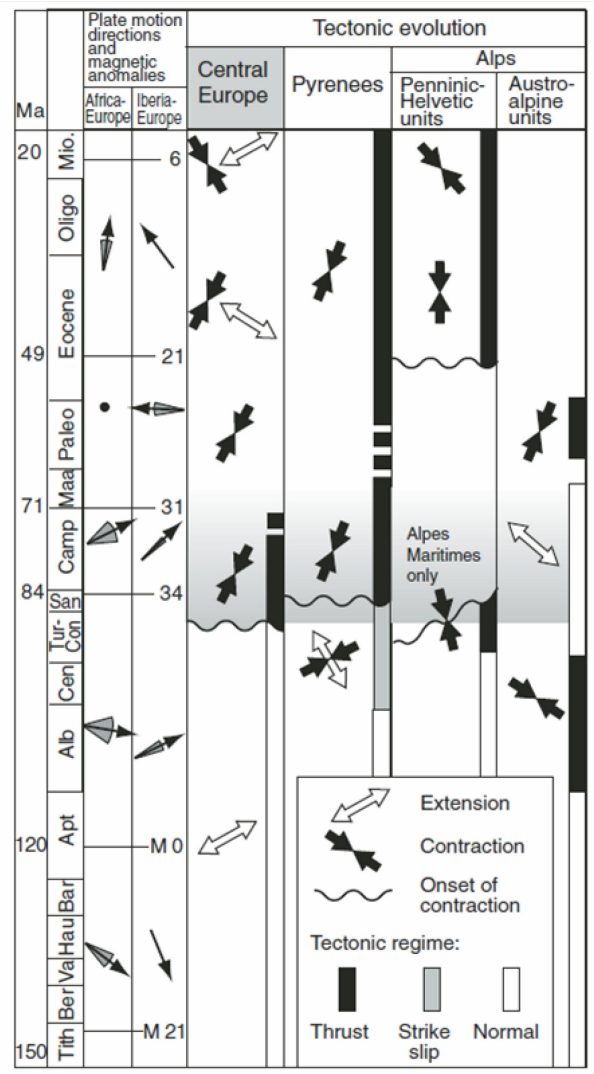

Fig. 3. Kinematic evolution in central Europe, Pyrenees and the Alps during Cretaceous and Cenozoic times (from Kley and Voigt, 2008).

The Cenozoic evolution of the North Alpine Foreland Basin was determined by the contemporaneous evolution of the Alpine orogenic system. The first stages of flexural loading of the European foreland are represented by the onset of subsidence in the Eocene, following collisional coupling of the European continental margin and the evolving Alpine nappes. Thrust loading caused by the advancing Alpine nappe systems (Latest Eocene and Early Oligocene) resulted in flexural down-bending of the European margin, rapid deepening and the development of tensional faults along with the reactivation of older fault systems (Genser, Cloething and Neubauer 2007). These EW-trending, S- and N-dipping faults (previously named syn- and antithetic normal faults, respectively) form traps, which contain the majority of oil accumulation in the Austrian Molasse Basin. Clastics derived from the rising Alps started to fill the deep-marine sediment-starved Molasse Basin from the Mid-Oligocene onwards (De Ruig 2003). During the Oligocene and Early Miocene the advancing Alpine nappe system overrode and partially scooped out the southern parts of the Molasse Basin. Cenozoic Molasse deposits are known to extend at least 40 km underneath the Alpine nappes (Fig. 4). Therefore Cenozoic sediments are divided structurally into the Autochthonous Molasse in front of and underneath the Alpine nappes and the Allochthonous Molasse. The Autochthonous Molasse rests generally undisturbed on the European foreland. The Allochthonous Molasse, including the Imbricated Molasse, is composed of tectonically moved Molasse sediments partially incorporated into the Alpine thrust sheets (Sachsenhofer, Gratzer, et al. 2006). During Eggenburgian to Ottnangian times rapid tectonic subsidence started in the E-part of the Austrian Molasse Basin accompanied by increasing sediment accumulation rates peaking during the Ottnangian (Genser, Cloething and Neubauer 2007). Persistent convergence between the European and Adriatic plates was probably largely accommodated by orogenetic- and lateral thickening. The widespread uplift of the entire Alpine region (from 6.0 Ma on) is most likely explained by distributed delamination and/or convective removal of over-thickened lithosphere along with N-ward spreading of the mechanical decoupling between mantle and crust of the subducted lithosphere, enhanced by erosional unloading (Genser, Cloething and Neubauer 2007). As a result of its asymmetric geometry thicknesses of the Cenozoic series range between a few meters in the north and more than 4000 m in the south close to the Alpine thrust front (Fig. 4) (Wagner 1998).

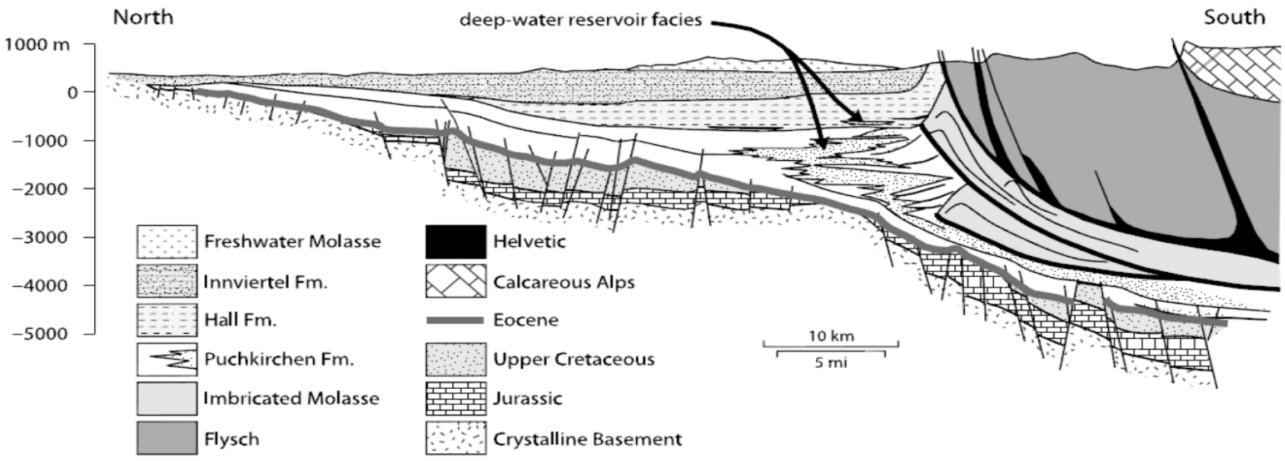

Fig. 4. Regional cross section through the Upper Austrian Molasse Basin (from De Ruig 2006, modified after Wagner 1996)

STRATIGRAPHY

PALEOZOIC

Late Paleozoic sediments are limited in Upper Austria to graben structures along the SW-margin of the Central-Swell-Zone (Fig. 2), a southeastern extension of the Landshut-Neuöttingen-High in Bavaria (Wagner 1998). This suggests that the formation of the Central-Swell-Zone, a major Mesozoic structural feature, is associated with a Late Hercynian fracture zone (Nachtmann and Wagner 1987).

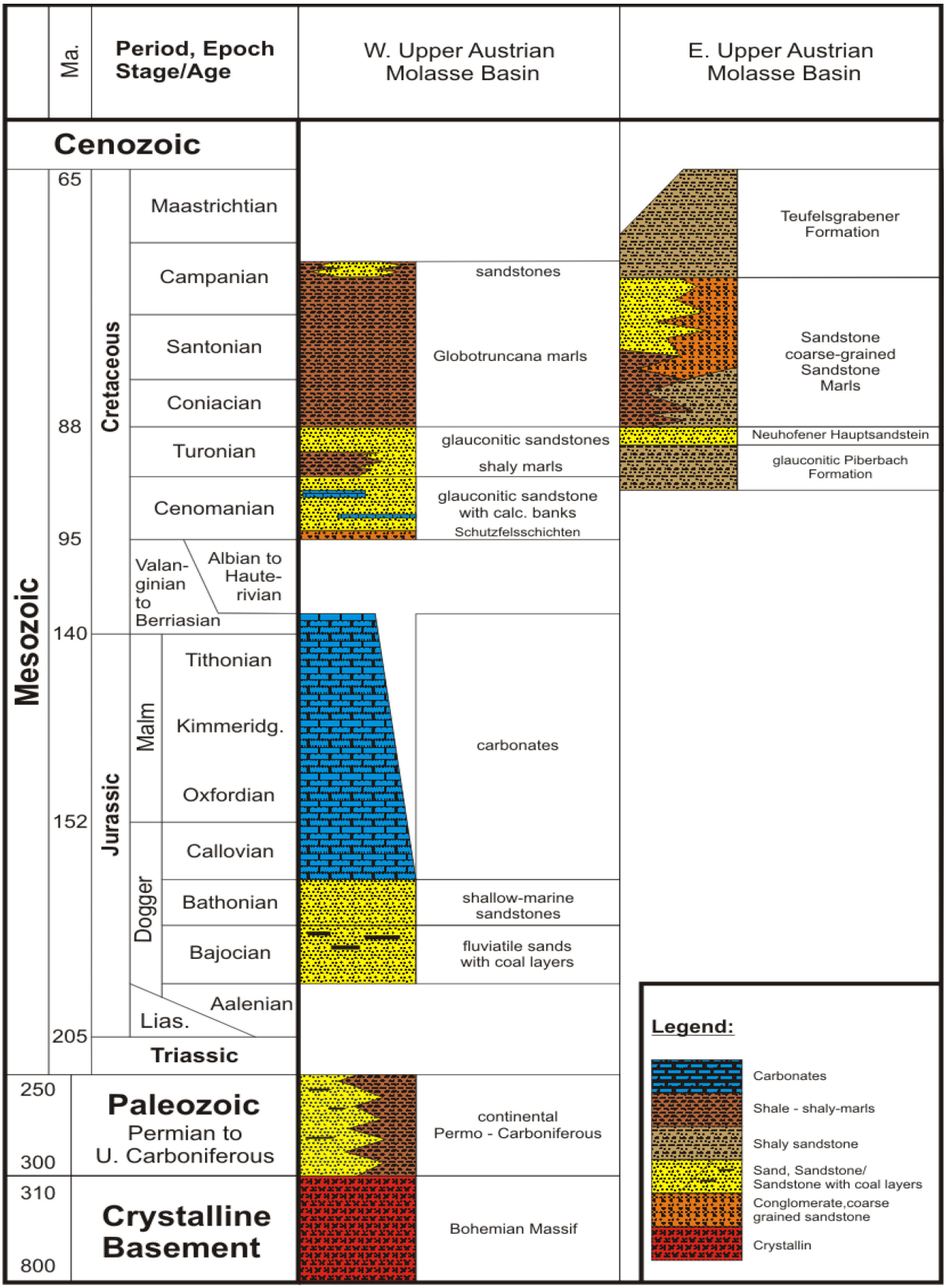

Fig. 5. Stratigraphic chart of the pre-Cenozoic basement in the Upper Austrian Molasse Basin (modified after Malzer, et al. 1993).

Jurassic facies distribution

Wagner (1998) divides the sedimentary evolution of the Central Paratethys in Upper Austria into the facies N- and S of the Central Swell Zone and the facies below or within the thrust sheets of the Imbricated Molasse (Fig. 5). The oldest Mesozoic sediments are of Middle Jurassic (Doggerian) age. They are composed of braided fluvial to shallow-marine sandstones with local thin coal seams. Their thickness ranges up to 60 m (Nachtmann and Wagner 1987). These clastic rocks are conformably overlain by micrites (Callovian) which grade upwards into biostromal carbonates with abundant sponges and chert nodules. Glauconitic limestones, a few meters thick, roughly represent the boundary between the Middle and Upper Jurassic (Nachtmann and Wagner 1987). In the west algal and sponge banks (Oxfordian, Kimmeridgian), up to 200 m thick, are capped by coral reefs. To the east they grade into oolitic grainstones and tidal flat deposits. Upper Jurassic facies show a progressive shallowing from the deeper shelf in the SW to the shallow shelf on the Bohemian Massif. This is demonstrated by the fully marine evolution of Upper Jurassic carbonates, an extensive carbonate platform succeeded by salt lagoon and tidal flat deposits (Purbeck facies). The maximum encountered total thickness of Jurassic carbonates is about 560 m (Fig. 6) in the well Hochburg 1 located SW of the Central-Swell-Zone (Wagner 1998). Deep karstification and frequent dolomitization are characteristic for Upper Jurassic carbonates. The top of the Jurassic and Purbeckian strata corresponds to a regional unconformity (Nachtmann and Wagner 1987).

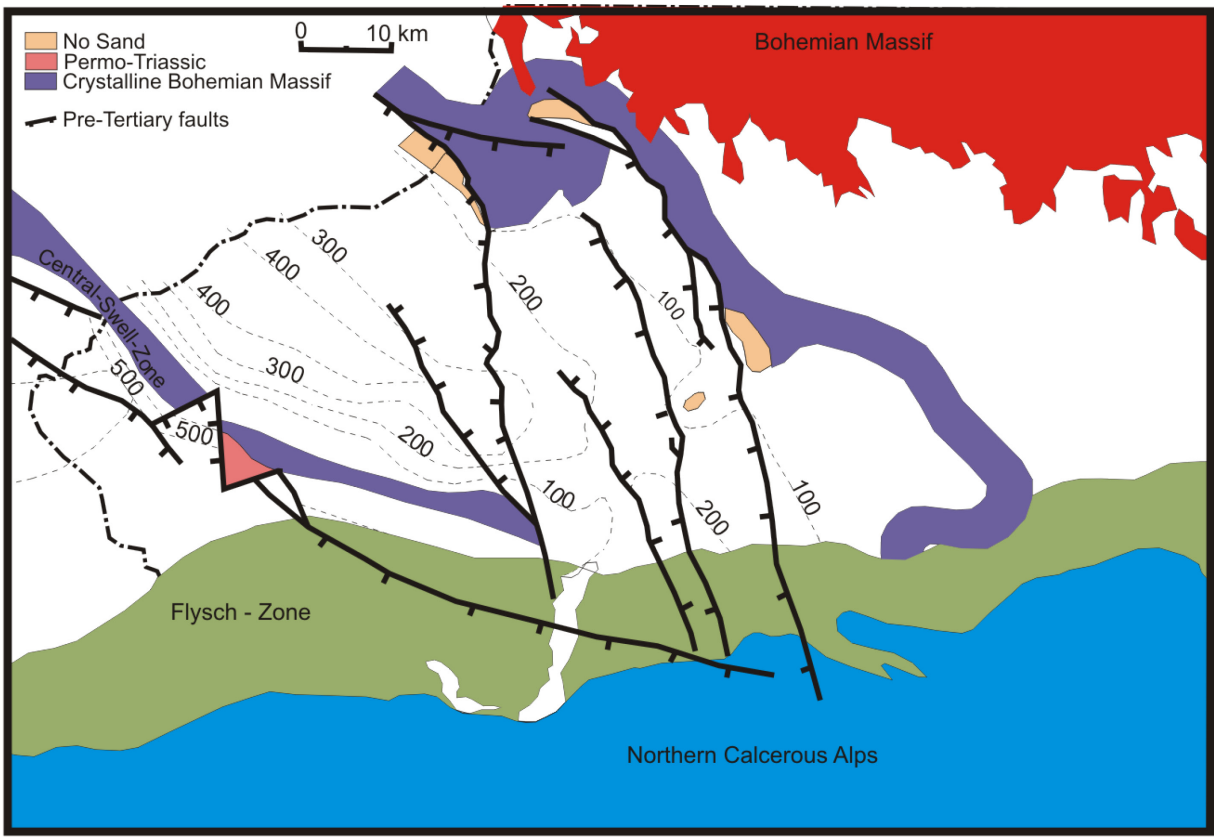

Fig. 6. Isopach map of Upper Jurassic carbonates along with the pre-Tertiary fault system. Thickness is in meters (modified after Nachtmann and Wagner 1987)

Cretaceous facies distribution

The unconformity separating the Jurassic carbonates from the overlying Lower Cretaceous strata represents the Early Cretaceous phase of basin inversion. This phase was accompanied by tectonic activity along NW-SE striking fault systems. The uplift associated with the above mentioned deformation event removed rocks up to 600 m thick (Nachtmann and Wagner 1987). Northeast of the Central-Swell-Zone the oldest Cretaceous deposit are termed Schutzfels Formation. It consists of light grey, white, red or green non-fossiliferous, coarse-grained fluvial sands. These beds infill the Upper Jurassic karst up to a depth of 100 m. They are overlain by Cenomanian coal-bearing marls which grade upwards into glauconitic sandstones of the Regensburg Formation. The Cenomanian deposits mainly consist of storm-dominated, shallow-marine, glauconitic sandstones that were deposited on a broad shelf with thicknesses between 15 and 70 m. Cenomanian clastics are conformably overlain by Lower Turonian shaly marls containing glauconitic storm-deposits in their upper parts. Upper Turonian to Upper Campanian sediments mainly consist of intensively burrowed mudstones accumulated under outer-

shelf conditions. During the Late Campanian some 300 m of shallow-water-sandstones were deposited NW of the Central-Swell-Zone, derived from the Bohemian Massif. The maximum drilled thickness of Cretaceous sediments is 800 m (Wagner 1998), however their original thickness probably ranged between 750 and 1000 m. No Maastrichtian and Danian sedimentary records have been encountered in the autochthonous series of the western Upper Austrian Cretaceous Basin. Throughout the Upper Austrian Molasse Basin the top of the Cretaceous succession corresponds to a regional unconformity, the so-called" base Eocene unconformity".

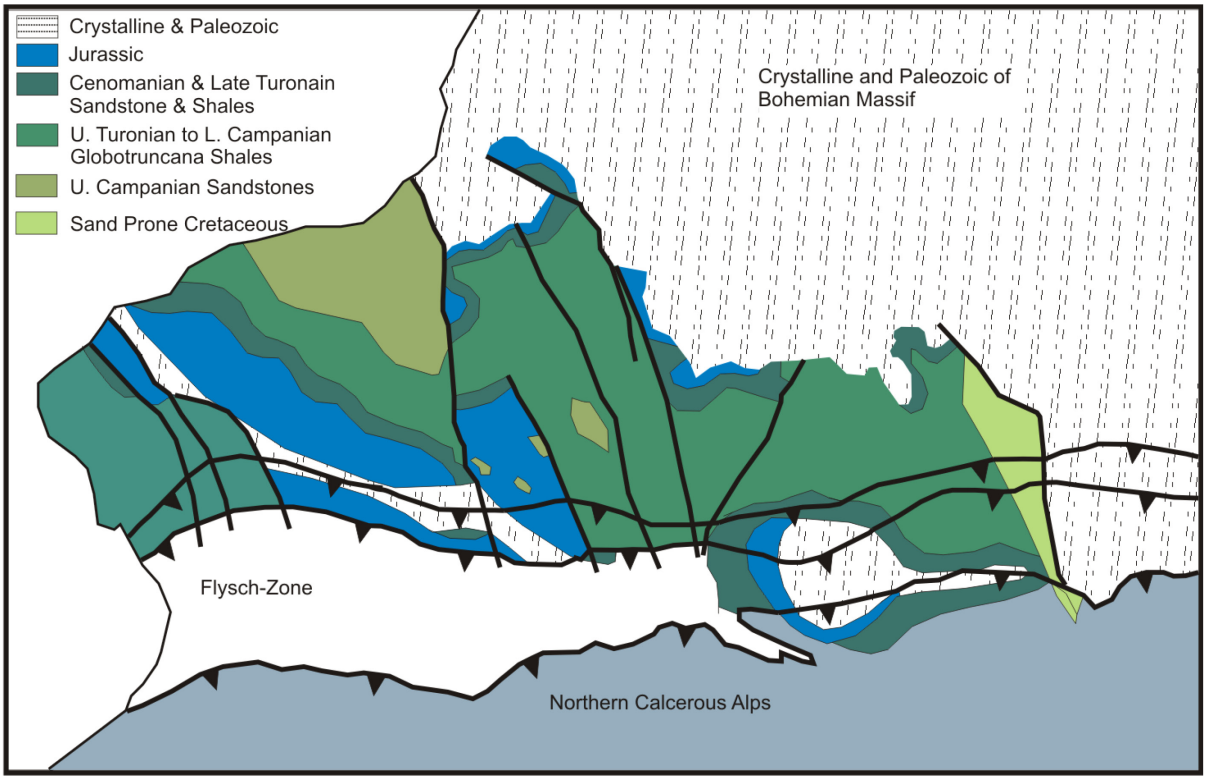

Fig. 7. Pre-Tertiary subcrop map with simplified faults displayed as black lines (modified after Wagner 1996).

CENOZOIC

In the Eocene the actual Molasse stage began with the deposition of fluvial and shallow marine sandstones, shales and carbonates (Fig. 8). During the Late Eocene the Tethys Sea progressively encroached the Mesozoic and Crystalline fault blocks. At the same time the Central-Swell-Zone separated the lagoon from the slope to the open marine realm. The different facies zones started in the north with fluvial flood plains crossed by meandering channels of the Voitsdorf Formation. The fluvial and limnic Voitsdorf Formation was transgressed by the Upper Eocene succession in the S and progressively younger Oligocene sediments to the N and NE. The subsiding floodplain is overlain by the paralic Cerithian Beds (Priabonian) and shallow marine sands of the Ampfing Formation. On top of the Central-Swell-Zone the Lithothamnium Limestones are centered and shed their debris to the N into the lagoon and S into the high energy open marine shelf.

During the latest Eocene and Early Oligocene the Molasse Basin subsided rapidly to deep-water conditions. This led to the development of a dense network of N- and S-dipping, E-W-trending normal faults (Nachtmann and Wagner 1987).
On the paleo-slope, the Schöneck Formation with thicknesses up to 30 m was deposited. This formation, formerly called Fischschiefer is a source rock for the Molasse oil (Wagner 1996). Contemporaneously Globigerina marls were deposited to the south. Bottom currents eroded deep into older sediments in front of the Alpine nappe system immediately followed by rapid sedimentation of slide material, turbidites and reworking of sediment. The Schöneck Formation is overlain by the Dynow Marlstone (Middle Kiscellian), a pure nannofossil chalk deposited in a basin with reduced salinity (Schulz, et al. 2004).

The Eggerding Formation (Banded Marls) consists of dark grey laminated pelites with thin white layers of nannoplankton and was deposited under conditions of the outer slope (Sachsenhofer, Leitner, et al. 2010). The overlying Zupfing Formation was deposited under the same conditions. It is characterized by hemipelagites and distal turbidites (Wagner 1998).

Rupelian sands record the onset of coarse clastic sedimentation in the deep-marine basin. These sands generally consist of fine- to medium-grained sandstones which are separated

by mudstone intervals. The stratigraphic interval between the Oligocene and the Early Miocene in the Upper Austrian Molasse is characterized by a thick succession of gravity flow deposits. These consist of the above mentioned Rupelian sands, the Lower Puchkirchen Formation (Untere Puchkirchener Serie), the Upper Puchkirchen Formation (Obere Puchkirchener Serie) and the basal parts of the Hall Formation. Accumulation of these up to 2000 m thick sediments took place between 30 - 20 Ma.

The Lower Puchkirchen Formation (Chattian) is traditionally subdivided from bottom to top into the "Liegende Tonmergel", the “Sand-Schotter Gruppe” (Sand-Gravel Group) and the locally developed mudstones of the "Hangende Tonmergel". The Upper Puchkirchen Formation (Aquitanian) is separated from the Lower Puchkirchen Formation by a semi-regional erosional unconformity (Hinsch 2008). The Upper Puchkirchen Formation is subdivided into four units by De Ruig and Hubbard (2006), who provide a comprehensive and detailed characterization of the Puchkirchen Formation. Both, the Lower and Upper Puchkirchen Formations contain a wide range of clastic lithologies including clast-supported sandy conglomerates, pebbly sandstones, fine- to coarse-grained sandstones, siltstones and mudstones. The Puchkirchen depositional system is characterized by a large, roughly W-E-trending, low sinuosity deep-water channel belt (De Ruig and Hubbard 2006) characterized by a variety of gravity flow processes, slurry flows, submarine slides and slumps.

The Hall Formation overlies the Puchkirchen Formation with another unconformity. Similar to the Puchkirchen Formation, the basal Hall Formation is characterized by deep-water deposits. The upper Hall Formation consists of NW-prograding muddy prodelta deposits (De Ruig 2003).

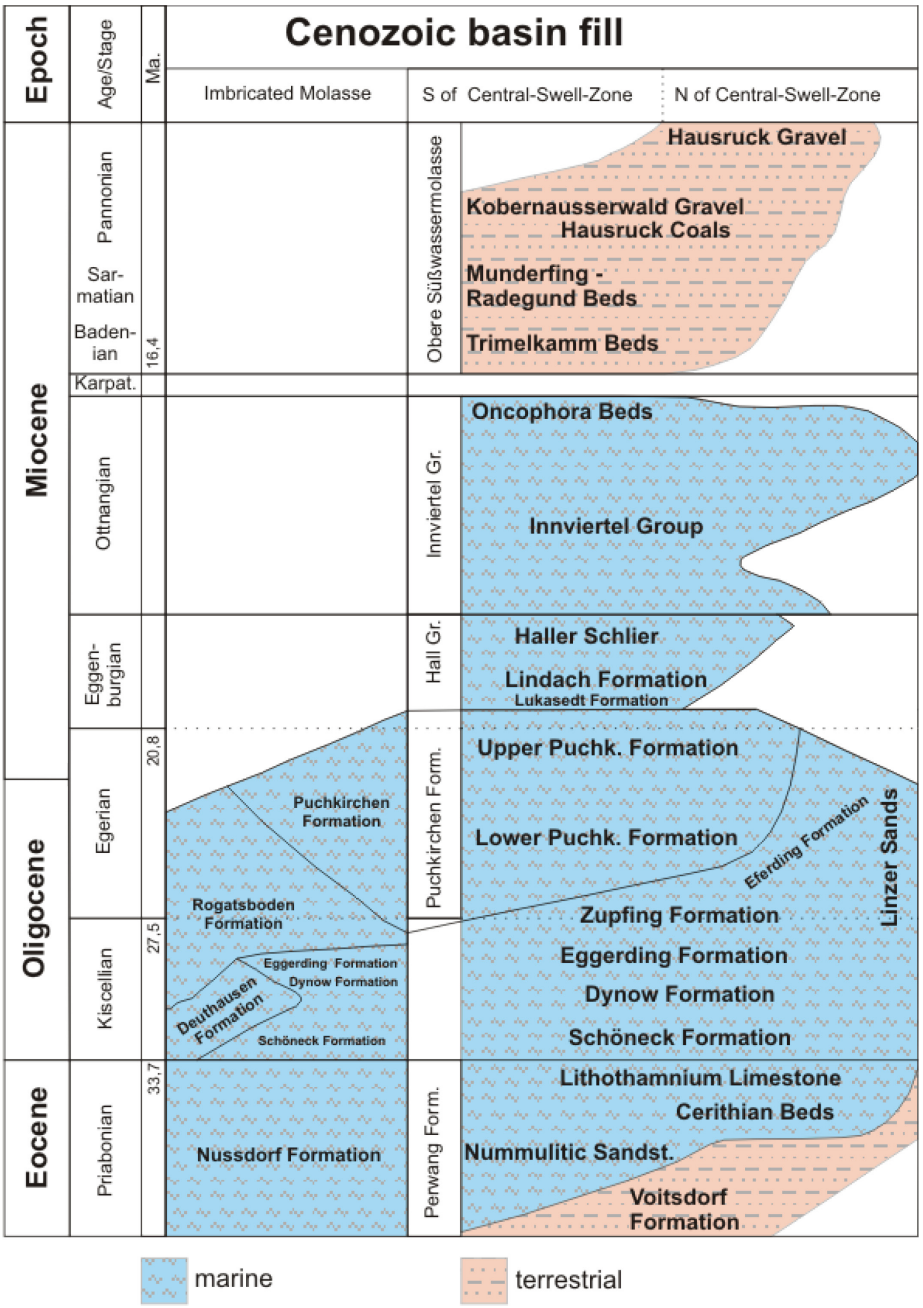

Fig. 8. Stratigraphy of the Cenozoic basin fill in the Upper Austrian Molasse (modified after Wagner, 1998)

HISTORY OF PETROLEUM EXPLORATION AND THE PETROLEUM SYSTEM

With the coincidental discovery of a shallow gas reservoir in the vicinity of Wels during the 1890's the exploration for oil and gas in Upper Austria began. This set the cornerstone for ongoing drilling and exploration until today. In 1917 Dr. Max Silberberg founded the "Wallerner Erdölgesellschaft m. b. H." in order to drill for oil in the surroundings of Wels. The first well, spudded in 1917, was not successful and abandoned. Subsequently a few kilometers away from the first one, the well "Schacht Paul" located in Bad Schallerbach was drilled during 1918. Again no hydrocarbons were found. Although unsuccessful in terms of petroleum, the borehole found thermal water. The thermal water bearing formation is produced until today and forms the base for a considerable number of health resorts in the surrounding area (Rockenschaub 1996). The limited drilling success of that time might be due to the fact that dowsing (dowse means "Wünschelrute" in German) was considered an adequate exploration tool. Decades later in 1956 the well Puchkirchen 1, drilled by RAG, was the first one to encounter a profitable oil field in the Upper Austrian Molasse Basin.

In the Upper Austrian Foreland Basin two different petroleum systems are present: A Mesozoic to lower Oligocene oil and thermal gas system and an Oligo-Miocene biogenic gas system (Wagner 1996).

The Oligocene Schöneck Formation is regarded as the main source rock for oil and thermal gas in the Molasse Basin (Schulz, et al. 2002). Besides that the Eggerding formation has some additional, but subordinate source rock potential (Sachsenhofer, Leitner, et al. 2010). The Schöneck Formation enters the oil window (4 -6 km depth) only beneath the Alpine nappes thus indicating long distance migration. Reservoirs are preferentially located on the upthrown side of W-E trending N-dipping normal faults (Nachtmann 1995). Reservoir rocks of this system are those aligned along migration paths with updip migration from deeper basin parts. Oil reservoirs are thus found in Doggerian sandstones and carbonates, Cenomanian and Upper Eocene sandstones, but also in Oligocene sandstones (Wagner 1998). However, Upper Eocene basal sandstones are most important. Seals are mainly provided by intraformational shales (Véron 2005).

Reservoirs for biogenic gas are Oligocene (Chattian) and Miocene (Aquitanian, Eggenburgian) turbiditic sandstones and sandy conglomerates of the Puchkirchen and Hall formation. Seals are provided by intraformational Oligocene and Miocene shales. Gas generation is suggested having taken place from Middle Oligocene time onwards. The gas is commonly trapped in compaction and stratigraphic structures, combinations of both and imbrication structures.

DATA AND METHODS

DATA

The "Trattnach-Dataset" covering an area of about 65 km² (E-W extension of 6.5 km and N-S extension of 10 km) was generously made available by RAG (Rohöl-Aufsuchungs AG) to the University of Leoben for research purposes. Along with 3D seismic data numerous wells and well-logs are part of this data set. Geographically the Trattnach oilfield is located in the Upper Austrian part of the Molasse Basin, some 40 km WSW of Linz. Seismic data was acquired in 2007 whereas well-data is considerably older. Interpretation of seismic data was primarily done on a pre-stack time migrated cube (PrSTM cube). The other important seismic volume is the semblance cube. Both cubes are part of the Trattnach dataset provided by RAG. Because of the frequent use of this dataset a seismic to well tie along with a Time-Depth (T/D) law had already been established and therefore only minor adjustments were necessary for the deeper parts of the cube (below the Cenomanian). However the T/D-law could not be used for the whole seismic volume due to the lack of well data; only three wells penetrated the entire Mesozoic succession within the area of interest. Hence all further work was done in two-way-travel time (TWT) bearing in mind the difference between time and depth.

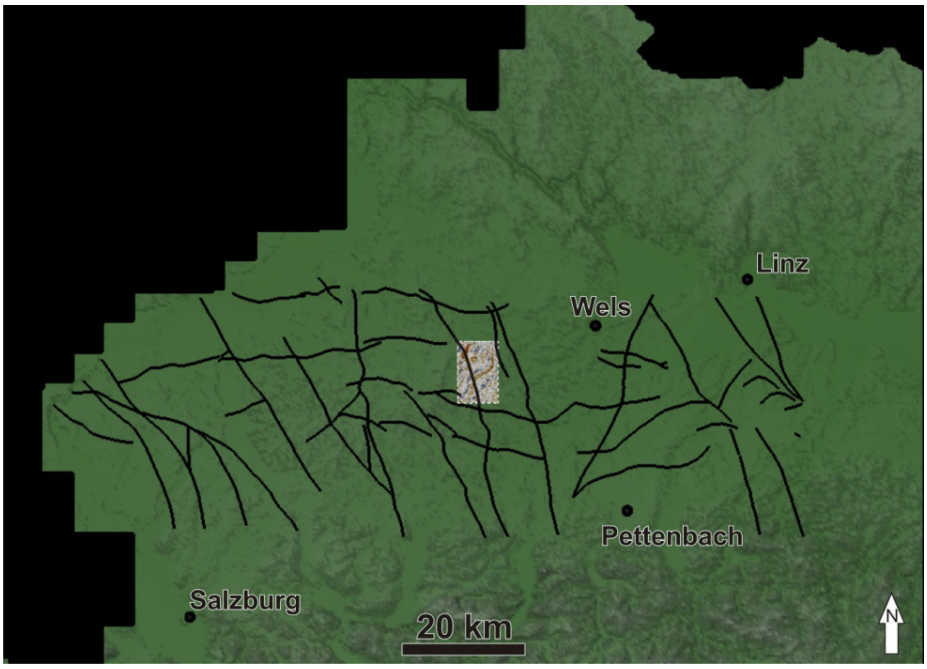

Fig. 9. Overview of Upper Austria, the location of the seismic cube and the major faults.

SEISMIC INTERPRETATION

STRATIGRAPHIC INTERPRETATION

Key horizons were identified by matching synthetic seismograms and 3D seismic data. Horizons were mapped using Petrel Software on variable inline and crossline spacing (bin size is 25x25 m) depending on resolution and traceability of the reflector. Horizons mapped from bottom to top are listed in Table 1 and presented in Fig. 10. Furthermore several additional intra-formational horizons were mapped.

Table 1: Interpreted Horizons:

Horizon (abbreviation)	Reflector	Quality
Top Basement (Top XBM)	peak	very poor
Base Cenomanian/Top Jurassic	trough	good
Top Cenomanian	zero-crossing	good
Top Turonian marl (Top TRTNM)	peak	fair
Top Mesozoic/Base Eocene	peak	good
Base Puchkirchen Formation (Base PS)	trough	good
Top Lower Puchkirchen Formation (Top LPS)	trough	fair
Base Hall Formation	peak	good

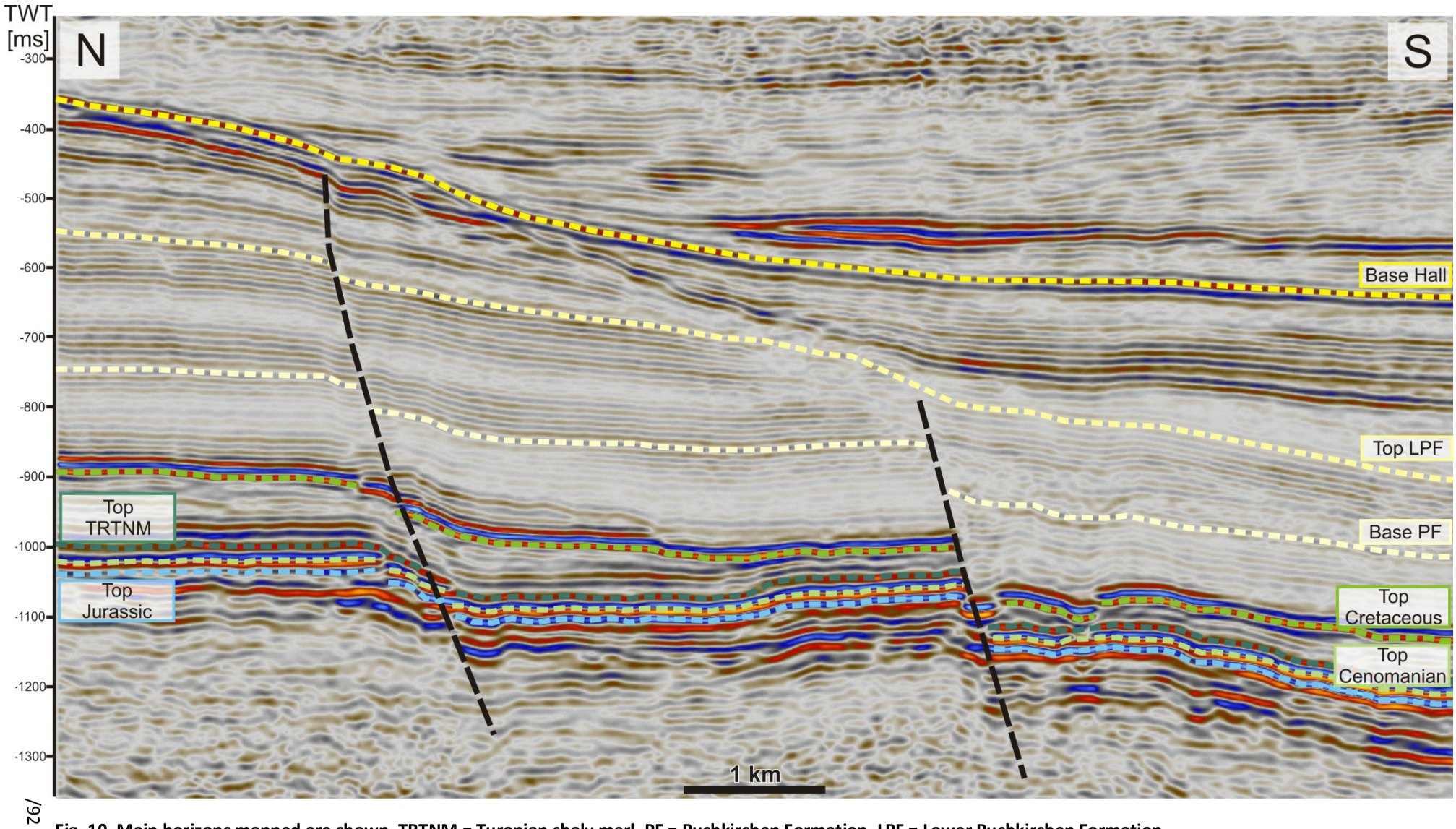

/92

Fig. 10. Main horizons mapped are shown. TRTNM = Turonian shaly marl, PF = Puchkirchen Formation, LPF = Lower Puchkirchen Formation.

FAULT INTERPRETATION

Previous fault interpretations by different authors were made available for this study. All of them were evaluated and if necessary were edited or extended. Interpretation was done rather conventionally, mapping faults line by line or by using ant-tracking and attribute maps. Two main fault systems were identified NNW-SSE trending older reverse faults and younger E-E trending normal faults (Fig. 11).

SEISMIC ATTRIBUTES

Seismic attributes, for a whole cube, as time-slice or along a surface (horizon-slice) were computed within Petrel© by Schlumberger and OpenDtect© by dGB Earth Sciences. Attributes created in Petrel are: ant-tracking and amplitude maps. With OpenDtect similarity maps and dip maps were calculated.

ANT-TRACKING

Ant-tracking is a proprietary tool within the Petrel software package and part of a workflow. This algorithm automatically extracts fault surfaces from fault attributes. The workflow is divided in four main steps: (1) seismic conditioning, reducing noise in the data, (2) edge detection, (3) edge enhancement and (4) interactive interpretation.

By using the existing semblance seismic volume all the prerequisites are fulfilled to apply ant-tracking directly. This workflow results in an attribute volume that shows three dimensional fault zones. For further information about this workflow please refer to Petrel manual of Schlumberger. The final step following ant-tracking would be automatic fault extraction. This step was tested, but because the results were not satisfactory, automatic fault extraction was not applied. Nevertheless ant tracking volumes are of tremendous help in interpreting and identifying faults. The operation can be performed before one single fault or horizon is mapped and thus guides subsequent interpretation. In order to test the reliability of "ant-tracked" fault zones they have been compared with faults mapped conventionally line-by-line. The result: ant-tracking provides useful guidance.

Nevertheless in order to improve reliability, several cropped ant tracking sub-cubes were calculated and positioned at the same stratigraphic intervals (Fig. 11). This was necessary because, for example the reflectors of Cenomanian strata are not a flat horizontal surface but displaced along normal faults. Hence the southern parts of the Cenomanian are considerably deeper (in TWT) compared to the northern part. This procedure, matching stratigraphy to ant-tracking sub-cubes was called stratigraphic ant-tracking.

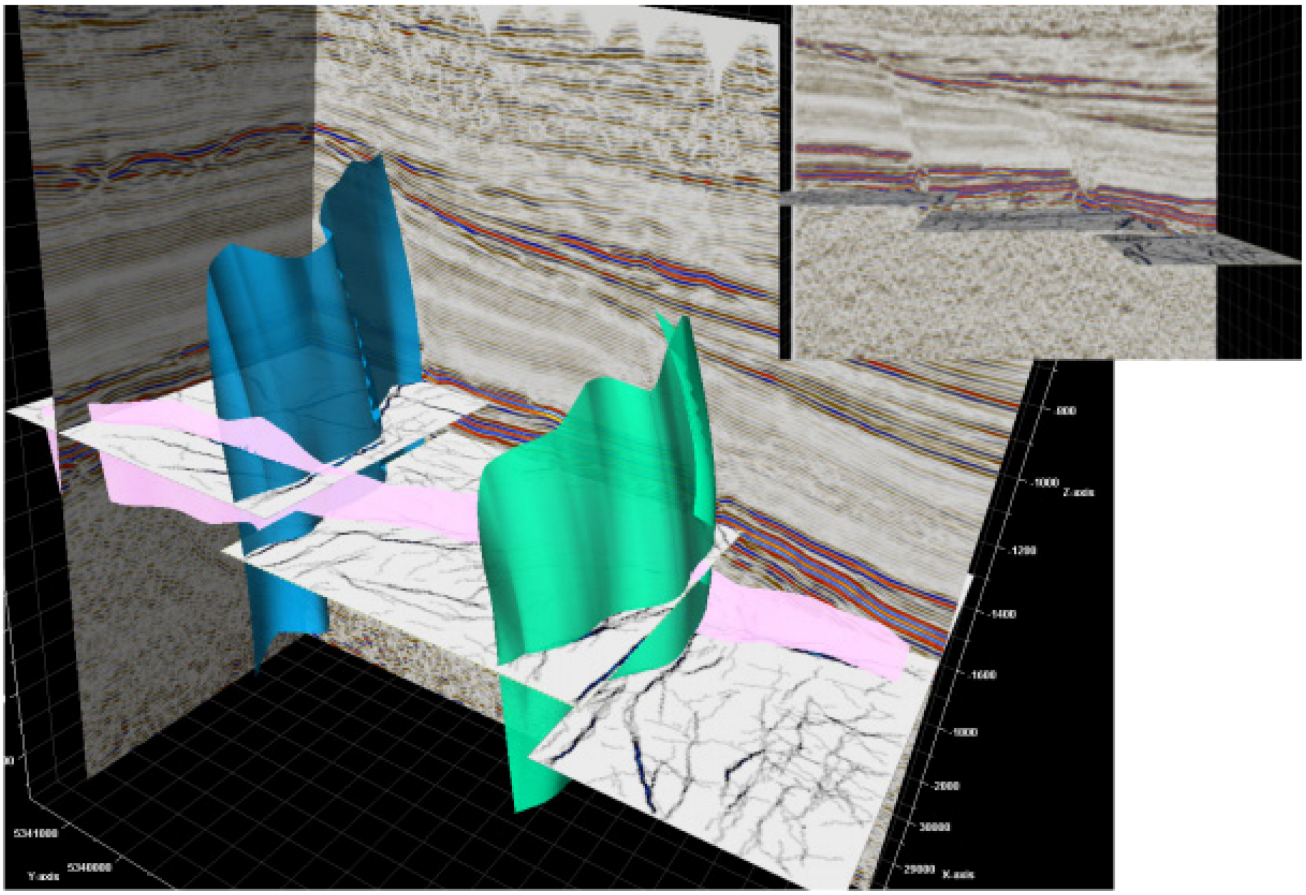

Fig. 11. Stratigraphic ant-tracking. Top right: position of the ant-tracking sub-cubes. Three conventionally mapped fault planes are show in blue, green and pink.

AMPLITUDE MAPS

EXTRACT VALUE

This utility extracts the input seismic value relative to a single horizon or an existing interpretation. It can be used on any seismic volume to extract any value.

RMS AMPLITUDE

The RMS amplitude helps in mapping hydrocarbon indications in the data and other geologic features, possibly karst, which are isolated from background features by amplitude response. RMS is the square root of the sum of the squared amplitudes (amp) divided by the number of samples (k), see equation below.

$$\sqrt{\frac{(\sum_i^n amp^2)}{k}}$$

RMS can be calculated for a single surface within a given TWT-window, between to surfaces or between two events e.g. zero-crossings. For computation the input seismic volume has to be chosen, in this case the PrSTM or as described below the semblance volume. Finally a new surface attribute is generated which can be colour coded.

ATTRIBUTES DERIVED FROM THE SEMBLANCE CUBE

Both amplitude map utilities (RMS and extract value) were used to compute maps from the semblance cube. The generated maps, Top Cenomanian and Base Eocene are a very good representation of structural features and topography, in time! The Top Cenomanian relief map clearly depicts all the main structural features like fault zones and other deformation structures. The topography of each map corresponds to the interpreted surface, the actual input along which the attribute was calculated and is emphasized by the chosen colour coding. Relief maps below (Fig. 12a,b) are displayed in a grey scale with a non-linear gradient emphasizing discontinuities in black.

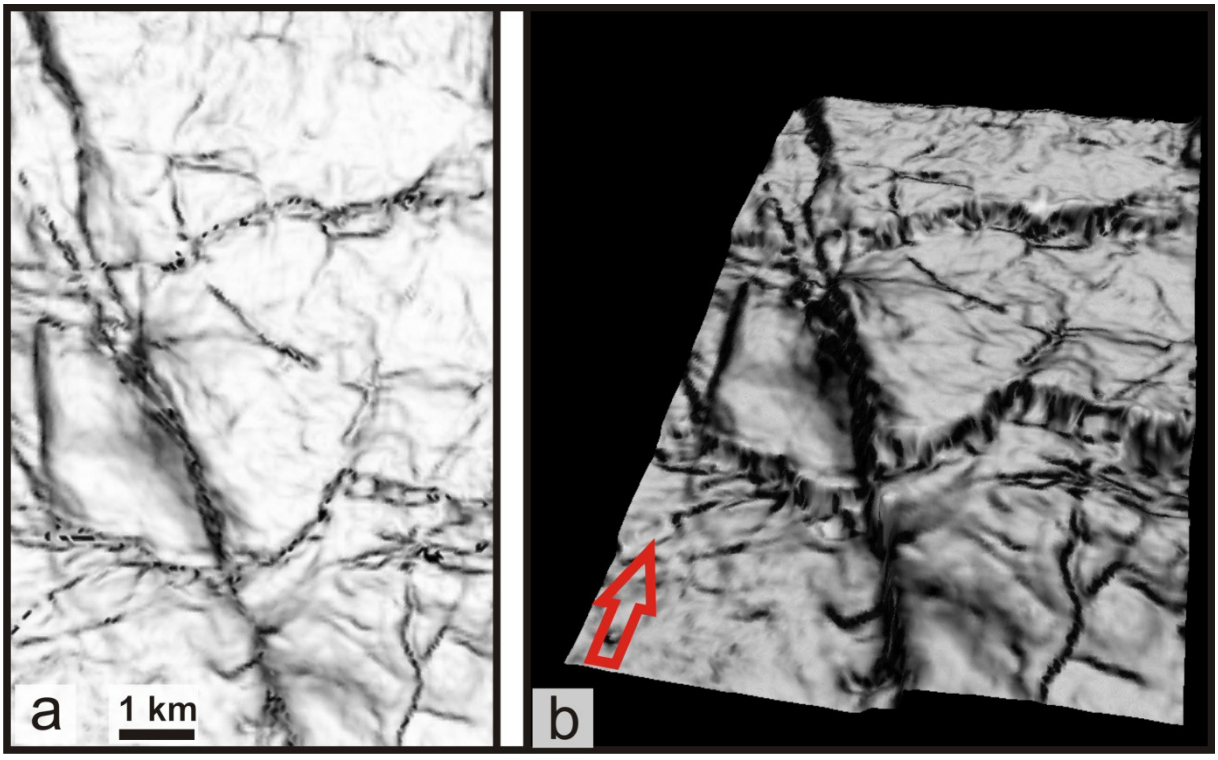

Fig. 12. a) Relief map in map view.
b) 3D flying carpet. Red arrow is indicating north.
Maps displayed in map view are always oriented with the top pointing north.

SIMILARITY MAP

The similarity is a multi trace attribute that returns trace-to-trace similarity properties (Fig. 13). It expresses how much two or more trace segments look alike. A similarity of “1” means that the trace segments are completely identical in waveform and amplitude. A similarity of “0” means they are completely dis-similar. The OpenDtect algorithm first searches for direction of the best match at every position (dip). Then the dip is used to calculate the similarity between adjacent traces.

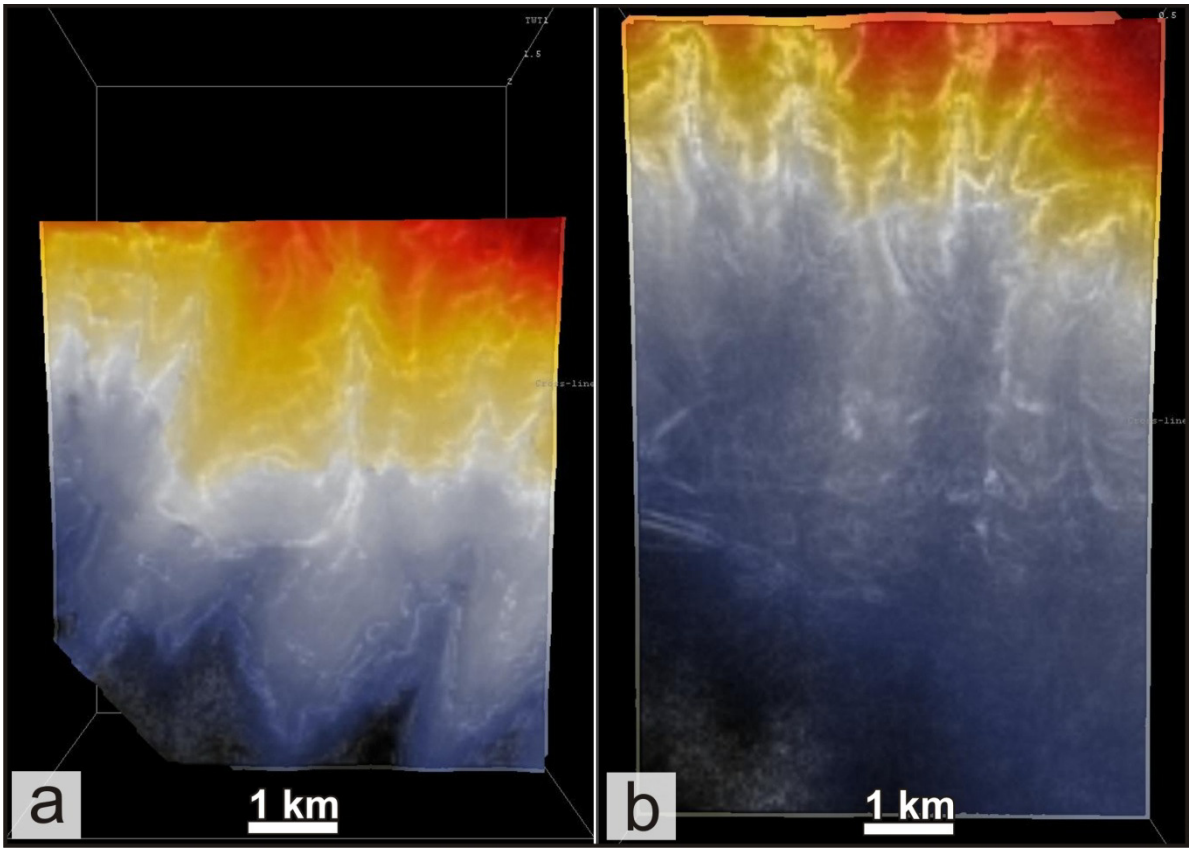

Fig. 13. Similarity maps with superimposed TWT. Red colours indicate shorter TWTs blue colours longer TWTs.
a) Intra Upper Puchkirchen Formation erosion surface.
b) Base Hall Formation erosion surface.

DIP MAP

The polar dip attribute is composed of extracted inline- and crossline dip (Fig. 14). The polar dip is calculated, referring to the OpenDtect manual, using the following equation:

$$\sqrt{(inline\ dip)^2 + (crossline\ dip)^2}$$

Thus the result is always larger than zero. The dip is a ratio between vertical length and horizontal distance either in time (TWT) or depth (meters). It represents the true (geological) dip.

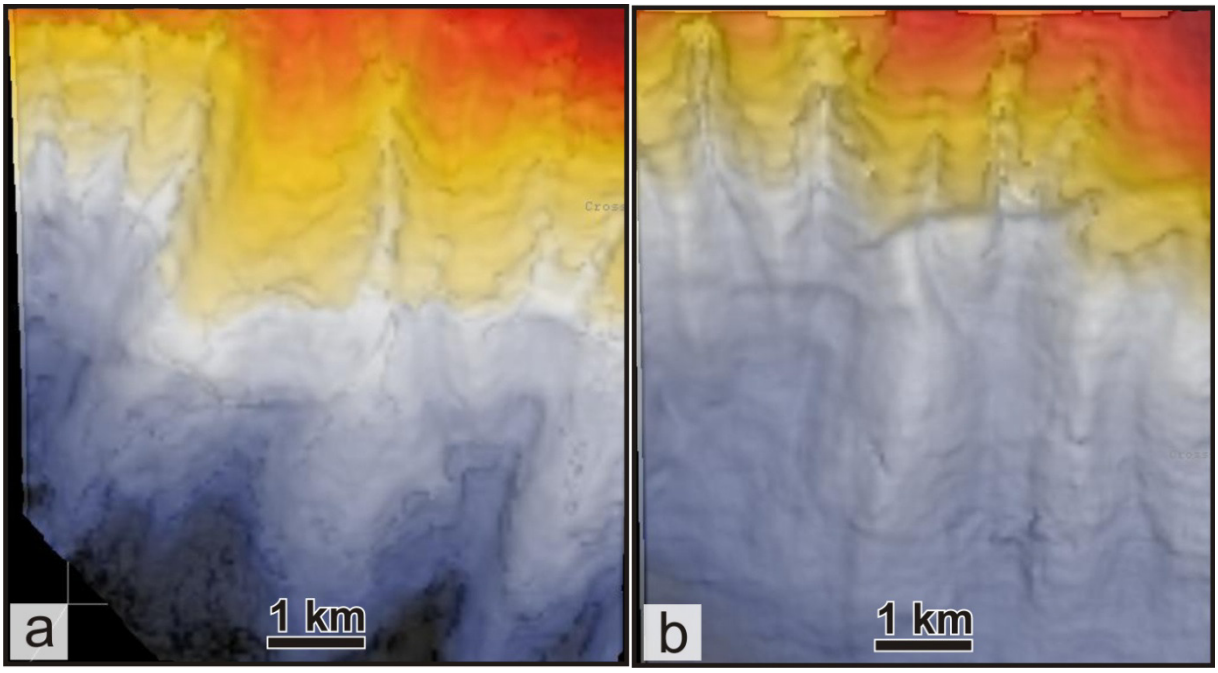

Fig. 14. Dip map with superimposed TWT. Red colours indicate shorter TWTs blue colours longer TWTs.
a) Intra Upper Puchkirchen Formation erosion surface.
b) Base Hall Formation erosion surface.

RESULTS

SEISMIC CHARACTERIZATION OF THE SEDIMENTARY RECORD (MESOZOIC AND PALEOGENE)

JURASSIC

Base Jurassic (Top Basement)

Due to the poor resolution of seismic data the definition of Top XBM (Top Crystalline Basement) is based on sparse well data (well tops from three wells) and a tentative mapping of a continuous reflector associated with Top XBM.

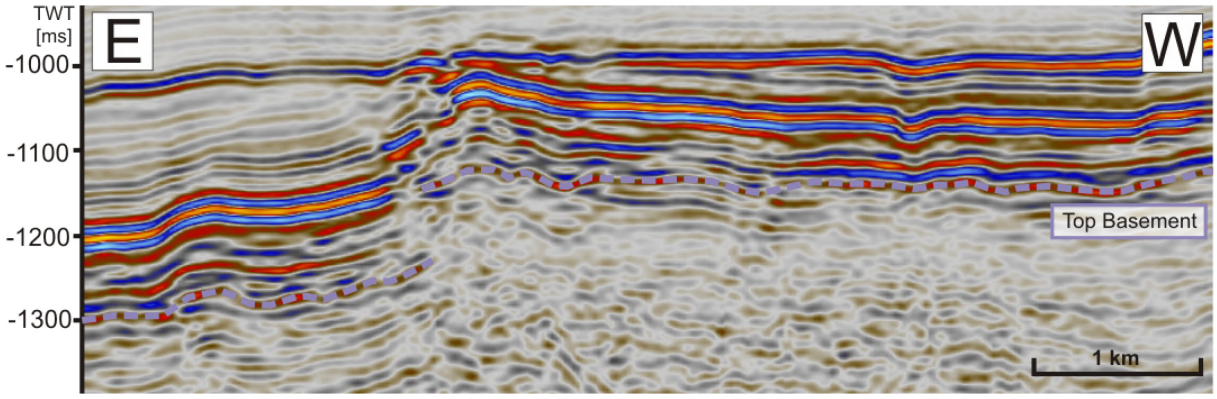

Fig. 15. E-W trending seismic profile displaying the Top Basement reflector in purple.

The unconformity separating the crystalline basement from the Jurassic sediments is not well resolved in the seismic data. Nevertheless top of the basement was interpreted as a reflector with a positive amplitude (peak, Fig. 15 and Fig. 16a). This reflector is warped, laterally not continuous, often chopped and therefore hardly traceable with an adequate reliability.

Top Jurassic

The Top Jurassic (Base Cenomanian) was defined as a trough by comparing well logs and 3D seismic data. The reflector Top Jurassic is defined by strong negative amplitudes, is easily traceable and covers the whole area of investigation (Fig. 16a). An angular unconformity between Jurassic and Cretaceous deposits, known from other parts of the Molasse Basin, is not apparent in the area of investigation.

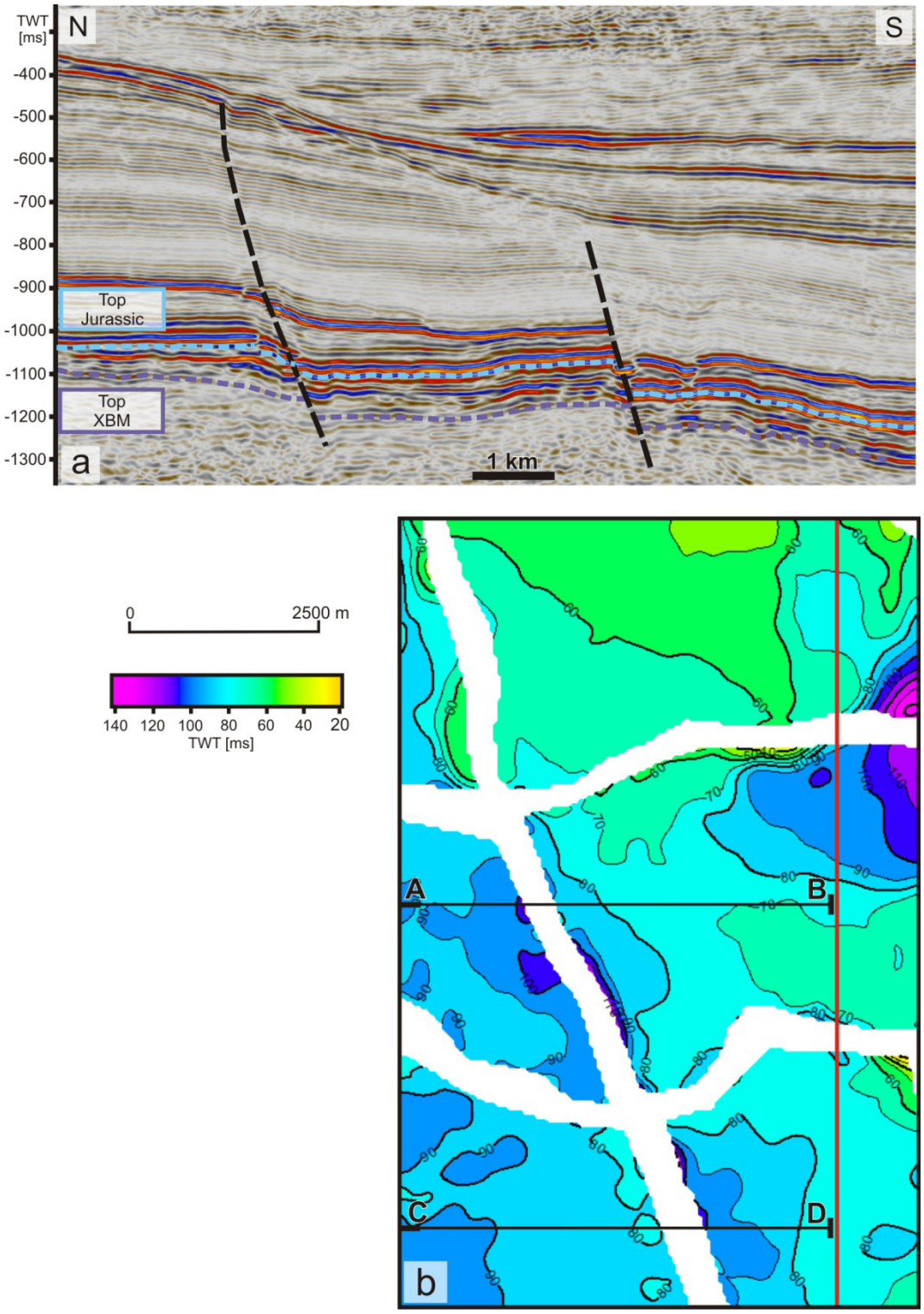

Fig. 16. **a) Seismic profile along the red line in Fig. 16b. The purple line represents the Top XBM reflector (Top Basement, Base Jurassic) and the blue line indicates the Top Jurassic (Base Cenomanian) reflector.**
b) TWT-thickness map of the Jurassic succession. Faults are whitened. A-B and C-D indicate the position of the seismic profiles in Fig. 17a,b.

TWT-thickness

As mentioned above, the definition of Base Jurassic is tentative so the TWT-thickness map in Fig. 16b should be interpreted with caution. The TWT-thickness map suggests that the Jurassic succession is rather uniform in thickness. It displays a general increase in thickness from NE to SW from 40 to 80 ms with an anomaly in the NE part exhibiting high thicknesses. However, it cannot be excluded that the thickness anomaly is due to erroneous mapping of Top XBM.

Seismic facies

Seismic facies of the Jurassic succession is laterally variable (Fig. 17). Intra-Jurassic reflection characteristics are ranging from continuous, low frequency, parallel and blurred reflectors in the S-parts (Fig. 17b) to laterally interrupted, in the N-part (Fig. 17a).

In the basal parts reflectors are sometimes wavy with reduced lateral continuity. The Jurassic consists of basal fluviatile and shallow marine sandstones succeeded by sponge bank, coral reefs and their debris deposited in high energy environments. These rocks are overlain by salt lagoon and tidal flat deposits (Wagner 1998). This variation in lithology and, thus, physical properties is reflected by an inhomogeneous and varying seismic facies.

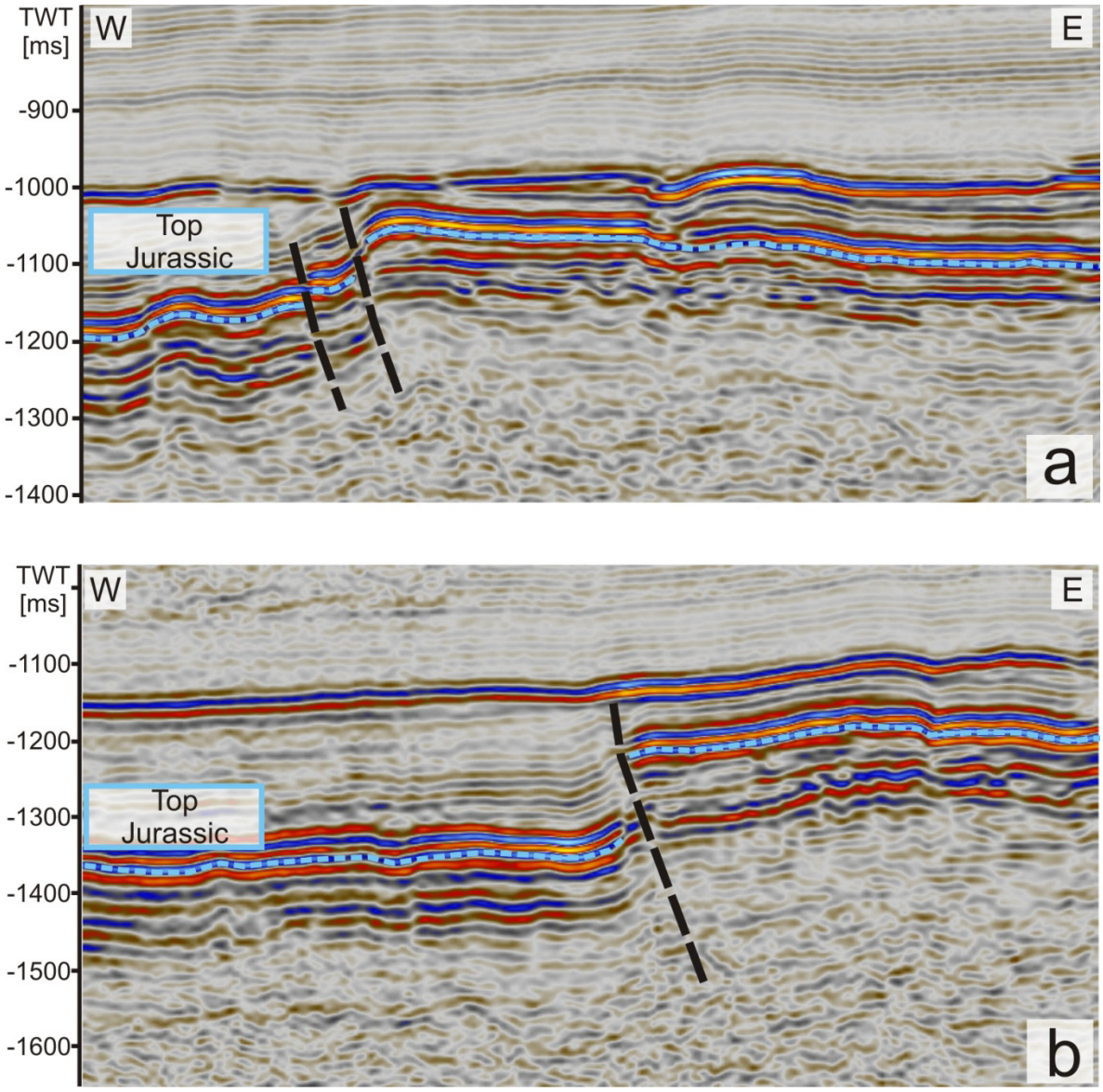

Fig. 17. Comparison of two W-E trending seismic profiles, highlighting the variable reflection characteristics of the Jurassic succession. Refer to text for explanation.

a) Northern seismic profile (A to B in Fig. 16b)

b) Southern seismic profile (C to D in Fig. 16b)

CRETACEOUS

Base Cretaceous
See Top Jurassic.

Top Cretaceous
The reflector Top Cretaceous (Base Eocene) is continuous, high in amplitude and is easily recognized by its unconformable relationship with the underlying Cretaceous rocks (Fig. 18a and Fig. 23). For further explanation see Base Eocene.

Fig. 18 provides a general overview of thickness and seismic facies of the entire Cretaceous succession, which will later be discussed in greater detail. The thickness distribution reflects a large-scale truncated anticline with an NW-SE trending axis. Thickness of the Cretaceous succession ranges from about 40 ms at the crest of the anticline to more than 200 ms in the SW part (Fig. 18b).

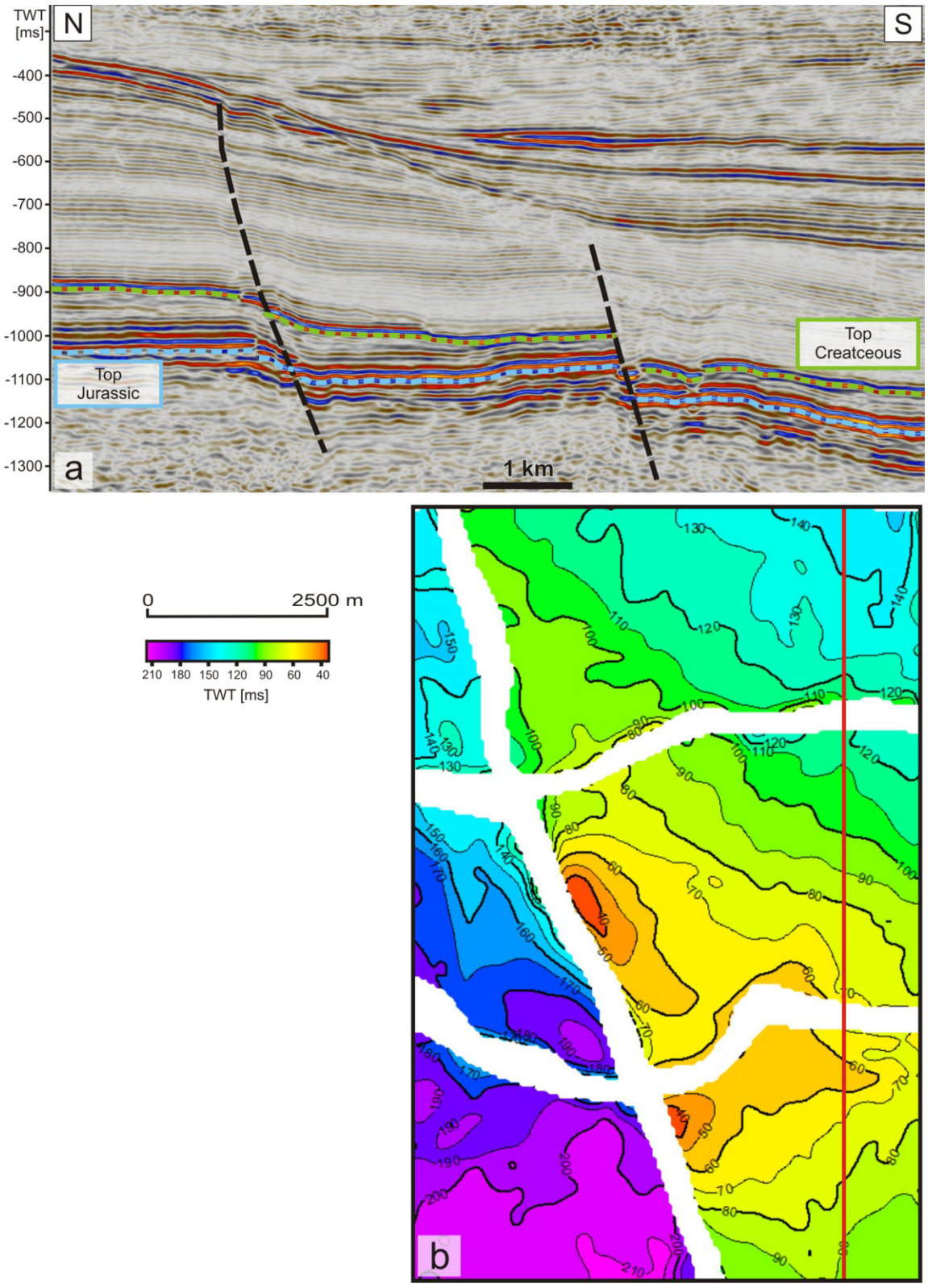

Fig. 18. a) Seismic profile along the red line in Fig. 18b. The blue line is the Top Jurassic (Base Cretaceous) reflector and the green line represents the Top Cretaceous (Base Eocene) reflector.
b) TWT-thickness map of the entire Cretaceous succession.

CENOMANIAN SUCCESSION

Base Cenomanian

The reflector Base Cenomanian (Top Jurassic) is defined by strong negative amplitudes, is easily traceable and covers the whole area of investigation (Fig. 19a and Fig. 20).

Top Cenomanian

The Top Cenomanian reflector is defined as a zero-crossing by synthetic seismograms. The reflector is well traceable throughout the entire seismic volume (Fig. 19a and Fig. 20).

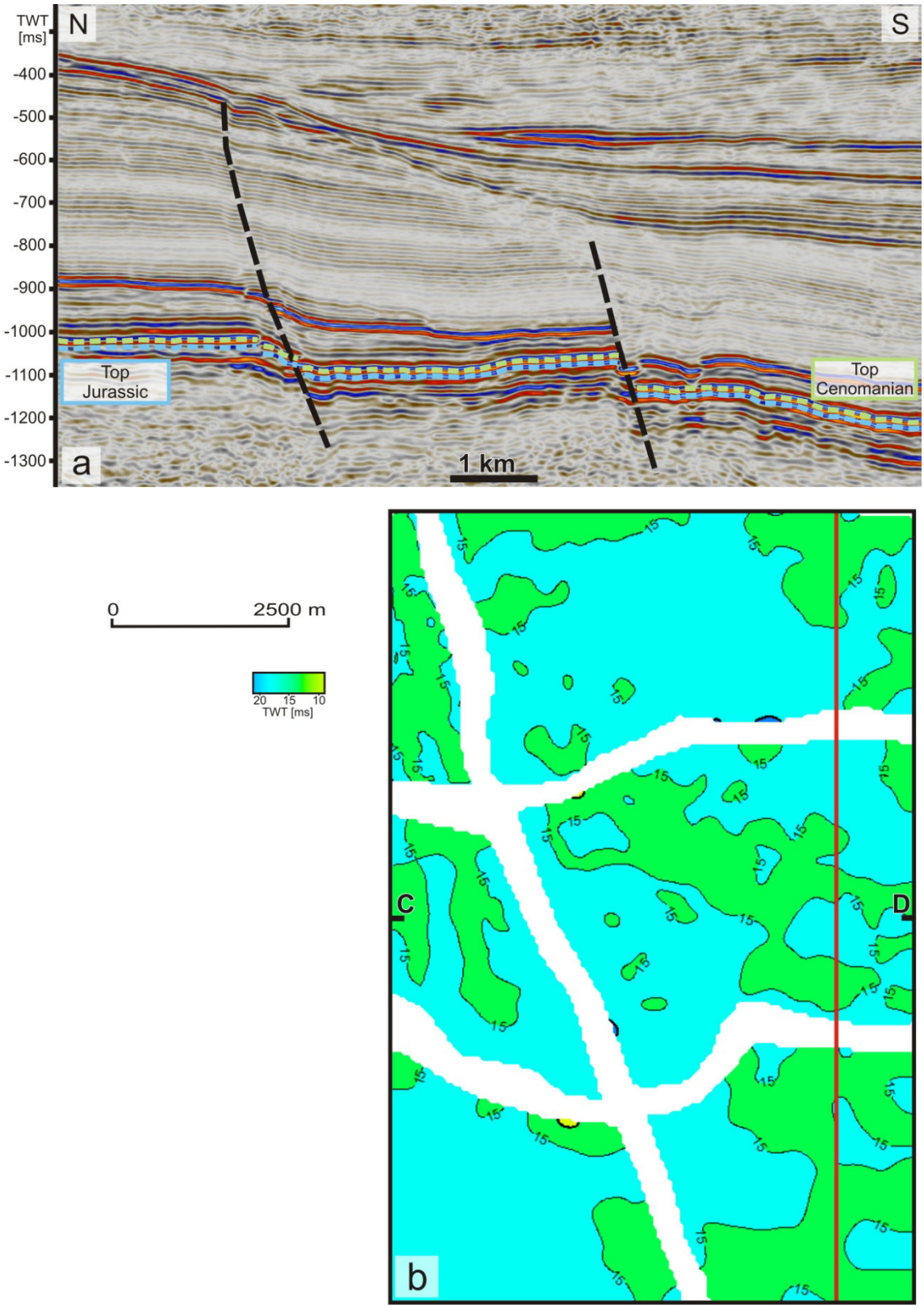

Fig. 19. a) Seismic profile along the red line in Fig. 19b. The blue line indicates the Top Jurassic (Base Cenomanian), light green line is the Top Cenomanian reflector.
b) TWT-thickness map of the Cenomanian deposits.

TWT-thickness

The TWT-Thickness of the Cenomanian succession is in the range of 10 to 20 ms (Fig. 19b) which equals roughly 15 to 35 m assuming an average velocity of 3500 m/s derived from well logs.

Seismic facies

Seismic facies is laterally uniform with parallel, continuous, high amplitude reflectors defining Base and Top Cenomanian and the only internal reflector (Fig. 20).

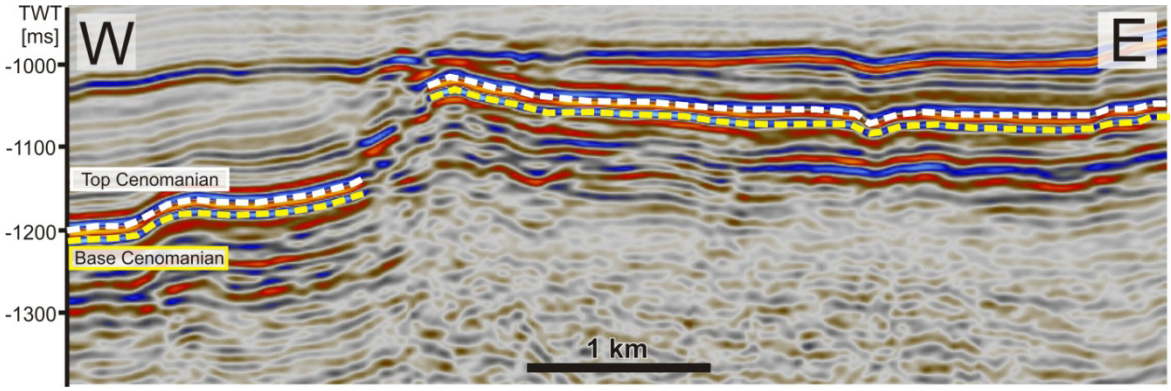

Fig. 20. Seismic section from C to D in Fig. 19. The yellow line is the Base Cenomanian (Top Jurassic) and the light yellow line is indicating the Top Cenomanian reflector)

Amplitude maps of Base Cenomanian did not show striking evidence for karstification of the underlying Jurassic carbonates, however karstification and infill of these karst structures by the Schutzfels Formation is well documented (e.g. Wagner 1996). The Schutzfels Formations infill karst structures up to 100 m deep with an unknown lateral extent. Thus large scale karstifications should be resolved in the seismic data, but could not be identified within the study area.

TURONIAN - SENONIAN

Base Upper Cretaceous (Top TRTNM)

The only Turonian reflector traceable throughout the seismic volume is the top Turonian shaly marl (Top TRTNM) reflector, defined by positive amplitudes and generally exhibiting a sharp, distinct peak (Fig. 21a). However it is not the actual top of the Turonian deposits. According to well logs these shaly marls are overlain by glauconitic sandstones which are not resolved on seismic data. Besides that, the Top TRTNM is well know and mapped in large parts of Upper Austria. It therefore represents an excellent Mesozoic marker horizon. The Top TRTNM is the base for the calculated Upper Cretaceous TWT-thickness.

In the Mesozoic succession of the Upper Austrian Foreland Basin the Cenomanian is overlain by Globotruncana marls and sandstones deposited during Early Turonian to Late Campanian times. Due to basin inversion during the Late Cretaceous and Early Paleocene, the above mentioned Upper Cretaceous strata became deeply eroded and are today unconformably overlain by Eocene sediments. This is exhibited by a major angular unconformity on seismic data (Fig. 21a).

On the crest of the anticline structure, erosion cut down into Turonian rocks deeply truncating Campanian, Santonian and Coniacian strata in a wide area around the crest (Fig. 21a and Fig. 21b). This makes it difficult to map and identify other, stratigraphically higher, Cretaceous reflectors.

Top Upper Cretaceous

The Top of the Upper Cretaceous succession is the Top Cretaceous (Base Eocene) reflector. For explanations refer to Base Eocene.

TWT-thickness

Fig. 21b shows the TWT-thickness between the Top TRTNM and Top Cretaceous. The greatly reduced thicknesses in the central part of the map are due to profound erosion.

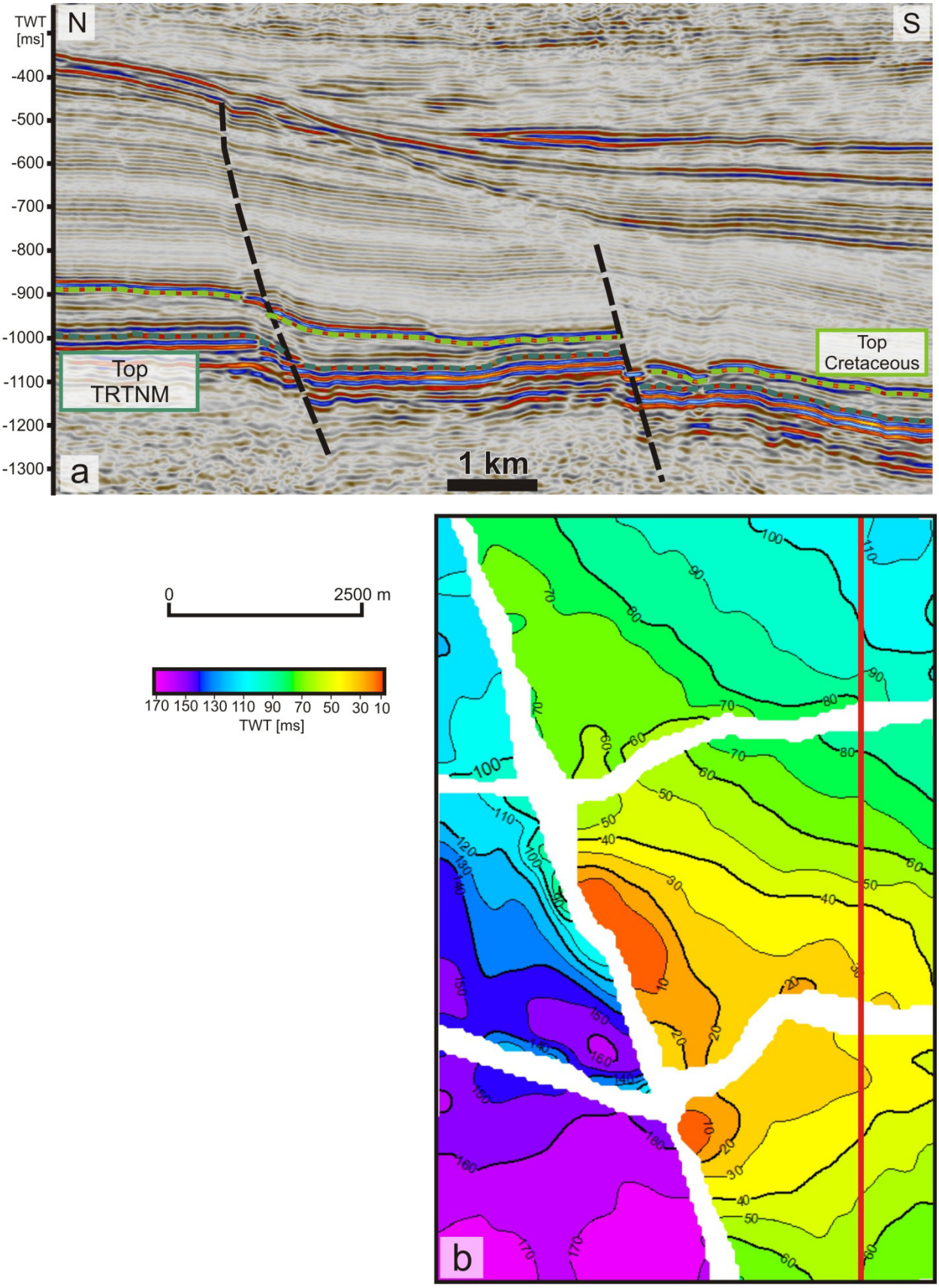

Fig. 21. **a) Seismic profile along the red line in Fig. 21b. The dark green line is the Top TRTNM (Turonian shaly marls) reflector and the light green line indicates the Top Cretaceous (Base Eocene) reflector.**
b) TWT-thickness map of the Upper Cretaceous, calculated between Top TRTNM and Top Cretaceous.

Thicknesses range from 0 ms at the crest of the anticline to more than 160 ms in SW-part (Fig. 21b). Again the figure stresses that Mesozoic TWT-thicknesses are greater on the western side of the NNW-SSE trending fault. Generally they are increasing from the north to the south.

Seismic facies

Internal Upper Cretaceous reflectors are stacked parallel with lower amplitudes than Cenomanian or Turonian ones (Fig. 21a). The frequency (number of reflectors per unit time) is generally increasing from the crystalline basement to the Top Mesozoic. If present, the reflectors are continuous and traceable but difficult to correlate with a specific stratigraphic unit, because of missing well information. This is because most wells drilled the anticline structure, where the uppermost Cretaceous layers are not preserved.

CENOZOIC

EOCENE AND LOWER OLIGOCENE

There is no Paleocene sedimentary record and the oldest Cenozoic sediments in the Molasse Basin are of Late Eocene age. Eocene sediments comprise the terrestrial Limnic Series followed by Cerithian Beds and Lithotamnium Limestone.

Base Eocene

The Base Eocene (Top Cretaceous) reflector is, as described before, continuous, high in amplitudes and is easily recognized by the unconformable relationship between the underlying Cretaceous and overlying Eocene rocks (Fig. 22a).

The relief map (Fig. 23) of the base Eocene surface displays patterns possibly linked to erosional processes (mass slides) within the Eocene/Lower Oligocene succession. Fault scarps are visible in the NW- and central part of the map.

Top Lower Oligocene

The top of the Lower Oligocene is defined by the Base Puchkirchen Formation (Base PF) reflector, which was identified using well tops and synthetic seismograms (Fig. 22a).

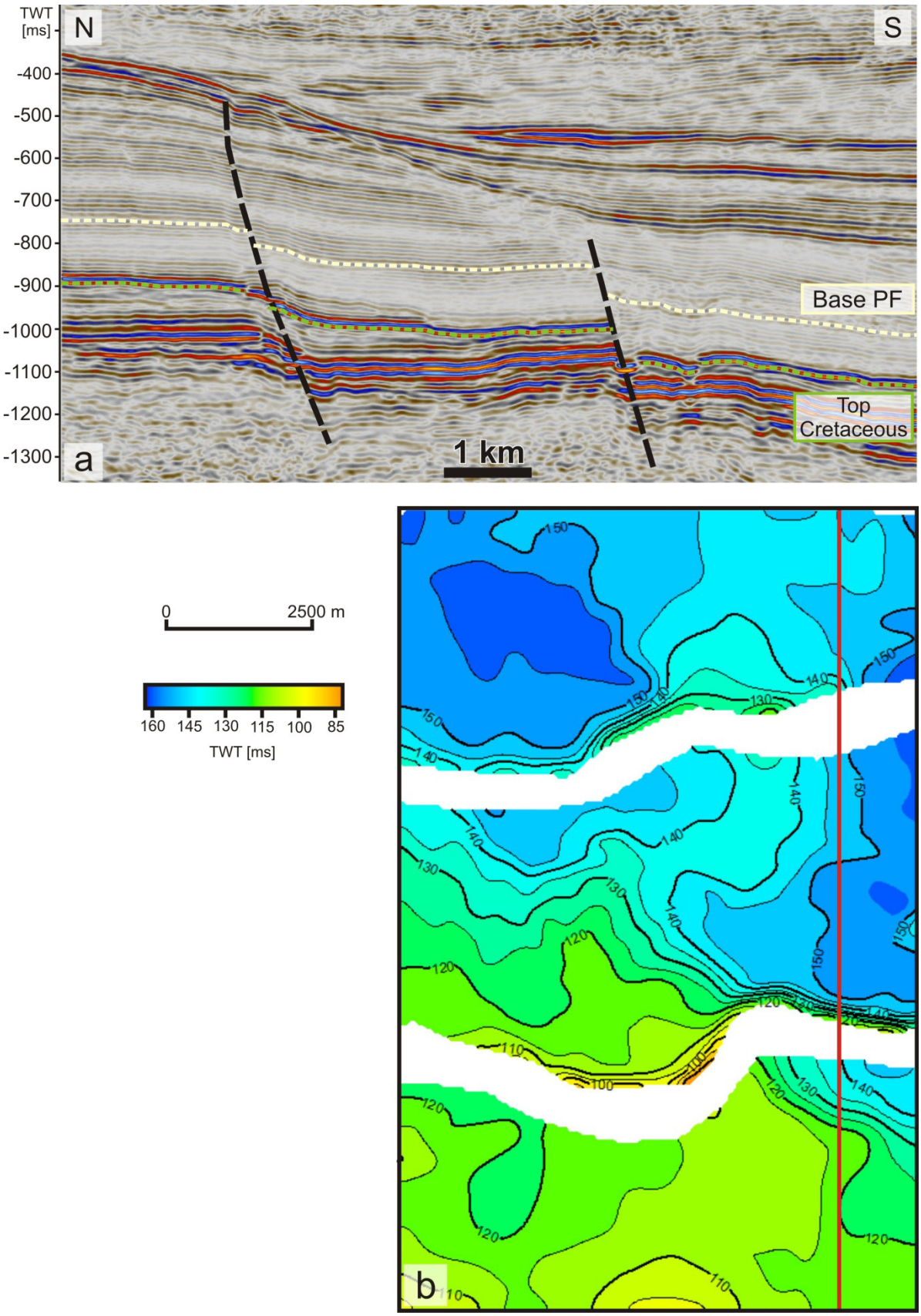

Fig. 22. **a) Seismic profile along the red line in Fig. 22b. The green line is the Top Cretaceous (Base Eocene) reflector and the light yellow line indicates the base of the Puchkirchen Formation (Base PF).**
b) TWT-thickness map of the Lower Oligocene sediments.

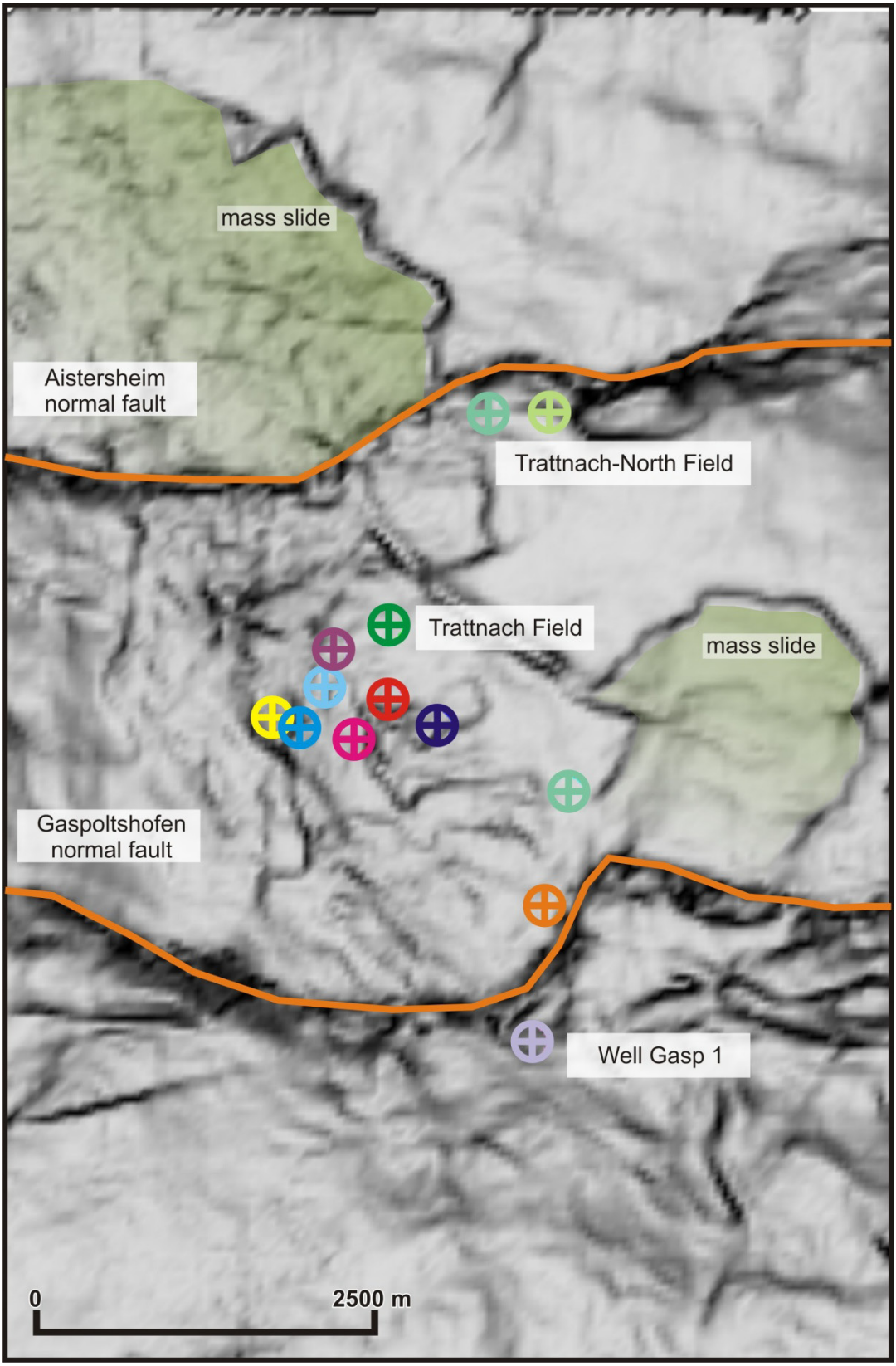

Fig. 23. Base Eocene relief map. Coloured circles are indicating well positions. The Trattnach and Trattnach North fields and the well Gaspoltshofen 1 (Gasp 1) are labeled. Mass slides are visible in the central eastern part and in the north-western parts of the map. E-W trending normal faults are indicated by orange lines.

TWT-thickness

TWT-thickness of the Lower Oligocene is in the range between 100 and 160 ms (Fig. 22b) with decreasing thicknesses from N to S and highest values in the north-western and the central eastern part.

Seismic facies

The seismic facies of the Lower Oligocene can be described as a set of laterally parallel layers with reduced amplitude and rather continuous spatial extension. Additionally reflectors are sometimes blurry and often truncated (Fig. 22a).

In the study area, the Lower Oligocene succession is characterized by the deep marine deposits of the Schöneck, Dynow, Eggerding and Zupfing formations.

The lower Oligocene is dominated by deep erosion of bottom currents followed by rapid sedimentation of slide material, turbidites and reworking of the sediment (Schulz, et al. 2002). These processes are visible in seismic sections and have been studied previously (Sachsenhofer and Schulz 2006, Sachsenhofer, Leitner, et al. 2010)

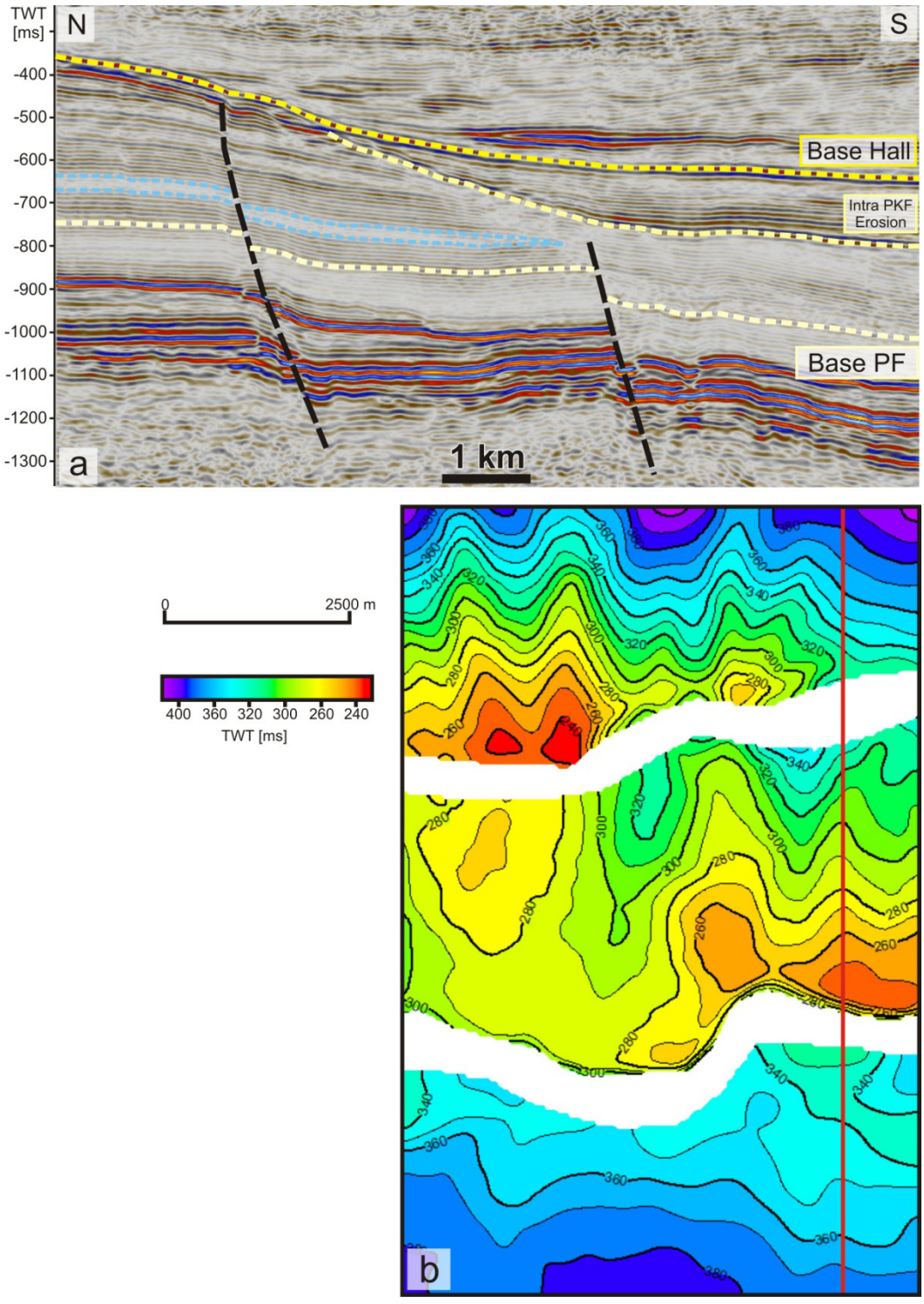

Fig. 24. a) Seismic profile along the red line in Fig. 24b. Light yellow line is the Base Puchkirchen Formation (Base PF) reflector; blue lines indicates a "wedge", capped by the intra Puchkirchen Formation erosional surface (intra PKF erosion) and the yellow line indicates the Base Hall Formation (Top PKF).
b) TWT-thickness map of the (Lower and Upper) Puchkirchen Formation.

The Late Oligocene to Early Miocene Puchkirchen Formation is characterized by a thick succession of gravity-flow deposits mainly consisting of sandstones.

Base Puchkirchen Formation

See Top Lower Oligocene.

Top Puchkirchen Formation

The Top Puchkirchen Formation (Base Hall) is represented by a reflector deeply truncating the upper parts of the Puchkirchen Formation (Fig. 24a).

Thus the reflector associated with the top of the Puchkirchen Formation is mapable throughout the seismic cube. It was identified as a trough (negative amplitudes) by matching well tops, synthetic seismograms and the seismic volume.

In Fig. 39 the map of the top of the Puchkirchen Formation is showing increasing TWT from N to S in a range between 340 to 620 ms. Fig. 39 provides of a relief map with superimposed TWTs. It depicts the erosional nature of this surface by indicating N-S trending canyons.

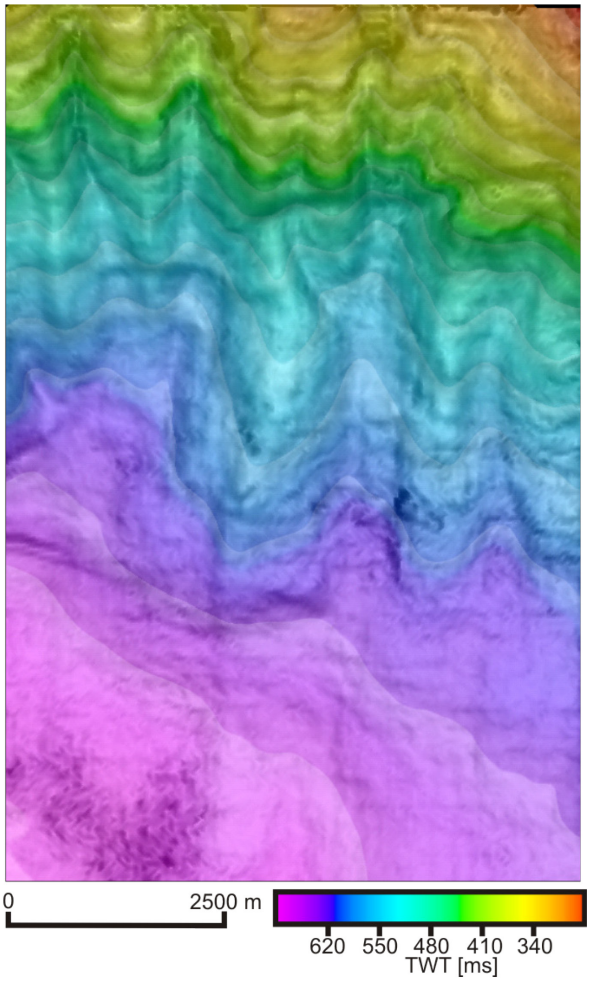

Fig. 25. Top Puchkirchen Formation (Base Hall) reflector. Displayed is a relief map with superimposed TWTs.

TWT-thickness

The TWT-thickness map in Fig. 24b is showing thicknesses generally between 250 and 400 ms with reduced thicknesses in the central part. Areas of significant erosion are identified by reduced thicknesses (Fig. 24b).

Intra-Puchkirchen Formation erosion

Besides this, there is also an intra-Puchkirchen Formation erosional surface visible in Fig.

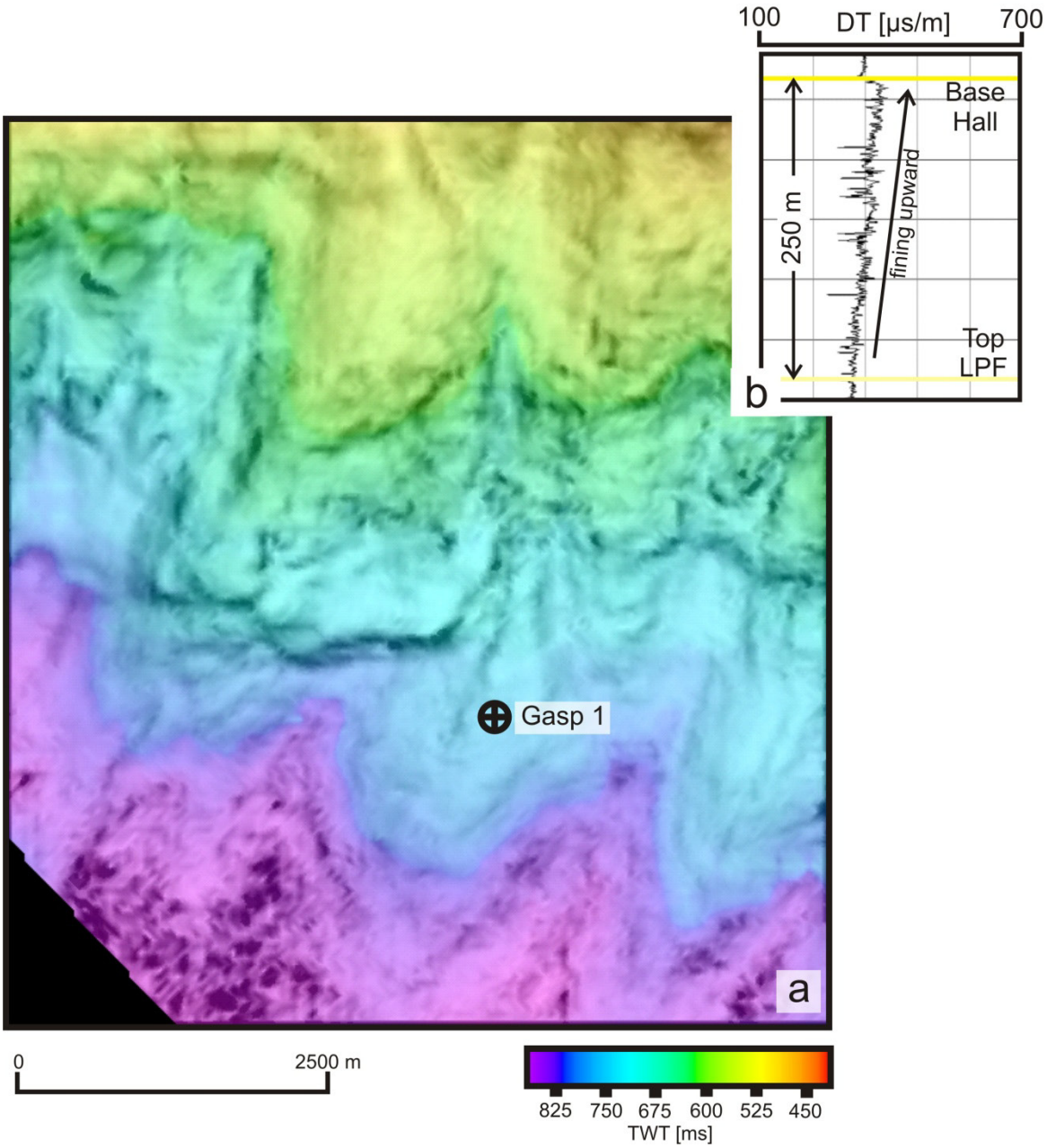

Fig. 26. **a) Intra Upper Puchkirchen Formation erosional surface displayed as a relief map with TWT overlay.**
b) DT log (in µs/m) of well Gasp 1 between the top of the Lower Puchkirchen Formation (Top LPF) and the base of the Hall Formation (Base Hall) is. See map for position of well Gasp 1.

24a represented by the reflector sharply cutting into Upper Puchkirchen sediments in the S-part of the seismic line.

The TWT-depth of the Intra Upper Puchkirchen Formation increases from N to S from 450 and to than 800 ms (Fig. 26). The Puchkirchen Formation consists, as previously mentioned, of deep marine gravity flow deposits. In Fig. 26 N-S trending canyons with sediment accumulation near the southern end of the canyons are visible. The transport direction of these sediments is roughly perpendicular to the main W-E transport of the Puchkirchen Formation. The surface is not affected by E-W trending faulting.

The DT log in Fig. 26 indicates an upward increase in travel-times indicating a fining upward trend within the Upper Puchkirchen Formation.

Seismic facies

The seismic facies suggests a tripartition of the Puchkirchen Formation (Fig. 24a). A lower part is characterized by parallel reflectors, which are sometimes blurry in the southern part of the study area. This part conformably overlain by a wedge with low amplitude reflectors. This wedge is pinching out towards the south and is therefore not present in the whole study area. The upper part of the Puchkirchen Formation is formed by a succession parallel reflectors forms the top of the Puchkirchen Formation. This succession is truncated in the south by the intra-Puchkirchen Formation erosion and by base reflector of the Hall Formation.

DEFORMATION STRUCTURES AND FAULT INVENTORY

MESOZOIC FAULT SYSTEMS

In Fig. 27 the relief map of the Top Cenomanian reflector is shown. It displays various patterns related to fault systems and deformation structures. The main structure is a NNW-SSE trending reverse fault (Trattnach reverse fault), which is discussed in the section dealing with Paleocene deformation structures.

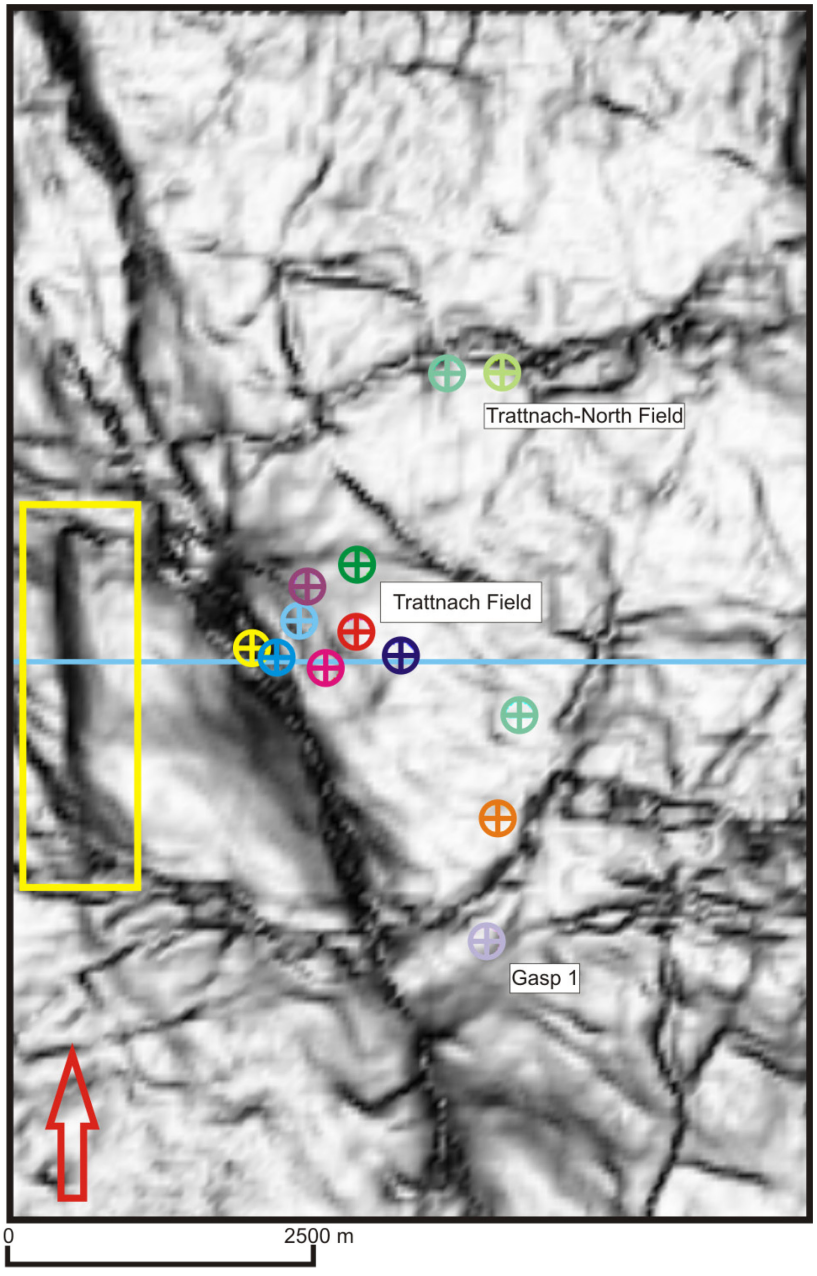

Fig. 27. Relief map of Top Cenomanian. Wells are indicated by circles; Yellow rectangle shows the location of a N-S trending bulge discussed in the text; Blue line shows the position of the seismic line displayed in Fig. 28.

The N-S trending bulge highlighted by the yellow rectangle in Fig. 27, Fig. 28 and Fig. 29 is about 3 km long and roughly 500 m wide and some tens of meters high. The western flank of the bulge is steeper than the eastern flank and is bordered by a reverse fault.

Top TRTNM is the uppermost folded reflector, hence it is the last reflector which was affected by the deformation process. In Fig. 29 indications for onlaps on the bulge from E and W are visible. The onlapping reflectors are overlain by a continuous reflector with a negative amplitude (blue).

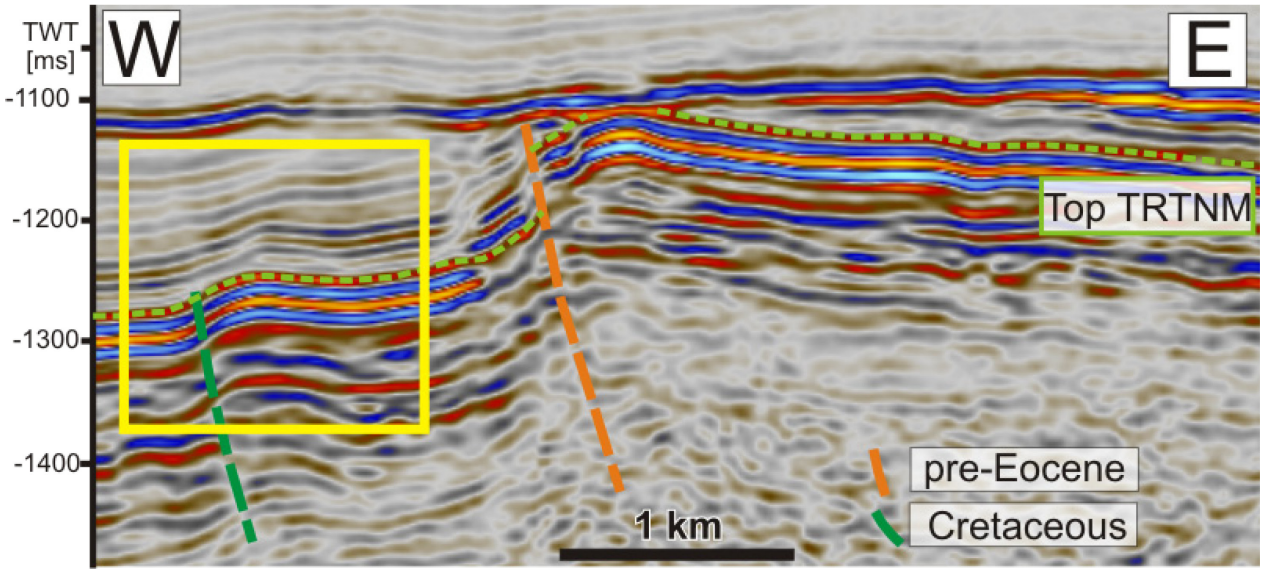

Fig. 28. W-E profile along the blue line in Fig. 27. The yellow rectangle indicates the location of the bulge.

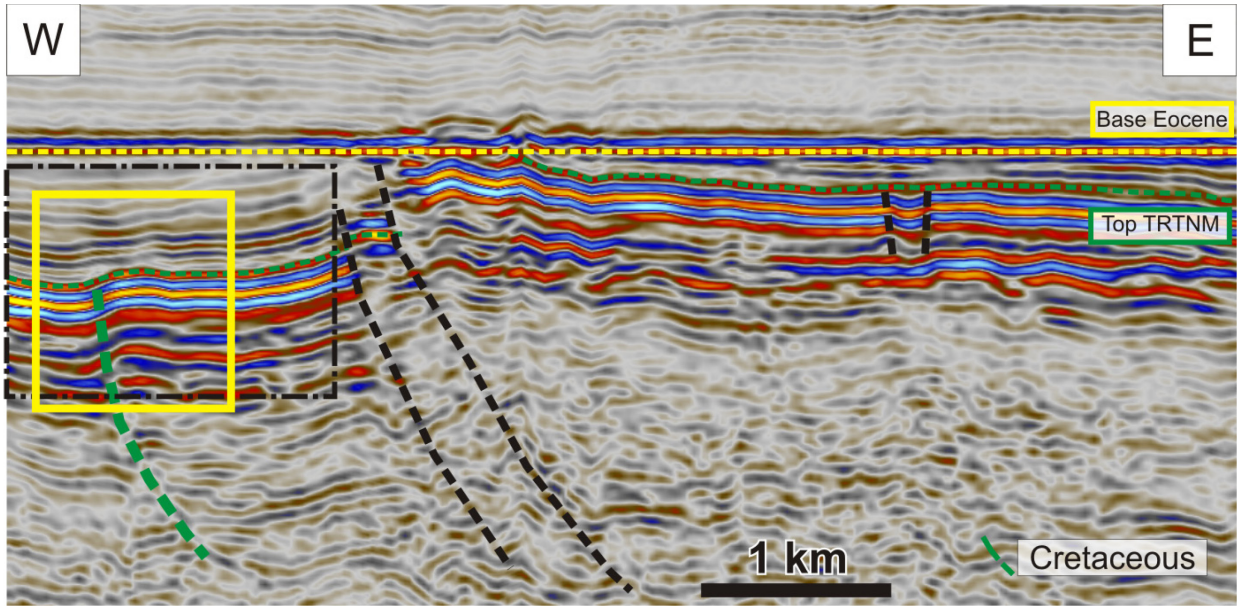

Fig. 29. Profile flattened on Base Eocene, about the same location as the section shown in Fig. 28. Black rectangle is the outline of Fig. 30.

The timeframe for this deformation phase is constrained by the above mentioned indications. Since Top TRTNM is continuous and overlain by onlapping strata (see Fig. 30) the bulge is interpreted to have formed during Late Turonian to Early Coniacian times.

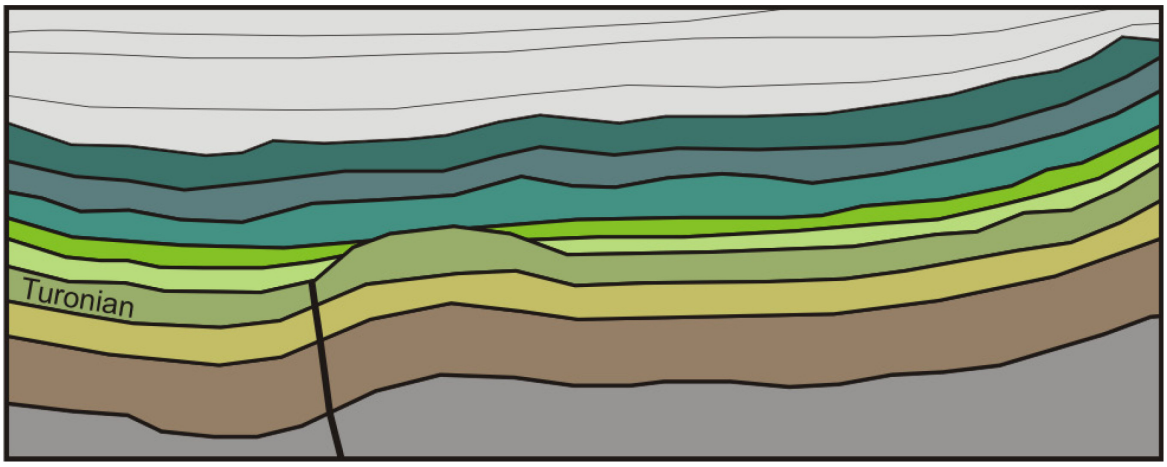

Fig. 30. Sketch showing the interpretation of the western part of the seismic line displayed in Fig. 29 (see black stipple-dotted rectangle in Fig. 29).

From the map in Fig. 27 it is obvious that there are no other strictly N-S trending deformation structures present in the part east of the NNW-SSE trending Trattnach reverse fault.

A similar intra-Upper Cretaceous bulge is also present in the northern part of the study area but here it is NNW-SSE trending.

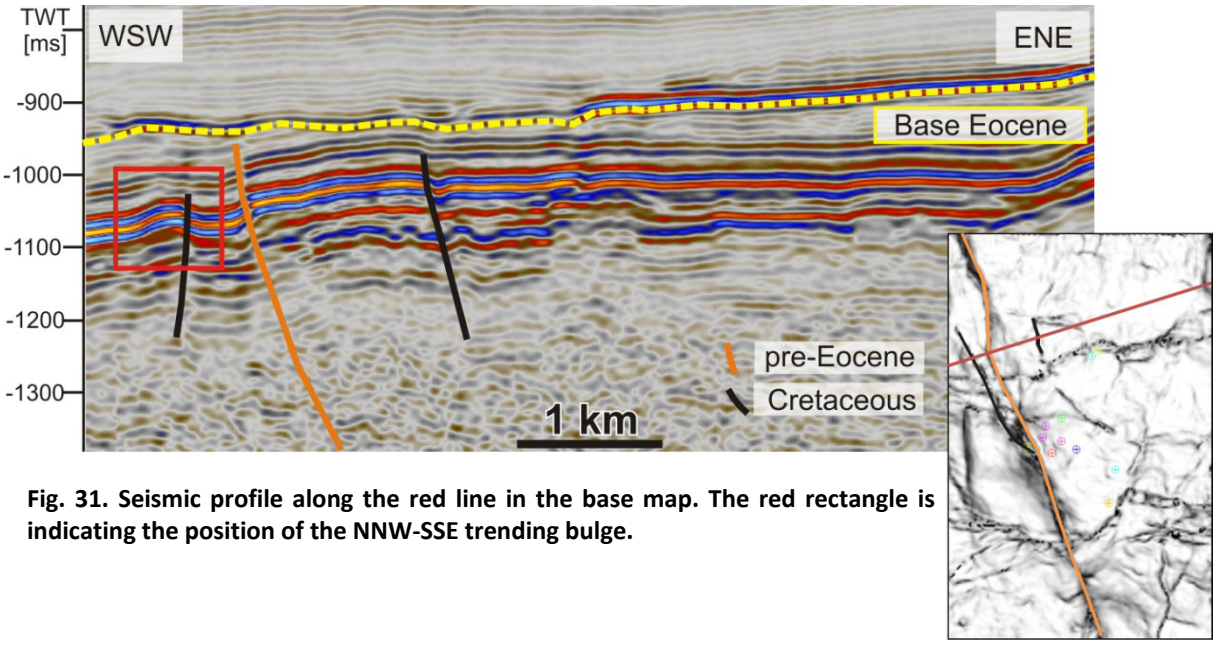

Fig. 31. Seismic profile along the red line in the base map. The red rectangle is indicating the position of the NNW-SSE trending bulge.

In Fig. 31 the bulge is located in the WSW-part of the seismic line. It is confined by a reverse fault to the east. The two Cretaceous faults (Fig. 31) are associated with the deformation event which triggered the evolution of the NNW-SSE trending bulge.

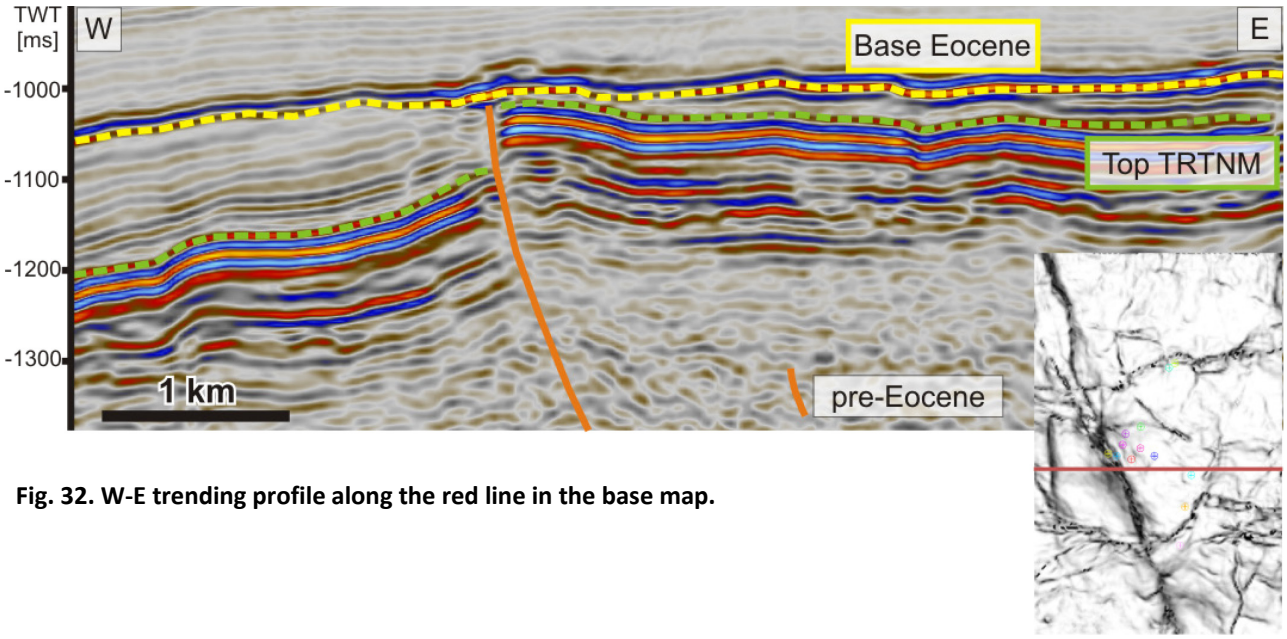

Fig. 32. W-E trending profile along the red line in the base map.

The dominant fault zone in the study area is the NNW-SSE trending Trattnach reverse fault displayed in Fig. 32. It extends through the whole area of investigation separating the western, deeper parts, from the east. This steep reverse fault is limiting the Trattnach mega-anticline (Fig. 33) to the W.

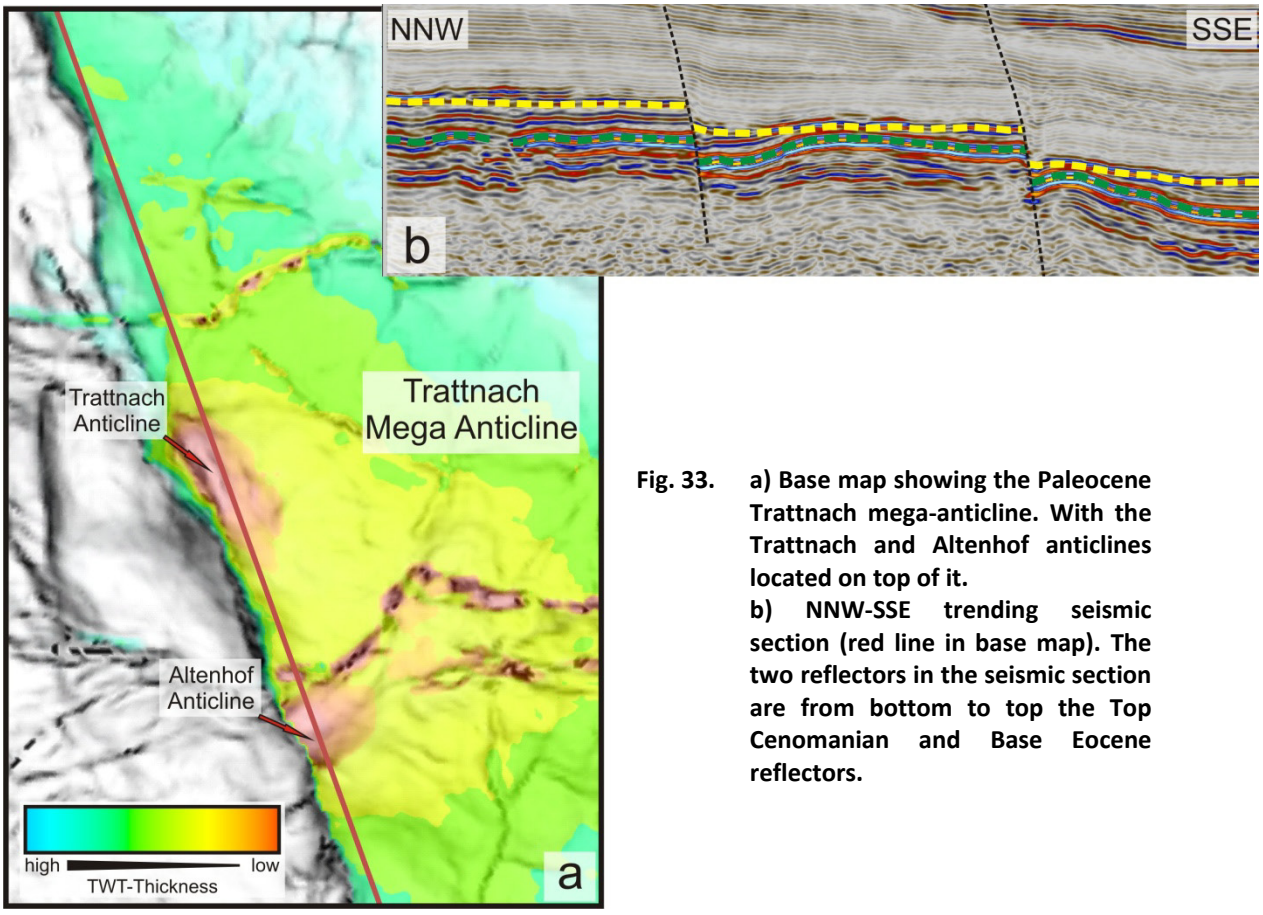

Fig. 33. **a) Base map showing the Paleocene Trattnach mega-anticline. With the Trattnach and Altenhof anticlines located on top of it.**
b) NNW-SSE trending seismic section (red line in base map). The two reflectors in the seismic section are from bottom to top the Top Cenomanian and Base Eocene reflectors.

The throw of the NNW-SSE trending Trattnach reverse fault is increasing from N-S from 40 to 100 ms two-way-travel time (about 50 to 200 m).

Along with the Trattnach reverse fault associated structures were developed. These structures have been apparently reactivated during the Cenozoic as normal faults. In Fig. 34 a reactivated fault is shown. It is situated to the NE of the Trattnach reverse fault. This specific fault is acting as a pressure barrier during oil production separating the Trattnach field from the Trattnach North field.

In Fig. 33a the Trattnach mega-anticline which evolved during the Paleocene is shown. The crests of it are coloured red because there the TWT-Thickness between top Cenomanian and base Eocene (respectively the green line and yellow line in Fig. 33b) is greatly reduced. The anticline has got two crests. The northern one, the Trattnach anticline hosts the Trattnach oil field. The southern one, termed here the Altenhofen anticline, was previously unknown. Unfortunately the structure seems to be open to the NE, at least in TWT. Therefore additional investigations are needed in order to determine

whether the anticline is closed. Interestingly, amplitude maps of the Cenomanian show anomalous high amplitudes in this area.

Precisely determining the time span for this deformation event is challenging, because the Late Cretaceous and Early Cenozoic was affected by uplift and intense erosion. Due to the formation of the anticline, erosion was greater E of the reverse fault. Thus sediment thicknesses in the W-part are higher. Unfortunately no wells were drilled within the W-part so no well tops exist, which would help in identifying single reflectors.

W of the reverse fault, Coniacian and Santonian, possibly even younger Cretaceous rocks are preserved. At the more elevated parts of the anticline erosion cut down into Turonian sediments whereas W of the Trattnach reverse fault Coniacian strata are still present (Fig. 32). Since Maastrichtian and Danian sedimentary records are missing all over the area and Mesozoic sediments of different age are unconformably overlain by Eocene rocks, a Late Cretaceous (Maastrichtian?) to Paleocene time for this deformation event is suggested.

Moreover it cannot be excluded that the Maastrichtian?/Paleocene deformation reactivated structures, which were formed during the Turonian and Coniacian, but this is not documented in the study area.

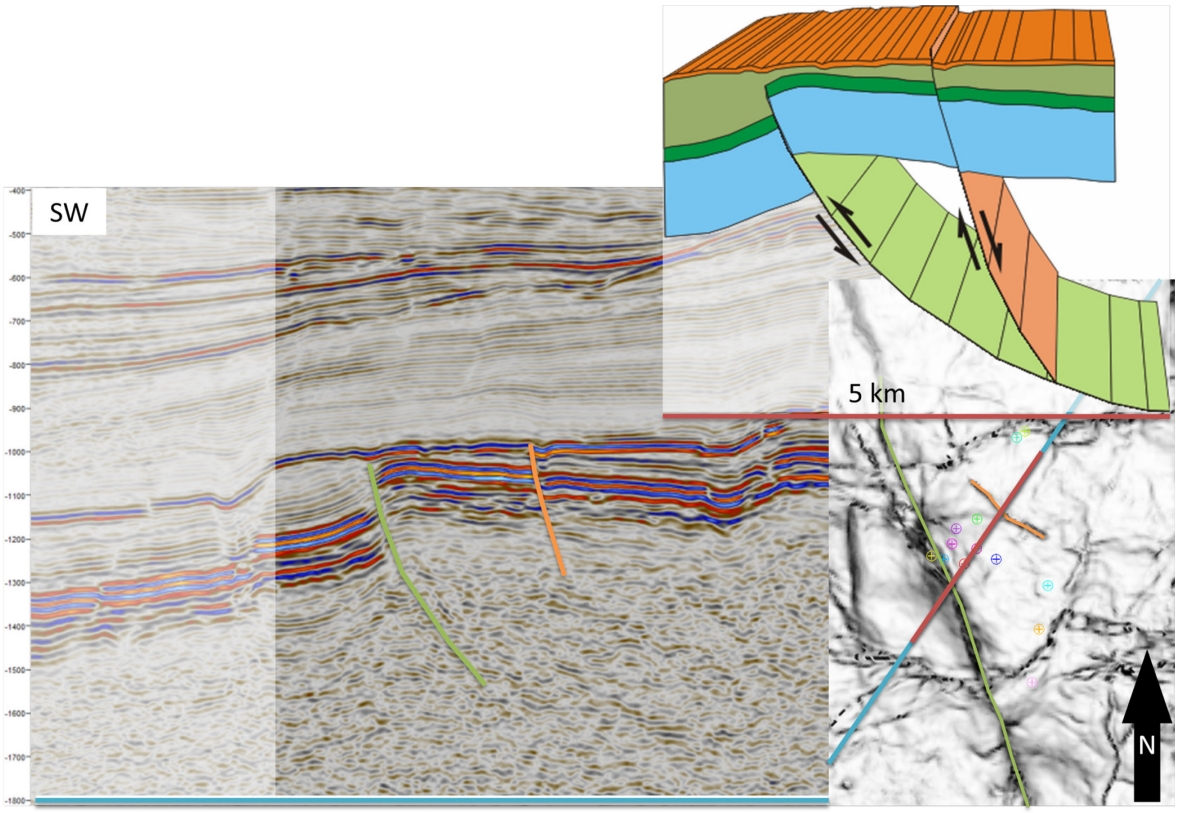

Fig. 34. Wrap up of the Late Cretaceous to Early Paleocene evolution. A random line oriented SW-NE (see base map, bottom right) with a length of about 10 km is displayed. The pre-Eocene Trattnach reverse fault in green and another reverse fault in orange are shown in the seismic profile. The orange reverse fault was reactivated during Eocene/Early Oligocene times.
Top right: Sketch of the deformation interpreted from the seismic section. In the shaded area the seismic line is crossing through a fault zone.

CENOZOIC FAULT SYSTEMS

The Cenozoic deformation is dominated by the formation of E-W trending normal fauls and reactivation of older fault systems. The northern fault is called Aistersheim normal fault, the southern one is termed Gaspoltshofen normal fault. Both fault zones exhibit a main S-dipping fault plane and a generally subordinate N-dipping fault plane. The development of these structures was triggered by flexural down-bending of the foreland crust due to the advancing Alpine nappe system from the Late Eocene and Early Oligocene times onwards. Tensional forces were accommodated by S- and N-dipping normal faults between the earliest Oligocene and late Egerian times. Frequently normal faults are observed, which do not fit to the predominantly E-W trending direction. These faults can be crescent shaped. Moreover graben structures are visible.

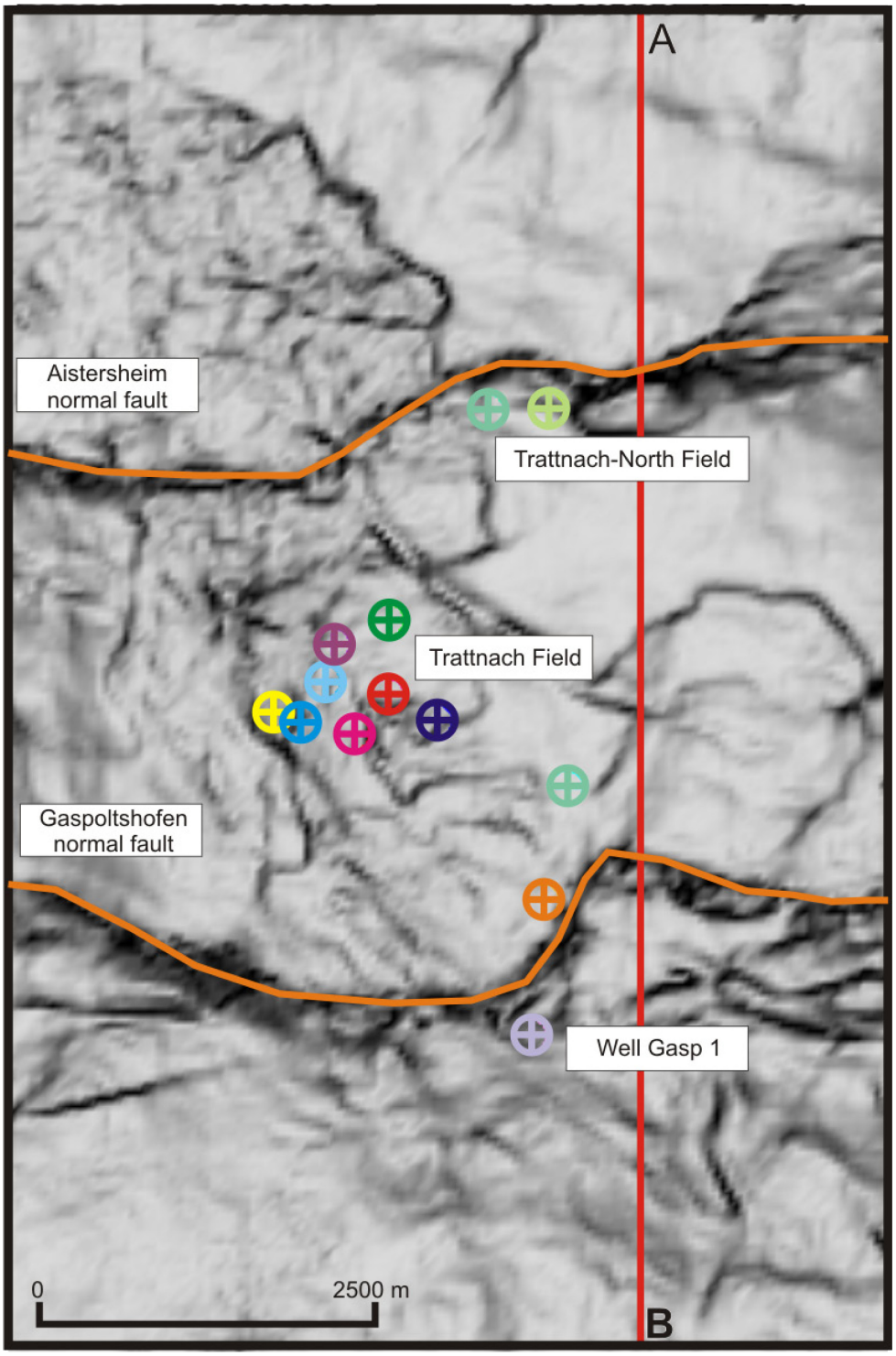

Fig. 35. Base Eocene surface relief map. Major Cenozoic normal faults are highlighted in orange.

In Fig. 35 the E-W trending faults are visible along with erosional patterns. These erosional patterns in the central and NW-part of the map are not initially linked with faulting but seem to represent the remnants of mass slide events during the Early Oligocene (Sachsenhofer, Leitner, et al. 2010).

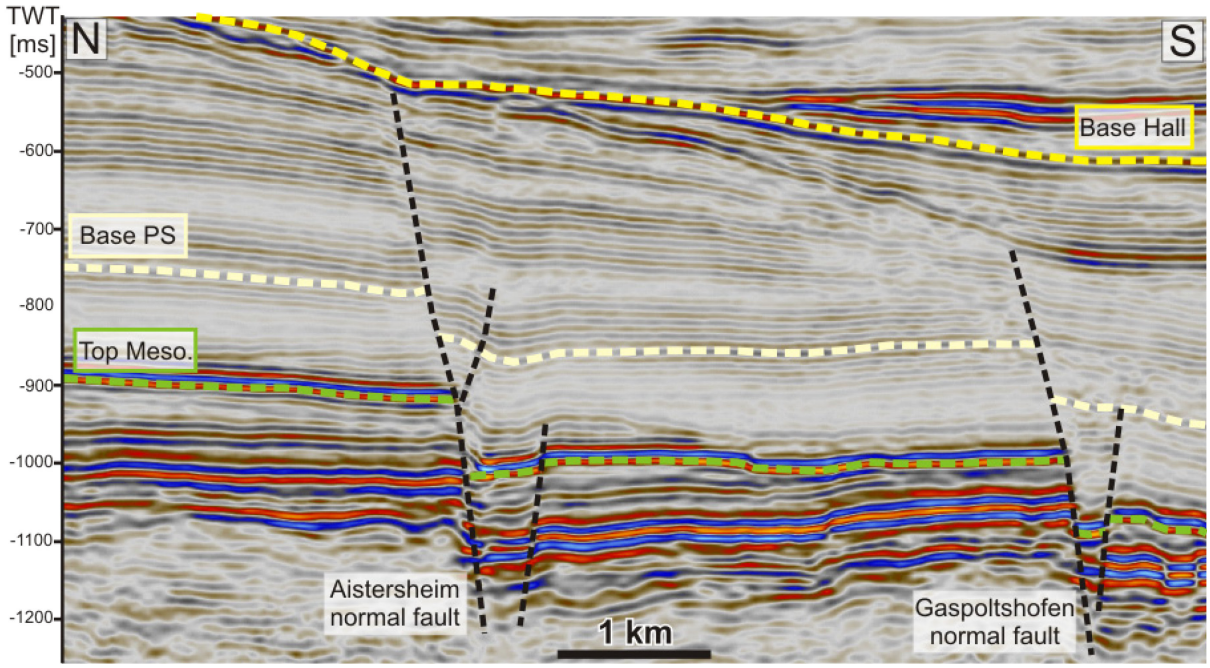

Fig. 36. N-S trending profile along the red line in Fig. 35. The Aistersheim and Gaspoltshofen normal fault systems are shown.

Initial activation of N- and S-dipping faults occurred contemporaneously. Later predominately the N-dipping faults died out, whereas the S-dipping faults remained active until the end of the Egerian. This is evident by the increasing throw from top to bottom (Fig. 37).

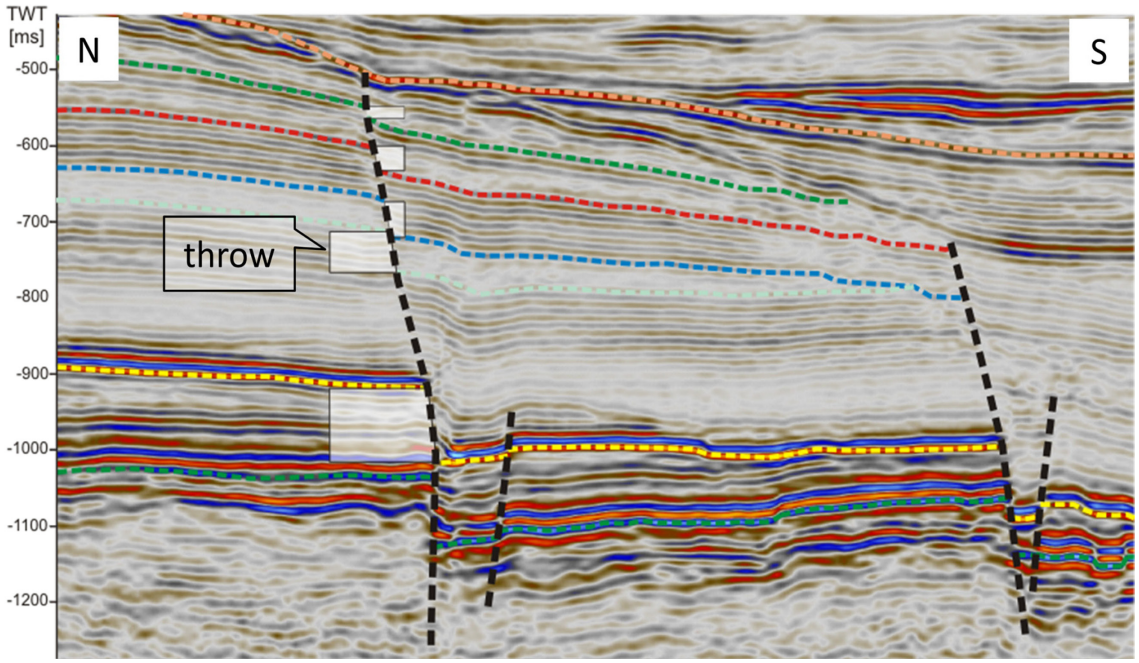

Fig. 37. Evolution of the Aistersheim normal fault. Initially the N- and S-dipping faults were activated contemporaneously during the earliest Oligocene. The continuing activity of the S-dipping faults until the end of Egerian is indicated by the increasing throw from top to bottom. A similar mechanism is assumed for the Gaspoltshofen fault system.

Branch faults associated with S-dipping normal faults are common and observed throughout the area of investigation.

Due to the multi-stage deformation of the Upper Austrian Molasse Basin, faults were frequently reactivated. Faults created during the Mesozoic, mainly as reverse faults, were reactivated during the extensional phase in the Cenozoic. This is important for the understanding of Cenozoic fault patterns. Many directions of faulting are predetermined. An example is the Gaspoltshofen Fault with its distinct S-shape in the central part. S shaped normal faults are rather unusual but having a look on a seismic line oriented perpendicular to the structure the fault seems to be just an ordinary one. In fact the direction is determined by Riedel and Anti-Riedel shears formed in the Mesozoic/Paleocene. These weakened zones were reactivated during Cenozoic normal faulting. Another example is the orange coloured fault in Fig. 34 emphasizing the importance of previously deformed areas in explaining the dynamic evolution of fault systems.

CENOZOIC BLOCK ROTATION

Another feature visible within the Puchkirchen Formation is apparent block rotation (tilting) in the central part of Fig. 38.

Carefully observing reflectors “a” and “b” (the two blue lines), an angular unconformity within the deposits of the Lower Puchkirchen Formation becomes visible. In the N-part of Fig. 38 the Base Puchkirchen, reflector “a” and reflector “b” are parallel. In the central part reflector “a” and “b” are forming a wedge with southward decreasing thickness and finally reflector “b” is truncating reflector “a”. Whereas S of the normal fault all three reflectors are again parallel. This suggests that reflector “a” was truncated after the block rotated/tilted to the NW and was subsequently overlain by the sediments above reflector “b”.

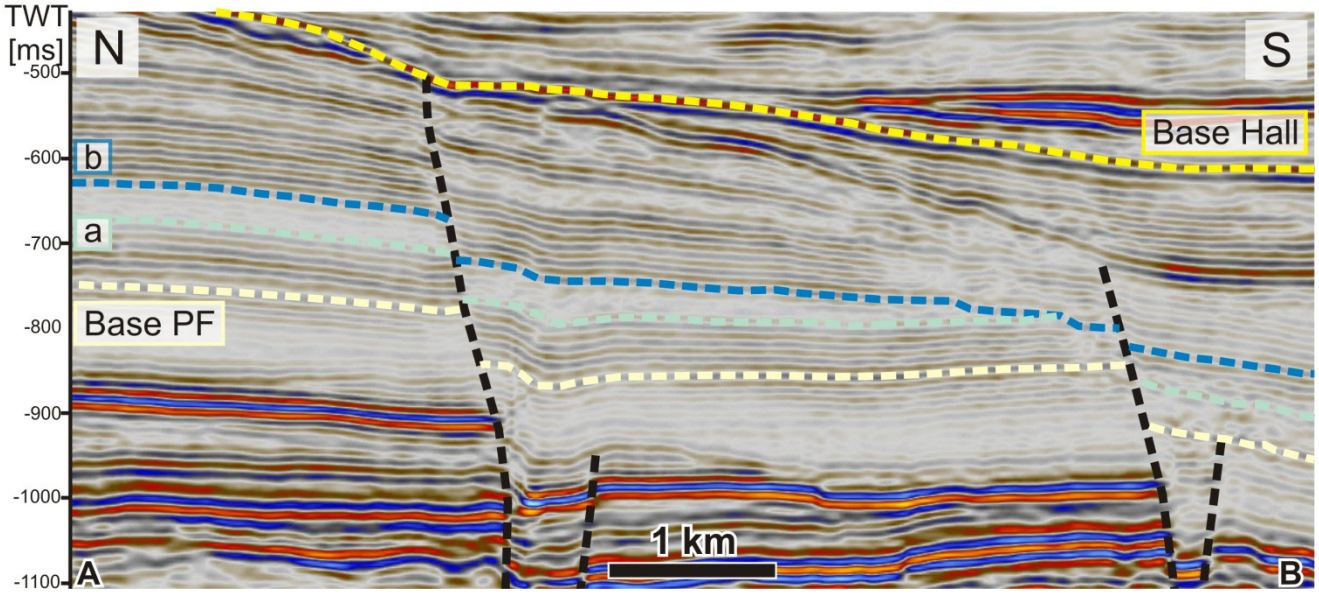

Fig. 38. N-S trending seismic profile. Light yellow line is Base Puchkirchen Formation, the light blue line is reflector "a" and the dark blue line is reflector "b".

Fig. 39 shows a TWT-thickness map of the sediment package bounded by the intra-Puchkirchen Formation reflectors "a" and "b" (Fig. 38). In general TWT-thickness decreases from N to S. Fig. 39 suggests that in the NW-corner of the red rectangle the distance between the two blue reflectors is higher than anticipated from the overall trend. This is due to the fact that the block rotated to the NW creating more accommodation space resulting in higher thicknesses.

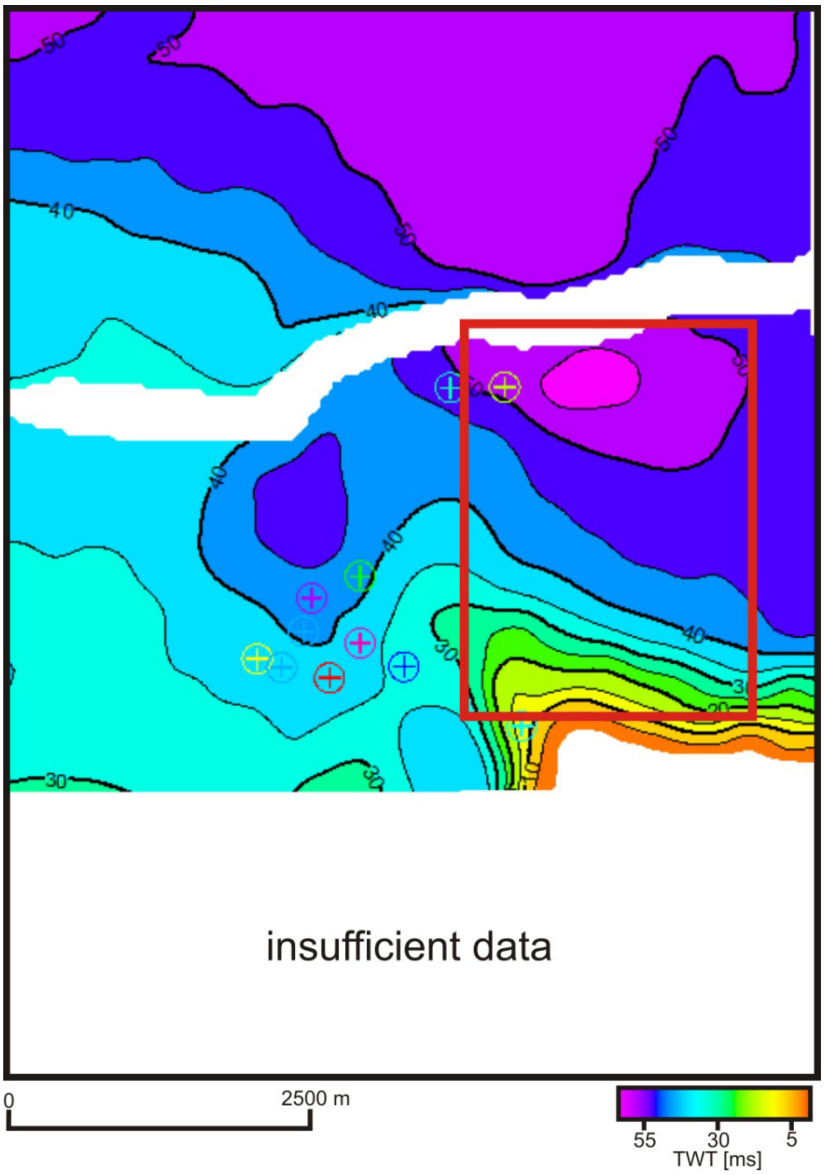

Fig. 39. TWT-thickness map between reflectors "a" and "b" in the Lower Puchkirchen Formation (see Fig. 38). The red rectangle indicates the area of block rotation.

The area within the red rectangle is the only place where a block rotation was observed within the Trattnach cube.

DISCUSSION AND INTERPRETATION

The evolution of deformation structures within the Upper Austrian Alpine Foreland is divided into three phases.

Phase one occurred during the Late Cretaceous (Turonian – Coniacian) and was followed by a Maastrichtian?/Paleocene deformation event (phase two). Finally, triggered by the steadily advancing Alpine nappe system, the third phase evolved.

Within this chapter, the evolution of the deformation events, linked to regional stress regimes, will be interpreted and where appropriate compared to existing concepts. These deformation phases are furthermore set into a regional geological context.

LATE CRETACEOUS DEFORMATION PHASE

During the Late Cretaceous the area today occupied by the Upper Austrian Molasse basin was situated on the southern shelf of the European continent. In the middle Late Cretaceous the first deformation phase formed the N-S trending buckling displayed in Fig. 40. As described previously the age of this deformation phase is constrained by the Turonian shaly marl reflector and the onlaps onto the bulge. Therefore it is suggested that this phase occurred during Late Turonian to Early Coniacian times. Similar structures formed in the study area N and S on the block west of the Trattnach reverse fault. However, comparable structures are not detected E of the Trattnach reverse fault. This might be due to Late Cretaceous and Early Paleocene erosion, which removed large parts of the Upper Cretaceous succession, thus preventing the detection of possible Turonian/Coniacian unconformities.

From the N-S direction it is concluded that the horizontal stress regime was E-W directed. The bulge exhibits a steeper western flank confined by a reverse fault. This processes, forming buckling and reverse faults caused by horizontal stresses (thrusting) is well known and described in literature e.g. by Butler (1982). Fig. 40 summarizes the regional stress pattern, the appearance of the bulge in map view and in a seismic profile.

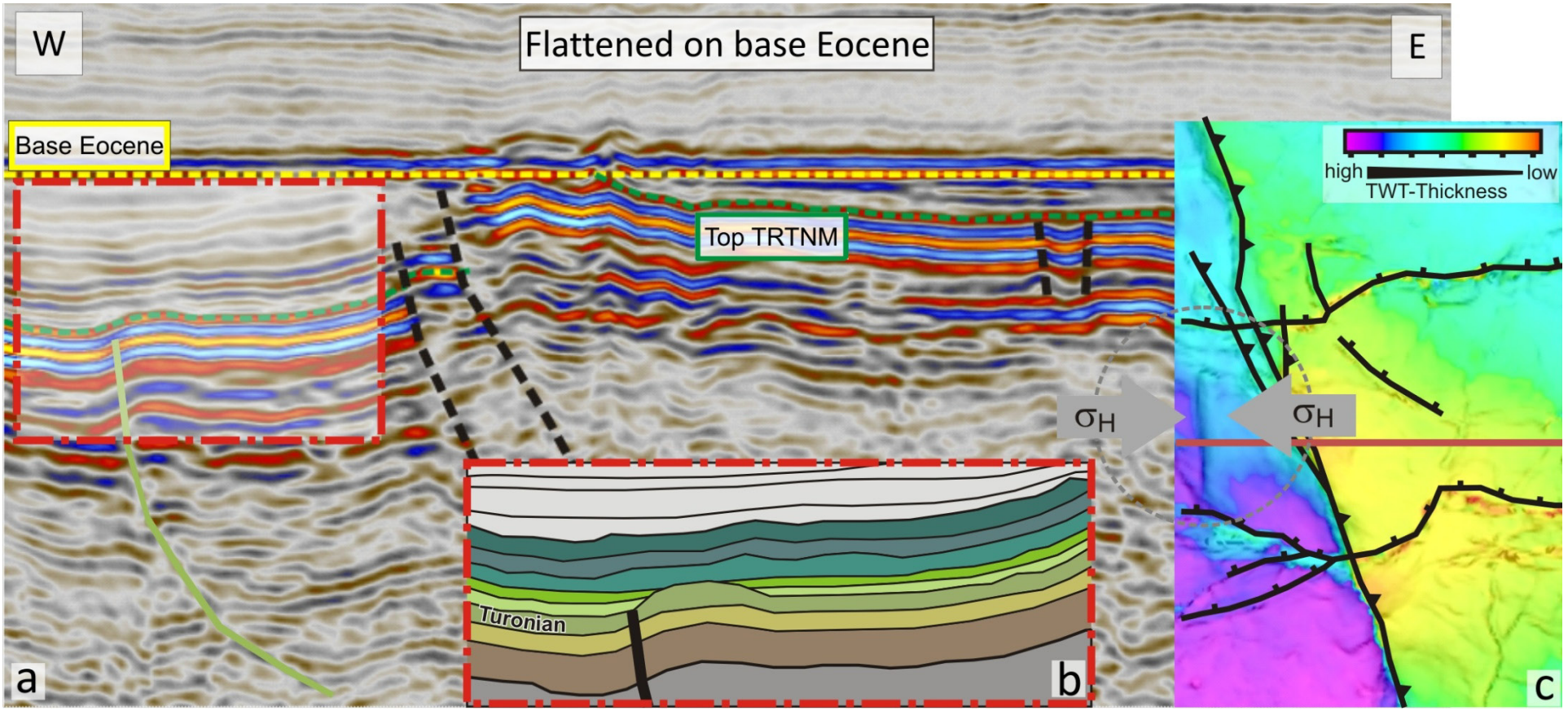

Fig. 40. **a) Flattened W-E trending X-line following the red line in Fig. 40c. The profile is about 6.5 km long.**
b) Sketch drawn from the seismic line is used to constrain the timing of the deformation phase. It displays the deformed Turonian shaly marl reflector (Turonian) and the overlying onlaps. The sketch is located within the red rectangle but not to scale.
c) The base map is compiled from the Top Cenomanian surface relief map with superimposed TWT-thickness of the Late Cretaceous.

It is worth noting that this deformation phase causing N-S trending buckling has not been described before in the Upper Austrian Foreland Basin. The driving tectonic forces exerting these compressional stresses on the European continent originate from the

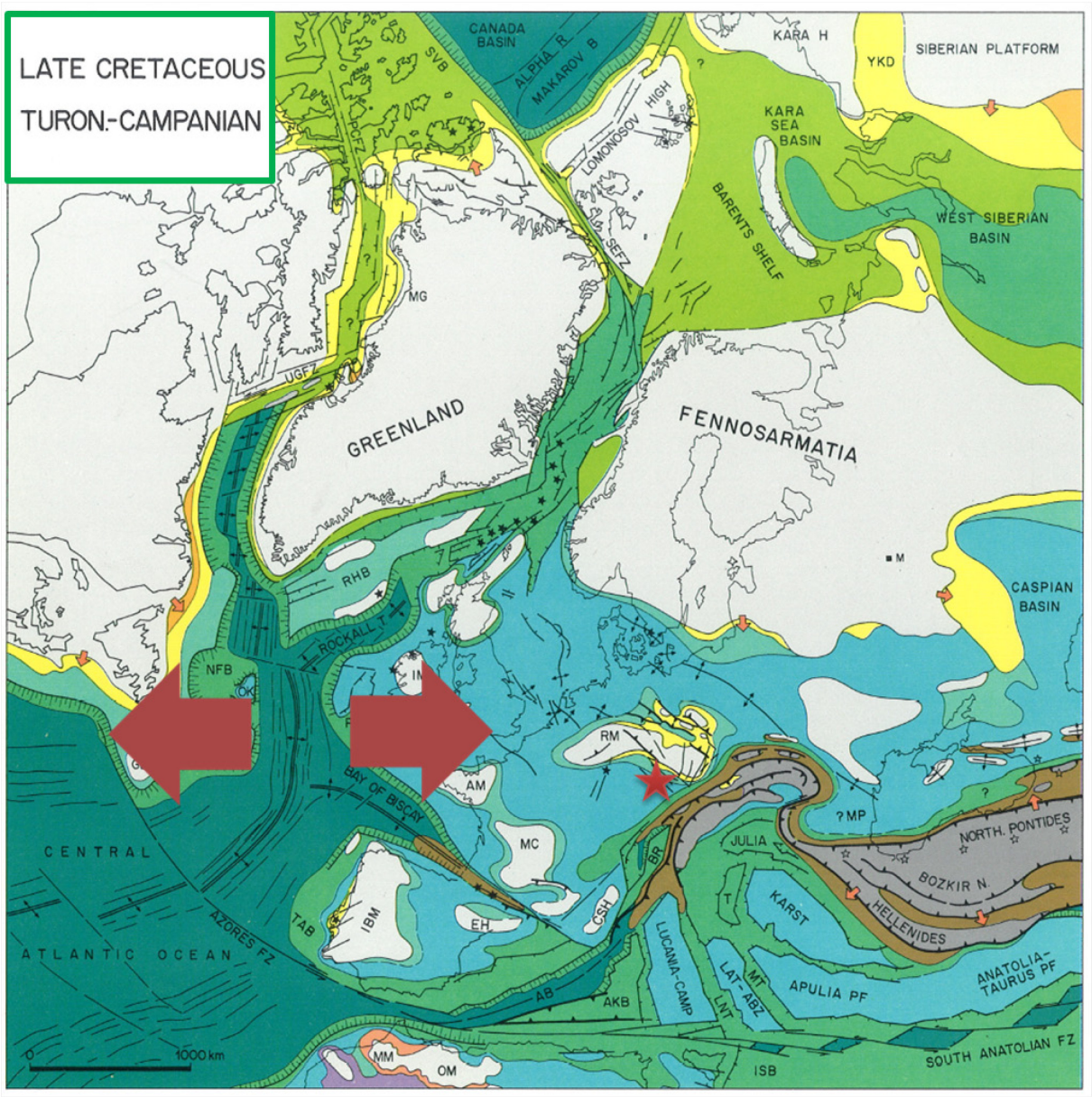

Fig. 41. Paleogeographic map of the Late Cretaceous. Red arrows indicate the direction of compressional stresses. Red star shows the approximate position of the Upper Austrian Foreland at that time. Modified from Ziegler (1988).

ocean spreading processes in the N-Atlantic during Turonian to Campanian times. In Fig. 41, showing a paleogeographic map of the Late Cretaceous, these driving forces are highlighted by red arrows.

Ziegler (1987) concluded that compressional deformation in Europe during the Late Cretaceous was linked to the initial phases of collision between the Austro-Alpine and the

Penninic nappe complexes and the Helvetic shelf. This processes would have exerted NE-SW directed compressional forces on the European plate, although thrusting was NW-SE directed.

Contrary to this widely accepted concept, Kley and Voigt (2008) have stated that NW directed thrusting in the Alps is an unlikely cause for NE-directed shortening on the European plate. Furthermore the paleogeographic location of the Cretaceous orogen precludes it from having exerted a N-ward push on central Europe. Reconstructions of the Western Mediterranean region and Central Europe in Late Cretaceous time place the Austroalpine units of the growing Alpine orogen far to the southeast of their present position. Still separated from the European passive margin by the subducting South Penninic ocean. Kley and Voigt (2008) suggest that the NNE-SSW directed intraplate thrusting is caused by a major change in relative plate motion between Africa and Europe and not Adria-Apulia. Before 120 Ma Africa was moving ESE, after 85 Ma Africa was converging against Iberia-Europe in a NE direction which is in good accordance with the direction of intraplate thrusting observed on the European foreland (Fig. 42). This suggests that the Late Cretaceous basement thrusts and inverted basins are not orogenic foreland phenomena but far-field intraplate structures that formed when the European foreland was pinched between Africa's and Baltic's cratonic lithosphere.

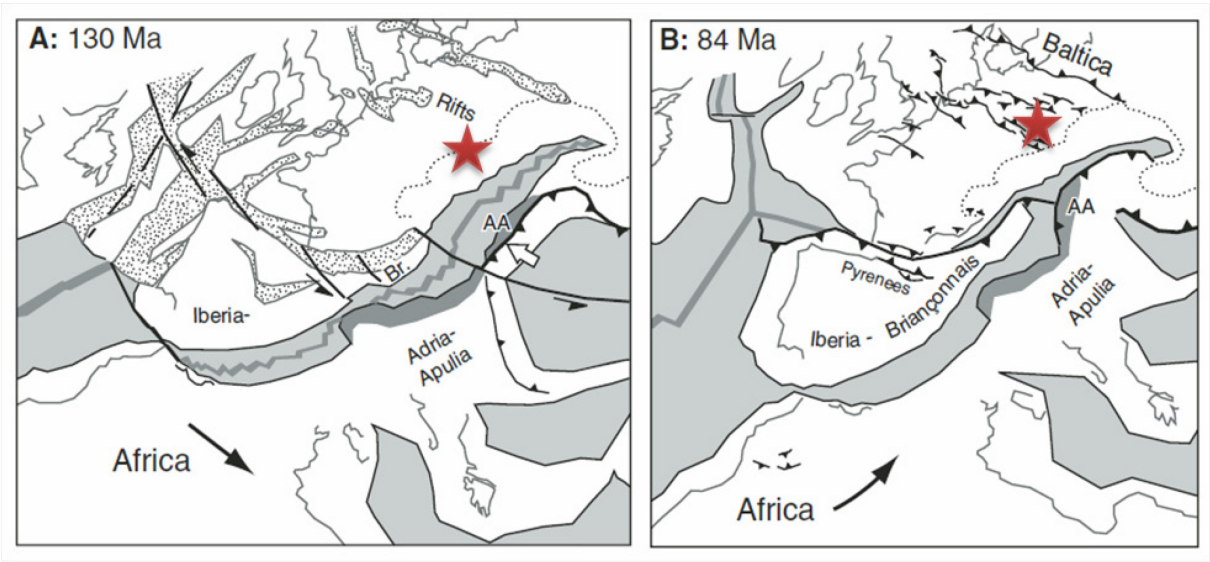

Fig. 42. Paleotectonic sketches at 130 Ma (left) and 84 Ma (right). Red stars indicate the position of the present-day Upper Austrian area at the given time. Modified after Kley and Voigt (2008).

Within the Trattnach area the northern NW-SE-trending bulge (Fig. 43) is indicating a possible NE-SW compressional stress regime. NW-SE trending deformation structures

(Fig. 42 and Fig. 43), might be a result of the before mentioned NE-SW convergence of Africa towards Iberia-Europe. These structures are evident in the Upper Austrian and German Molasse Basin and contemporaneous with the E-W directed compression caused by sea-floor spreading in the realm of the N-Atlantic ocean.

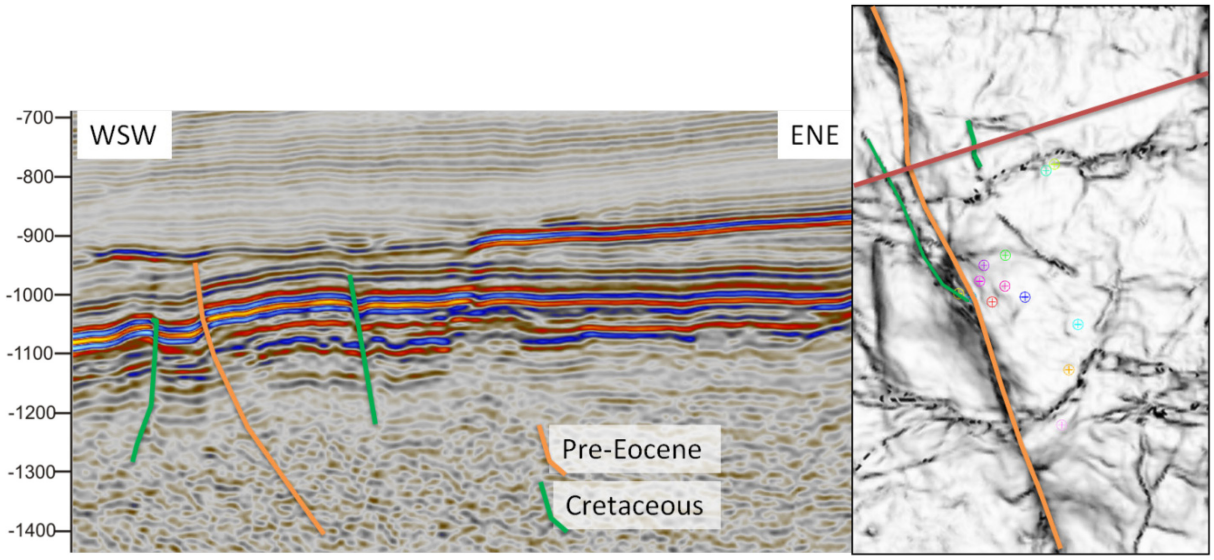

Fig. 43 NNW-SSE trending bulge and Late Cretaceous faults (green) associated with E-W and NE-SW compression. TWT is in ms; length of the seismic profile is about 6 km.

Effects of Late Cretaceous compressional deformation are displayed in Fig. 43 using a seismic profile and a base map. The two faults highlighted in green are of the same age (latest Turonian to Early Coniacian) whereas the orange one, the Trattnach reverse fault, is of pre-Eocene, probably Paleocene age. These two Turonian to Campanian faults along with the NNW-SSE trending bulge are the main indications for a contemporaneous deformations phase which was directed NE-SW and are therefore probably linked to the convergence of Africa towards Iberia-Europe. Combining E-W and NE-SW directed compressional deformation, with varying intensity, is one way to explain these structures. Literature suggests two possible directions of horizontal stresses. These are E-W and NE-SW directed compression. From the given data it is difficult to conclude whether the existing structures were formed by a single stress regime, or by a combination of the two mentioned regimes.

Fig. 44 highlights that Late Cretaceous deformation in the Upper Austrian Foreland Basin was not restricted to the study area. The N-S trending seismic 2D line is located in the western part of Upper Austria close to the German border. The profile is located south of

the Central Swell Zone whereas the Trattnach area is located north of it. The timing of the deformation, Late Turonian to Early Coniacian, is the same as in the Trattnach area. In Fig. 44a, a structure caused by compressional deformation is visible along an apparently S-dipping reverse fault. The north dipping fault located about 1 km to the south of the reverse fault is of Eocene age.

The sketch drawn from the seismic line (Fig. 44b) points out the time constraints of the deformation phase and the actual shape of the tectonic feature. Although strike-slip movements cannot be excluded, the present day shape of this structure is interpreted as an inverted halfgraben. The halfgaben (Fig. 44c) had possibly formed during a Jurassic extensional phase and was inverted during the Late Cretaceous (Turonian to Coniacian) times. Because only a single 2D line was available, the regional extent and alignment of the inverted halfgraben cannot be constrained.

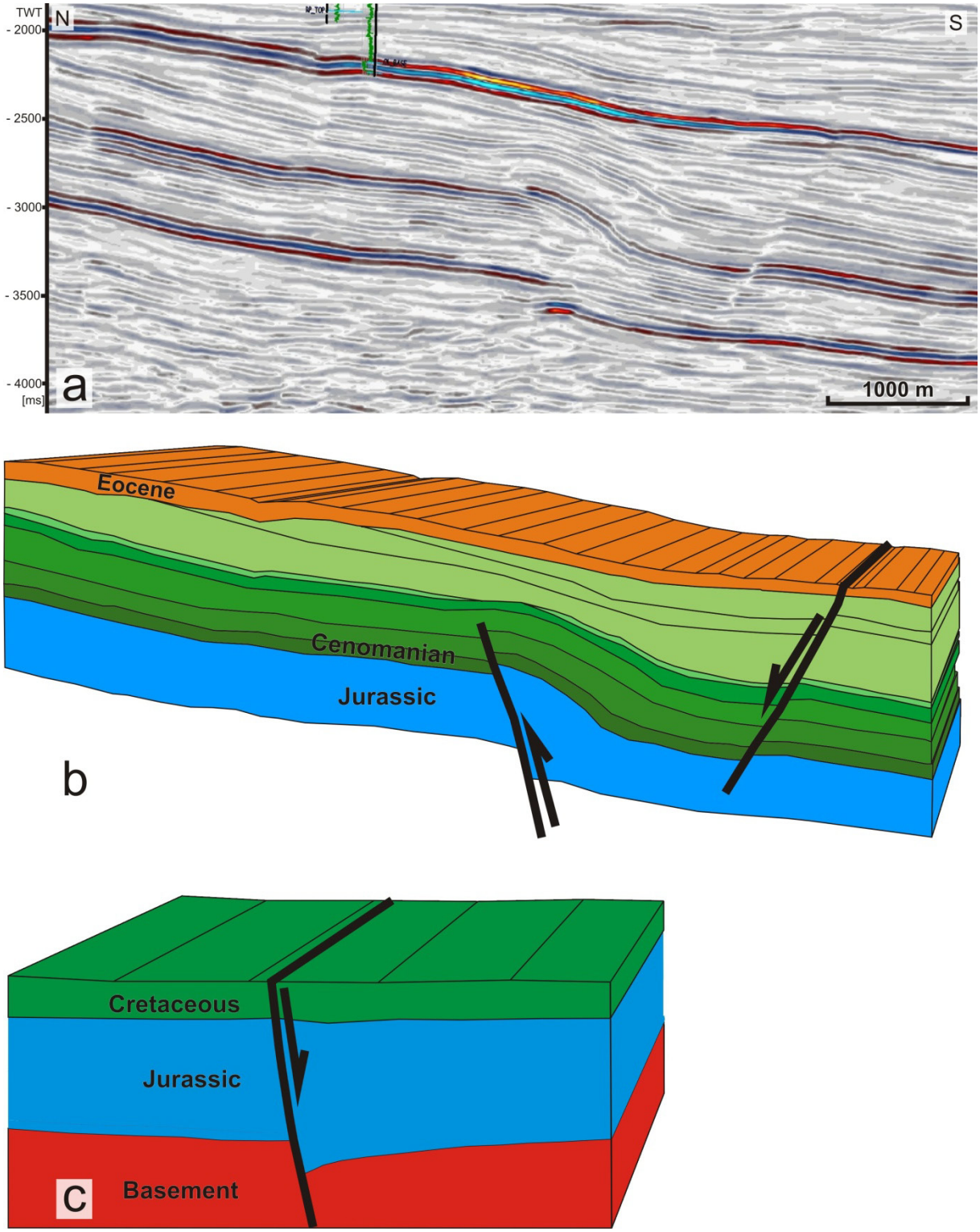

Fig. 44. Composite display of the Late Cretaceous deformation phase in the western part of the Upper Austrian Molasse Basin.

a) N-S trending seismic profile.

b) Interpretation drawn from the profile in Fig. 44a.

c) Sketch of the Jurassic halfgraben which was later inverted to its present day shape in Fig. 44b.

PALEOCENE DEFORMATION PHASE

The second deformation phase is the one which affected the Mesozoic sedimentary record the most. Before discussing the structures within the study area, the regional tectonic evolution during the Paleocene is described broadly following Dèzes et al. (2004). The Paleocene deformational structures in the Upper Austrian Foreland are caused by compressive stresses. During the Late Cretaceous convergence rates between Africa and Europe decreased sharply and during the Late Maastrichtian and Early Paleocene dropped to practically zero. This is explained by strong mechanical coupling of the African and European plates across the Alpine-Mediterranean orogen. During the Late Paleocene Western-, Central Europe along with the East-European craton and North Africa were affected by intense intraplate compression. By that time the S-ward subduction of the Alpine Tethys beneath the Austro-Alpine orogenic wedge was apparently completed. Closure of the Alpine Tethys resulted in the collision of the Austro-Alpine orogenic wedge with the European foreland in the E-Alpine domain. This caused the build-up of intraplate compressional stresses in the foreland.

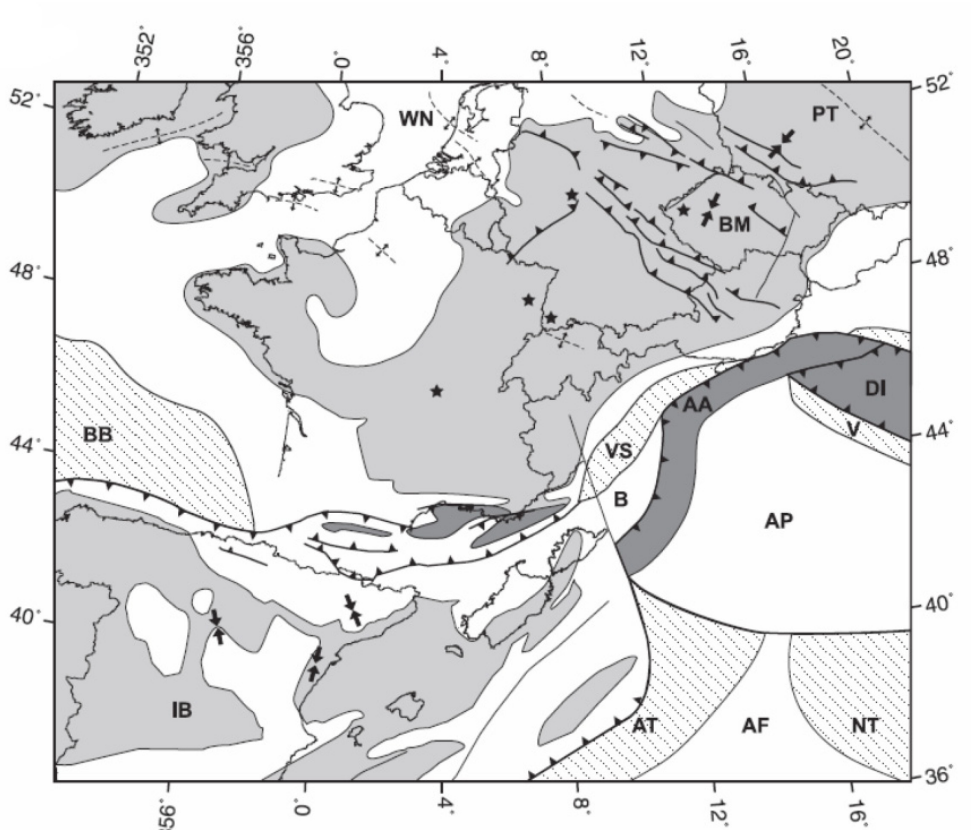

Fig. 45. Paleotectonic sketch map of the Late Paleocene. Legend: dark grey: orogens, light grey: areas of non deposition, white: sedimentary basins, stippled: oceanic basins, stars: volcansim, arrows: maximum horizontal compressional stress direction (Bergerat 1987, Blès and Gros 1991, Schumacher 2002), thick dashed line: axis of lithospheric fold. Abbreviations: AA: Austro-Alpine orogen; AF: Africa; AP: Apulia; AT: Alpine Tethys; B: Briançonnais; BM: Bohemian Massif. From Dèzes et al. (2004).

As shown in Fig. 45 maximum horizontal compressive stresses for the Late Paleocene are NE-SW directed in the Bohemian Massif. The pattern and dip direction of the reverse faults in the central European region (in Fig. 45) are a result this direction.

The paleotectonic sketch map from Dèzes et al. (2004; Fig. 45) suggests that NW-directed regional tectonic forces were causing NE-SW directed compression on the European foreland. Those stresses were caused by the N to NW directed collision of the Austro-Alpine orogenic wedge with the European foreland. Comparing this to the investigations from the Upper Austrian Foreland, especially the Trattnach area, shows good accordance of the interpreted paleostress directions. Hence is should be allowed to infer paleostress regimes from structures interpreted from seismic data.

Addressing NE-SW directed stress originating from N to NW directed tectonic forces, Wessely (1987) suggested a radial distribution of stresses around the South Bohemian Basement Spur (Fig. 1). A present-day radial stress orientation in eastern Austria is

documented by Reinecker and Lenhardt (1999 and 2010) south of the Molasse Basin for the Northern Calcerous Alps.
I speculate that, if this particular orientation of horizontal stresses is present today, the same mode of reorientation could be valid for the Paleocene as well.

This second deformation phase formed two prominent features. The first one is the Trattnach mega-anticline structure spanning from the NW to the SE and the second one is the Trattnach reverse fault confining the anticline to the west.
In Fig. 46 both features are displayed:

- The Trattnach mega-anticline with its two crests, the Trattnach anticline in the central part and the Altenhof anticline farther south.
- The NNW-SSE trending Trattnach reverse fault.

Maximum horizontal stress directions are indicated by the diagram in Fig. 46 along with Riedel and Anti-Riedel shear directions. Intraplate forces during the Paleocene were NE directed, within the Trattnach area, towards the Bohemian Massif which was acting as a rigid block causing NE-SW compressional deformation.
Along with the NNW-SSE trending Trattnach reverse fault NE-SW shortening caused deformation perpendicular to the maximum horizontal stress, parallel and along Riedel and/or Anti-Riedel shear zones. The alignment of Riedl and Anti-Riedel shears is indicated by the diagram in Fig. 46. The Riedel shears are NNE-SSW directed and Anti-Riedel shears are ESE-WNW trending. Along these directions deformation was possible during the Paleocene. One prominent fault ("Y") is situated between the Trattnach and Trattnach North fields (Fig. 46).

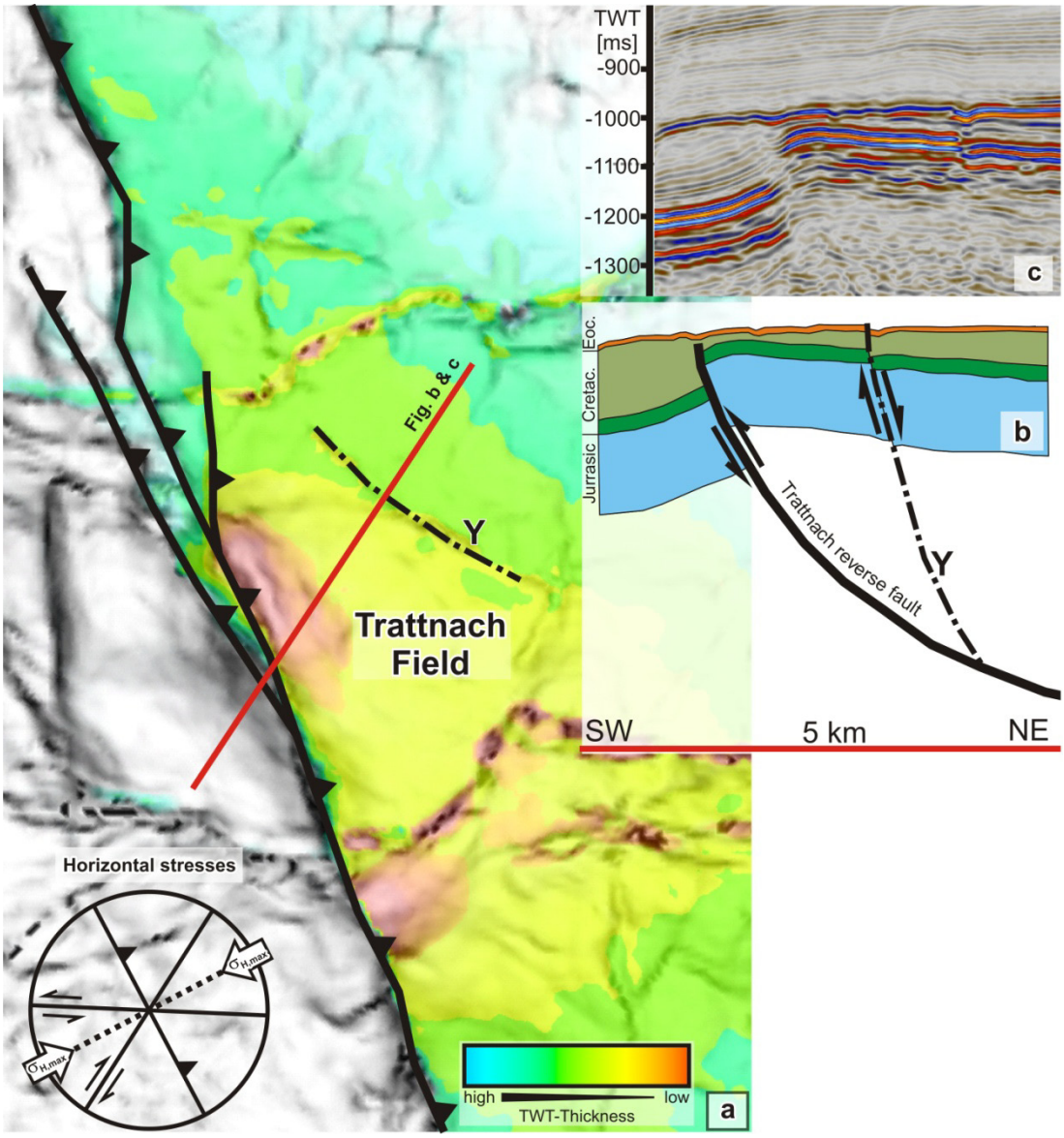

Fig. 46. a) Relief map with a TWT thickness map overlay.
b) Sketch is illustrating the deformation
c) Seismic profile along the red line in Fig. 46a is displayed.

The fault labelled "Y" is of importance because it acts as a pressure barrier between the Trattnach and Trattnach-North field. This fault was activated during the Paleocene by compressional forces, possibly forming a pop-up structure together with the Trattnach reverse fault. During the phase of flexural down-bending of the European foreland under the advancing Alpine nappe system this fault was reactivated as a NW-dipping, crescent shaped normal fault.

Bachmann et al. (1987) interpreted the seismic profile in Fig. 47. They concluded that the fault SW of the Central Swell Zone (synonymous for Landshut-Neuoettingen High) and the

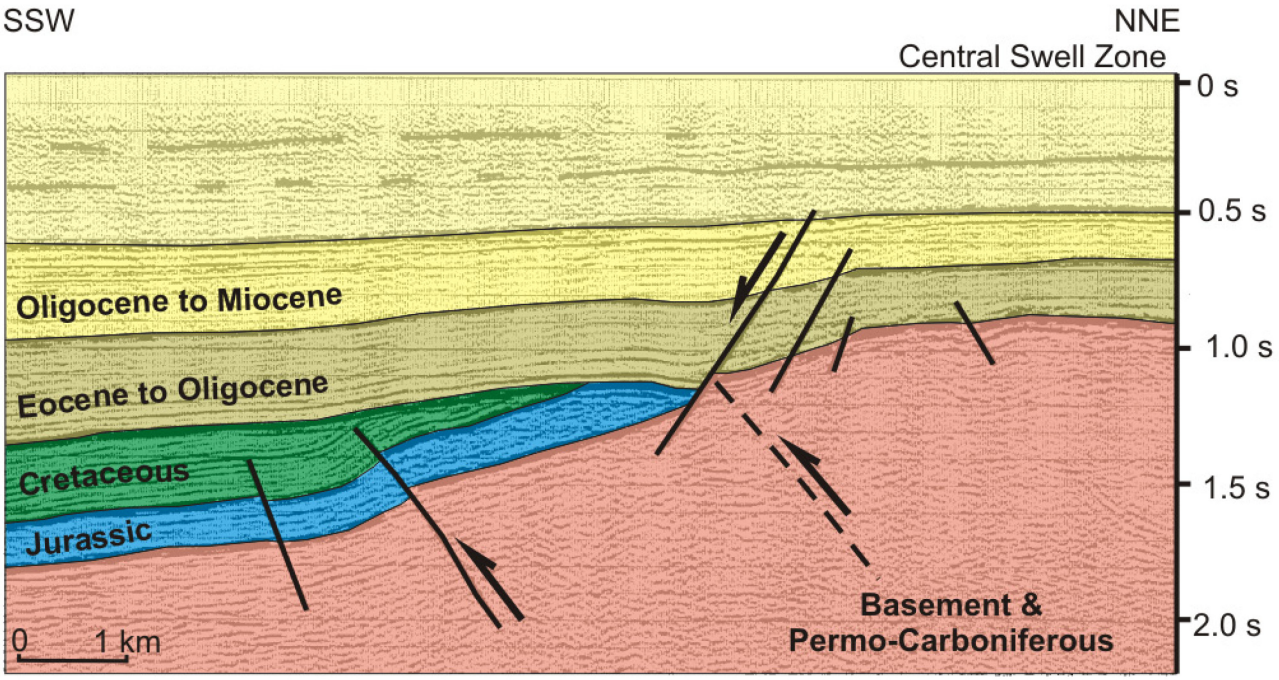

Fig. 47. SSW-NNE trending seismic profile approximately 65 km west of the Trattnach area in Bavaria (Germany). The reverse fault at the SW-edge of the Central Swell Zone is superimposed by younger normal faults and not visible in the seismic profile. But its location can be inferred from a parallel profile. Two Cretaceous reverse faults are present in the SSW part. Modified from Bachmann et al. (1987).

one 3 km to the SSW are reverse faults. The Landshut-Neuoettingen High is bordered by a major reverse fault on its SW-margin. They derived a vertical throw in the order of at least 1500 m and a horizontal displacement of more than 1000 m for this reverse fault.

The normal faults in this area are significantly younger and are associated with extensional deformations during the Oligocene and Miocene. Comparing the interpretations of Bachmann et al. (1987) and the recent findings presented within this thesis the Late Cretaceous and Paleocene deformation structures are similar. Concerning timing, paleostress directions and general appearance it is suggested that these structures were formed by the same mechanisms. Bachmann et al. (1987) conclude that the inversion phase during the Latest Cretaceous and Early Paleocene formed these structures and that they result from transpressional wrench tectonics.

Nachtmann and Wagner (1987) postulated that these foreland deformations are a result of dextral strike-slip movements. However within the research done for this thesis no clear indications for extensive strike-slip faulting, certainly necessary to achieve vertical

displacements of 1500 m or more, were found. Fault interpretation and structural analysis suggests predominately dip-slip movement with, which cannot be excluded, minor strike-slip components. The Trattnach fault is interpreted as a reverse fault after carefully examining other possibilities.

Moreover, strike-slip deformation forming the Trattnach fault seems to be unlikely due to the following reasons:

Seismic interpretation did not show clear signs like flower structures (Zolnai 1991). Another issue is that dextral strike-slip movements are suggested in literature for the entire Upper Austrian Molasse Basin (Wagner 1996). However the anticline and the branch faults of the Trattnach reverse fault (Fig. 46) suggest that sinsitral movement is the only plausible strike-slip mode, which could have formed the anticline and the branch faults at the same time. However, sinsitral strike-slip movement is not documented in the Upper Austrian Molasse Basin.

In addition, looking on seismic profiles (Fig. 43 and Fig. 46), it is apparent that the reverse faults W and E of the Trattnach reverse fault were formed during the Turonian and Coniacian. So they are considerably older. Therefore these faults are not branch faults of the Trattnach reverse fault but individual faults. The Trattnach reverse fault was formed during the Paleocene, or possible from the Maastrichtian onwards. Thus, these faults are not related to each other.

EVOLUTION OF CENOZOIC NORMAL FAULTING

Discussing the evolution of Cenozoic normal faults, I would like to briefly recall the tectonic evolution of the European foreland following Genser et al. (2007).

The Cenozoic evolution of the Molasse Basin was determined by subsidence in the Eocene followed by collisional coupling of the European continental margin and the evolving Alpine nappes. Flexural down-bending, rapid deepening and the development of tensional faults was the result of thrust loading during the latest Eocene and Early Oligocene.

The evolution of these E-W trending normal faults is interpreted within this section. The Aistersheim and the Gaspoltshofen normal fault systems were both first active during the earliest Oligocene accommodating S directed tensional forces (Fig. 48). N-dipping (antithetic) faults were developed contemporaneously with the S-dipping (synthetic) faults. During the Early Oligocene not only the major normal fault systems developed but also a number of older faults were reactivated. Although, having small throws those reactivated faults can be of importance. As an example, fault “Y” in Fig. 46 is a reactivated reverse fault. Fig. 48 displays Cenozoic normal faults on a N-S trending profile and on a base map. N-dipping faults are forming graben like structures in conjunction with the S-dipping major faults. These graben structures are not present along the whole length of the fault. The S-shape of the southern Gaspoltshofen normal fault is another prominent feature displayed on the base map. This particular shape is the combined result of the reactivation of older compressional faults and Cenozoic normal faulting. During the Paleocene weakened and therefore fault prone areas were formed in a NNE trending direction. These Paleocene structures are interpreted as (Anti-)Riedel shear zones as mentioned earlier. With the onset of flexural down-bending of the European continental margin these weakened zones were preferred directions of deformation. Hence the Gaspoltshofen fault is rather sharply bent along this zone.

The base map in Fig. 48 highlights another finding. The formation of the NNW-SSE trending Trattnach reverse fault was terminated before the deposition of basal Eocene sediments. Moreover, this suggests that the relief created by Paleocene deformation processes had already been peneplaned at that time. These findings are in accordance with literature.

Normal faulting in the Upper Austrian Molasse Basin was active until the end of the Egerian.

Cenozoic block rotation in the Trattnach area is a tectonic event never described before in the Austrian Molasse Basin. Like normal faulting this deformation is related to the crustal down-bending. Theory and constraints of block rotation in collisional foredeeps are described by Bradley and Kidd (1991) in their paper on flexural extension of the upper continental crust in collisional foredeeps. They conclude that rotational backtilting of fault blocks is a common feature associated with flexural extension and down-bending of lithosphere in collisional processes.

In Fig. 48 the block rotation is highlighted by colours. The reflectors coloured in blue are the uppermost ones affected by N-ward rotation. Towards the south they became, due to their backtilting, truncated by the overlying strata, coloured in a faded yellow. Since sediments affected by block rotation are a part of the Lower Puchkirchen Formation it is suggested that the deformation happened between the latest Oligocene and Early Miocene. This would be contemporaneous with the phase when the advancing Alpine nappe system overrode and partially scooped out the southern parts of the Molasse basin.

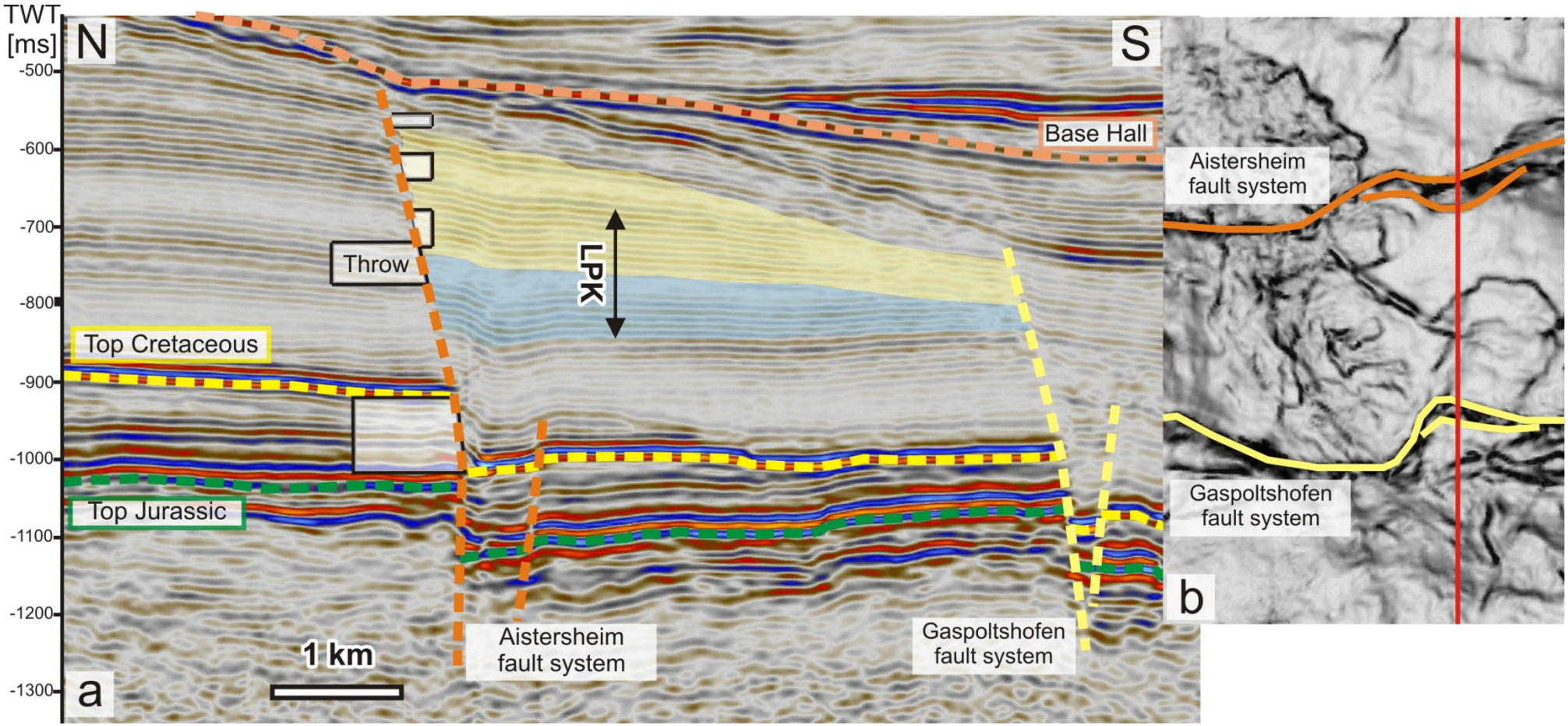

Fig. 48. **a) N-S trending seismic profile along the red line in Fig. 48b.**
b) Relief map of the Base Eocene (Top Cretaceous).
For explanation please see text.

CONCLUSION

The Upper Austrian Molasse Basin and its underlying Mesozoic succession are transsected by a variety of fault systems. Two main directions can be observed, NNW-SSE trending Paleocene reverse faults and younger E-W trending normal faults. A majority of hydrocarbon reservoirs is linked to these deformation structures (Nachtmann 1995).

Within the study area three deformational events can be distinguished:

(1) The oldest deformation phase interpreted in the Mesozoic succession of the Alpine foredeep took place during the latest Turonian and early Coniacian. Sea-floor spreading in the N-Atlantic realm induced intraplate compressional stresses on the European foreland. This stresses formed a N-S trending bulge displayed in Fig. 40.

The bulge has got an approximate length of 3 km, is 500 m wide and a few tens of meters high. It is confined by a reverse fault along its steeper western flank. The accurate N-S alignment of the bulge is apparent in Fig. 40b. The interpretation in Fig. 40c highlights the evolution of the bulge. The youngest folded reflector is the Top TRTNM (Turonian shaly marls) which is overlain by onlapping reflectors. On top of these, continuous deposits of the uppermost Cretaceous are capping the structure. Another deformation structure, showing the same timing exists only a few kilometres westwards from this one.

(2) Paleocene deformation in the Upper Austrian Molasse Basin is characterized by NE-SW compression. The deformation structures formed as a result of the collision of the Austro-Alpine unit with the European foreland (Dèzes, Schmid and Ziegler 2004). The Trattnach reverse fault and the Trattnach mega-anticline are the results of this event which are displayed in Fig. 33 and Fig. 46.
Along with the Trattnach reverse fault and the anticline deformation structures were formed perpendicular and parallel to the horizontal stresses and/or as (Anti-)Riedel shears. The fault NE of the Trattnach fault labelled "Y" in Fig. 46 is acting as a pressure barrier between the Trattnach and the Trattnach North field.

(3) Form the Eocene onwards, E-W trending normal faults (Fig. 48)were formed as a result of thrust loading and flexural down-bending of the foreland by the advancing Alpine

nappe system. The Aistersheim and Gaspoltshofen fault system were formed by these processes.

The N- and S-dipping normal faults were formed contemporaneously during the earliest Oligocene. The S-dipping faults were active until the end of the Egerian which is indicated by the increasing throw from top to bottom. Whereas formation of the N-dipping faults generally terminated earlier.

A block rotation occurred during the deposition of the Lower Puchkirchen Formation (Fig. 48) where a block tilted, W of the Trattnach reverse fault, to the N and was eroded in the S.

This concludes the interpreted tectonic evolution of the Cenozoic Molasse Basin and its underlying Mesozoic basement.

LITERATURVERZEICHNIS

Bachmann, G. H., M. Müller, and K. Weggen. “Evolution of the Molasse Basin (Germany, Switzerland).” *Tectonophysics*, 1987: 77-92.

Bergerat, F. “Stress fields in the European Platform at the time of Africa-Eurasia colission.” *Tectonics*, 1987: 99-132.

Blès, J.-P., and Y. Gros. “Stress field changes in the Rhone Valley from the Miocenne to present.” *Tectonophysics*, 1991: 265-277.

Bradley, D. C., and W.S.F. Kidd. “Flexural extension of upper continetal crust in collisional foredeeps.” *Geological Society of America Bulletin*, 1991: 1416-1438.

Butler, R. W. “The terminology of structures in thrust belts.” *Journal of Structural Geology*, 1982: 239-245.

De Ruig, M. J. “Deep Marine Sedimentation and Gas Reservoir Distribution in Upper Austria.” *OIL GAS European Magazine*, 2003: 64-73.

De Ruig, M. J., and S. M. Hubbard. “Seismic facies and reservoir characteristics of a deep-marine channel belt in the Molasse forelnad basin, Puchkirchen formation, Austria.” *AAPG Bulletin*, 2006: 735-752.

Dèzes, P., S. M. Schmid, and P. A. Ziegler. “Evolution of the European Cenozoic Rift System: interaction of the Alpine and Pyrenean orogens with their forelnad lithosphere.” *Tectonophysics*, 2004: 1-33.

Genser, J., S.A.P.L. Cloething, and F. Neubauer. “Late orogenic rebound and oblique Alpine convergence: New constraints from subsidence analysis of the Austrian Molasse basin.” *Global and Planetary Chnage*, 2007: 214-223.

Hinsch, R. “New Insights into the Oligocene to Miocene Geological Evolution of the Molasse Basin of Austria.” *OIL GAS European Magazine*, 2008: 138-143.

Kley, J., and T. Voigt. “Late Cretaceous intraplate thrusting in central Europe: Effect of Africa-Iberia-Europe convergence, not Alpine collision.” *Geology*, November 2008: 839-842.

Kollmann, K. “Die Öl- und Gasexploration der Molassezone Oberösterreichs und Salzburgs aus regional-geologischer Sicht.” *Erdöl-Erdgas Zeitschrift*, 1977: 36-49.

Malzer, O., F. Rögl, P. Seifert, L. Wagner, G. Wessely, and F. Brix. “Die Molassezone und deren Untergrund.” In *Erdöl und Erdgas in Österreich*, 281. 1993.

Nachtmann, W. “Bruchstrukturen und ihre Bedeutung für die Bildung von Kohlenwasserstoff-Fallen in der Oberösterreichischen Molasse.” *Geol. Paläont. Mitt. Innsbruck*, 1995: 221-230.

Nachtmann, W., and L. Wagner. “Mesozoic and Early Tertiary evolution of the Alpine foreland in Upper Austria and Salzburg, Austria.” *Tectonophysics*, 1987, Compressional Intra-Plate deformation in the Alpine Foreland ed.: 61-76.

Reinecker, J., and W. A. Lenhardt. “Present-day stress field and deformation in eastern Austria.” *Int. Journ. Earth Sciences*, 1999: 532-550.

Reinecker, J., M. Tingay, B. Müller, and O. Heidbach. “Present-day stress orientation in the Molasse Basin.” *Tectonophysics*, 2010: 129-138.

Rockenschaub, A. “Von der Erdölbohrung zum Heilbad - Bad Schallerbach.” *Oberösterreichische Heimatblätter*, 1996: 390-402.

Sachsenhofer, R. F., and H. M. Schulz. “Architecture of Lower Oligocene source rocks in the Alpine Foreland Basin: a model for syn- and post-depositional source-rock features in the Paratethyan realm.” *Petroleum Geoscience*, 2006: 363-377.

Sachsenhofer, R. F., et al. “Deposition, erosion and hydrocarbon source potential of the Oligocene Eggerding Formation (Molasse Basin, Austria).” *Austrian Journal of Earth Sciences*, 2010: 73-99.

Sachsenhofer, R. F., R. Gratzer, W. Tschelaut, and A. Bechtel. “Characterisation of non-producible oil in Eocene reservoir sandstones (Bad Hall Nord field, Alpine Foreland Basin, Austria).” *Marine and Petroleum Geology*, 2006: 1-26.

Schulz, H. M., R. F. Sachsenhofer, A. Bechtel, H. Polesny, and L. Wagner. “The origin of hydrocarbon source rocks in the Austrian Molasse Basin (Eocene - Oligocene transition).” *Marine and Petroleum Geology*, 2002: 683-709.

Schulz, H.-M., A. Bechtel, T. Rainer, R. F. Sachsenhofer, and U. Struck. “Paleoceanography of the western Central Paratethys during nannoplankton zone NP 23-the Dynow Marlstone in the Austrian Molasse Basin.” *Geologica Carpathica*, 2004: 311-323.

Schumacher, M. E. “Upper Rhine Graben: the role of preexisting structures during rift evolution.” *Tectonics*, 2002.

Sissingh, W. “Tectonostratigraphy of the North Alpine Foreland Basin: correlation of Tertiary depositional cycles and orogenic phases.” *Tectonophysics*, 1997: 223-256.

Véron, J. “The Alpine Molasse Basin - Review of Petroleum Geology and Remaining Potential.” *Bull. angew. Geol.*, 2005: 75-86.

Wagner, L. R. “Tectono-stratigraphy and hydrocarbons in the Molasse Foredeep of Salzburg, Upper and Lower Asutria.” *MASCLE, A., PUIGDEFÀBREGAS, C., LUTERBACHER, H.P. & FERNANDÈZ, M (eds) Cenozoic Foreland BAsins of Western Europe. Geological Society Special Publications, 134*, 1998: 339-369.

—. “Stratigraphy and hydrocarbons in the Upper Austrian Molasse Foredeep (active margin).” *Wessely, G. & Liebl, W. Oil and Gas in Aplidic Thrustbelts and Basins of Central and Eastern Europe, EAGE Special Publications No. 5*, 1996: 217-235.

Wessely, G. “Mesozoic and Tertiary evolution of the Alpine-Carpathian foreland in eastern Austria.” *Tectonophysics*, 1987: 45-59.

Ziegler, P. A. “Evolution of the Arctic-North Atlantic and the Western Tethys.” *AAPG Memoir 43*, 1988.

—. “Late Cretaceous and Cenzoic intra-plate compressional deformation in the Alpine foreland - a geodynamic model.” *Tectonophysics*, 1987: 389-402.

Ziegler, P. A., S. Cloething, and J.-D. van Wees. “Dynamics of intra-plate compressional deformation: the Alpine foreland and other examples.” *Tectonophysics*, 1995: 7-59.

Zolnai, G. “Continental Wrench-Tectonics and Hydrocarbon Habitat.” *Continuing Education Course Note Series 30*, 1991.

LIST OF FIGURES